SMALL IS DIFFERENT

Emergent behavior in the nanoscale

THE INTERSECTION OF TWO MAJOR EMERGENT MOVEMENTS

* *SCIENCE AND TECHNOLOGY AT THE NANOSCALE*

* *COMPUTATIONAL MICROSCOPIES – COMPUTERS AS TOOLS FOR DISCOVERY*

Small is Different

The non-scalable regime

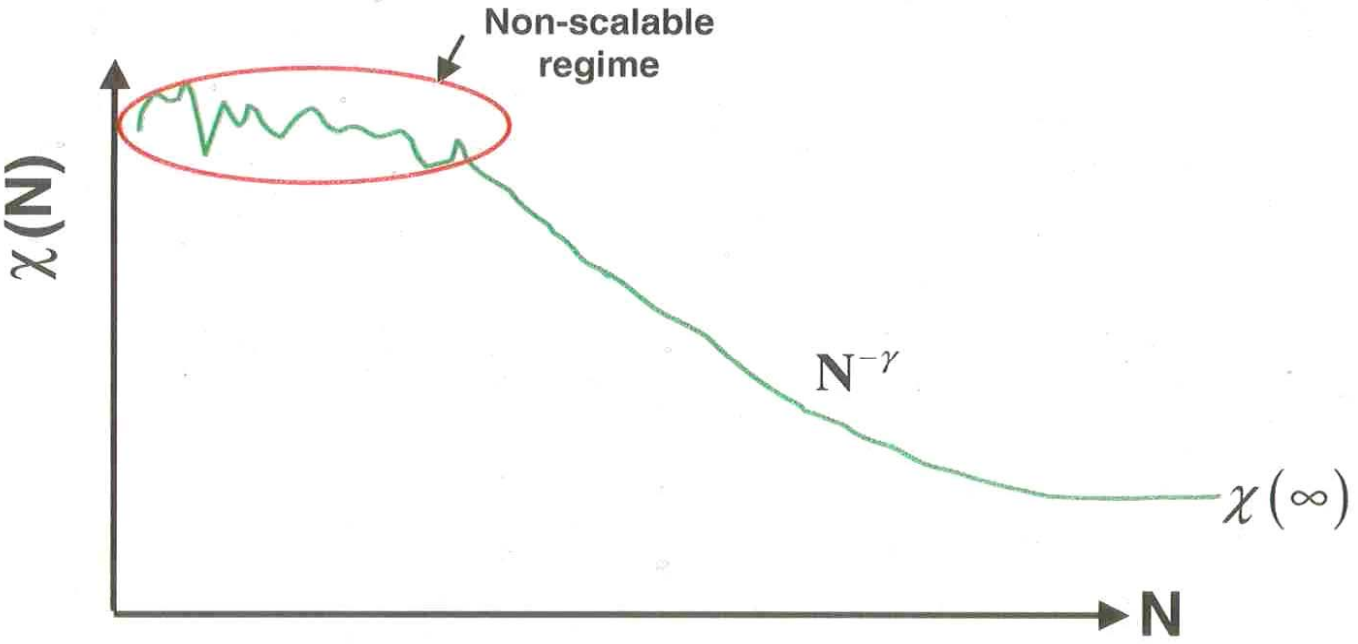

SMALL IS DIFFERENT

Nano

(Nānos (Greek) dwarf)

$= 10^{-9}$ meter

1nm $= 10^{-7}$ centimeter

$= 10$ Ångströms

λ ← characteristic length (phenomenon dependent) as material "

L ← physical extent

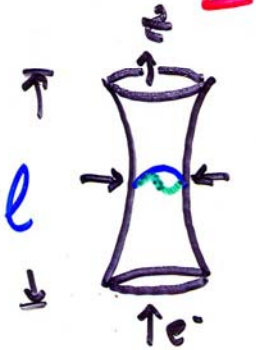

$\ell < \ell_e$

ballistic

λ_F electronic wavelength (Fermi)

L diameter of wire

⇒ quantized conductance

$G = \frac{dI}{dV}$

$2e^2/h$

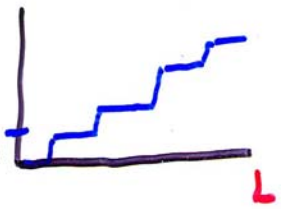

classical :

- Enhanced mechanical strength (dislocation loop dimensional
- layering of confined fluids
- fluctuations (nanojets)

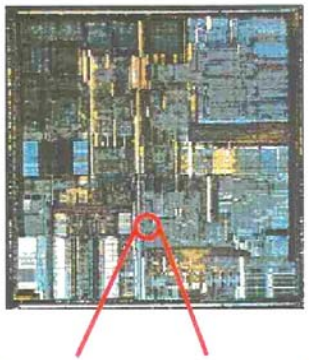

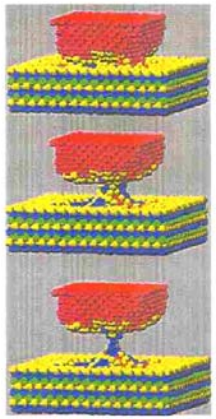

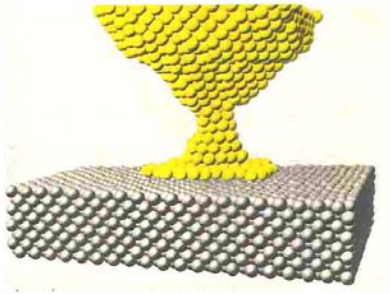

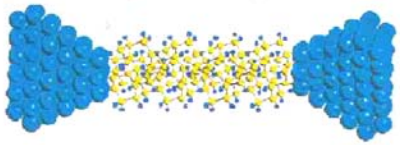

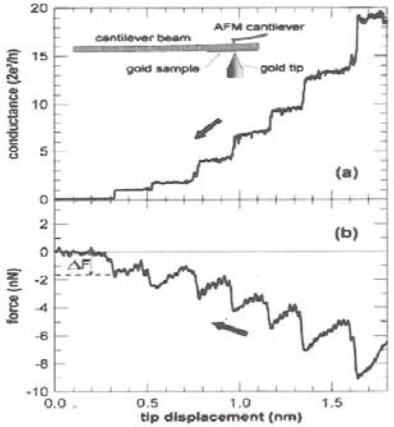
cantilever beam
AFM cantilever
gold sample
gold tip
conductance (2e²/h)
(a)
(b)
force (nN)
ΔF
tip displacement (nm)

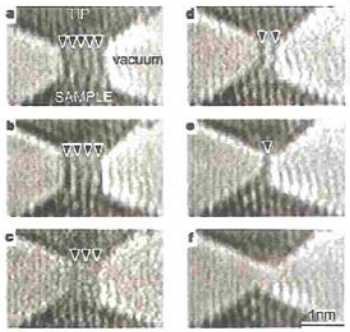
TIP
vacuum
SAMPLE
1nm

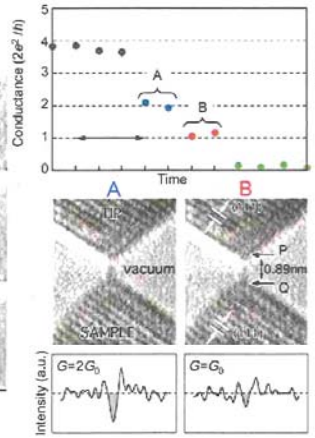
Conductance (2e² / h)
A
B
Time
TIP
vacuum
SAMPLE
P
0.89nm
Q
Intensity (a.u.)
G=2G₀
G=G₀

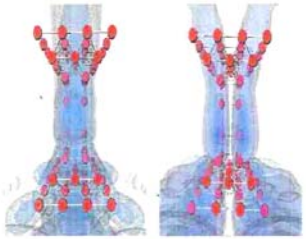

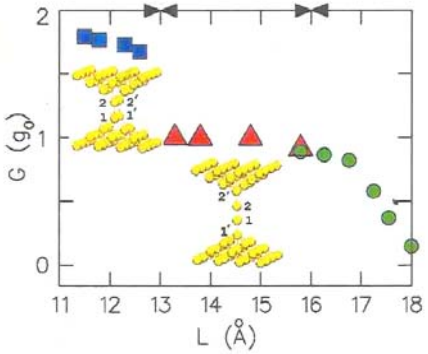
G (g₀)
L (Å)

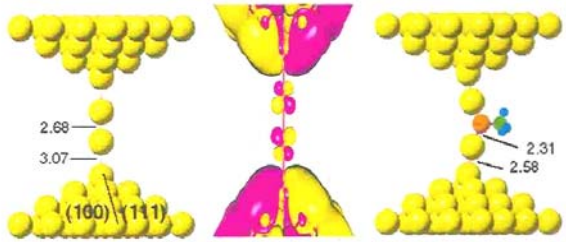
2.68
3.07
(100)
(111)
2.31
2.58

Nano-Scale Matter

- **Nature: Novel Phenomena**
  - reduced length and time scales
  - emergent phenomena
  - not merely scaling down!!
- **Experiment and Theory: New Strategies and Methodologies**
  - ultra-high saptio-temporal resolution
  - atomic-scale manipulations
  - simulations (quantum *ab-initio* and classical)
- **Science-driven Novel Technologies**
  - New design concepts; new opportunities

THE INTERSECTION OF TWO MAJOR EMERGENT MOVEMENTS

* SCIENCE AND TECHNOLOGY AT THE NANOSCALE

* COMPUTATIONAL MICROSCOPIES – COMPUTERS AS TOOLS FOR DISCOVERY

Viewing the nano-scale

--Pat Dehmer

atomic abacus

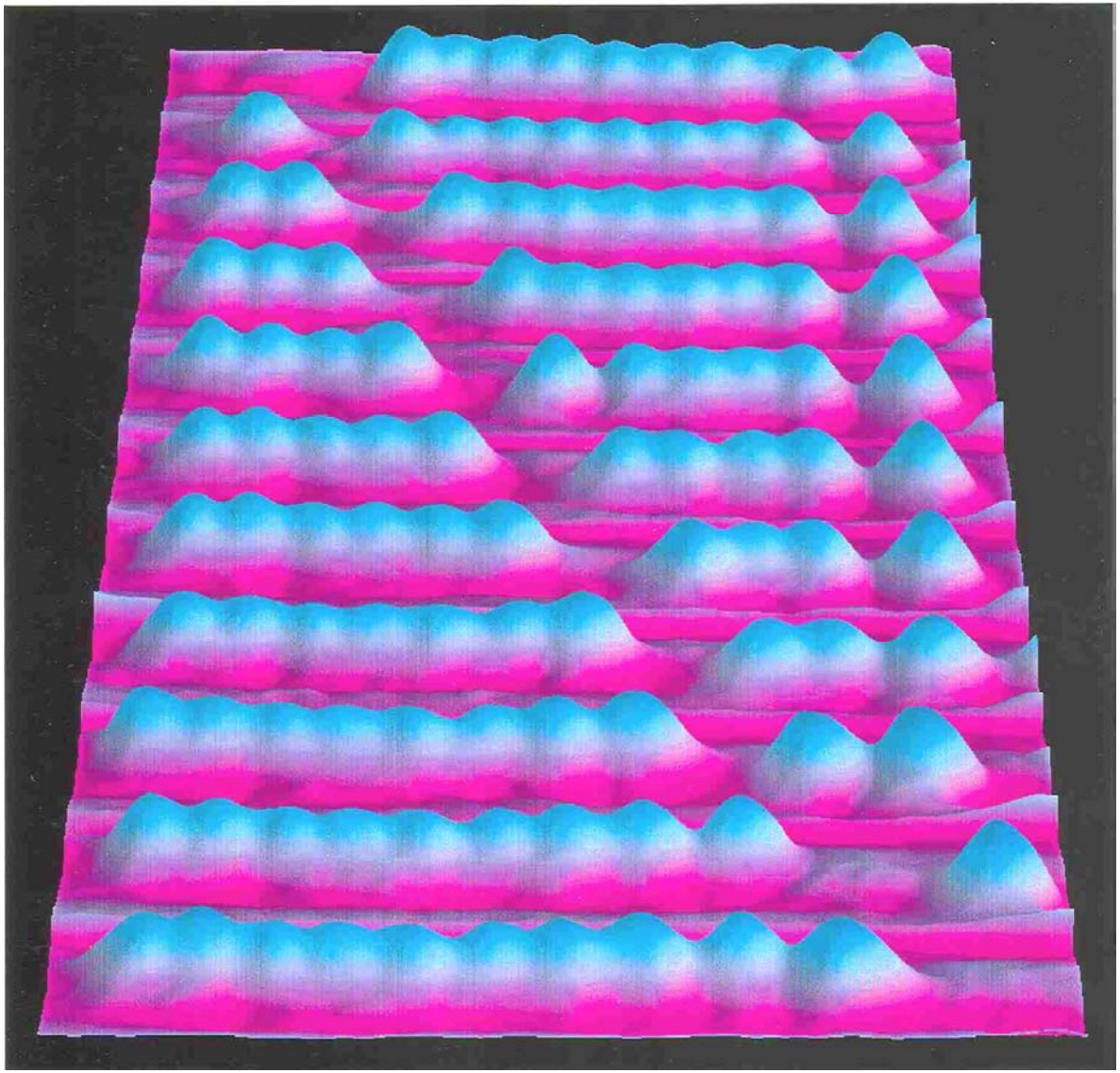

Richard Feynman

Power cost of information transfer?

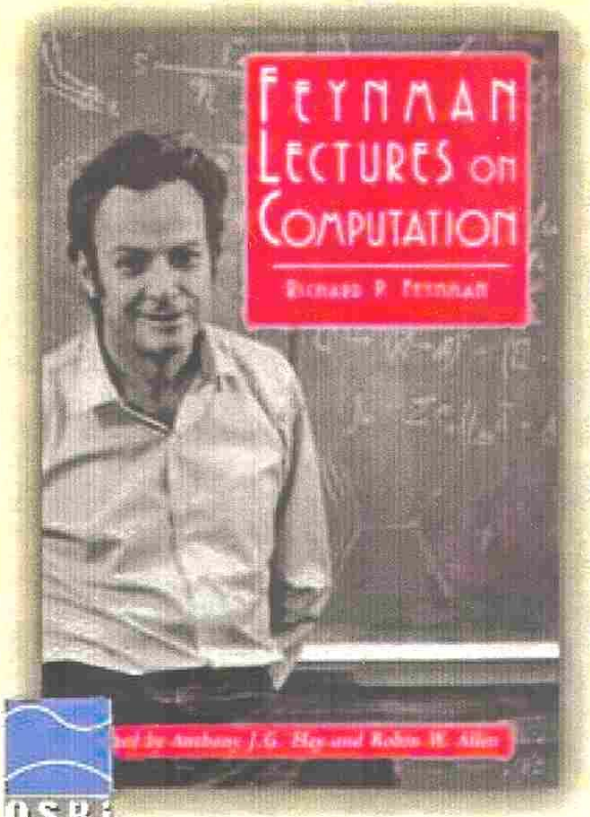

$$P = nk_BT \frac{d}{c} \nu^2$$

- P = power
- k_B = Boltzman constant
- T = temperature
- d = transmission distance
- c = speed of light
- ν = operating frequency
- n = number of parallel operations

QSRi

hp invent

Computational Microscopy

- Simulations of materials properties and processes
- Computational experiments
- Interpret (analysis of observations)
- Unify (sets of observations)
- Predict

Classical Evolution

Molecular dynamics
MD

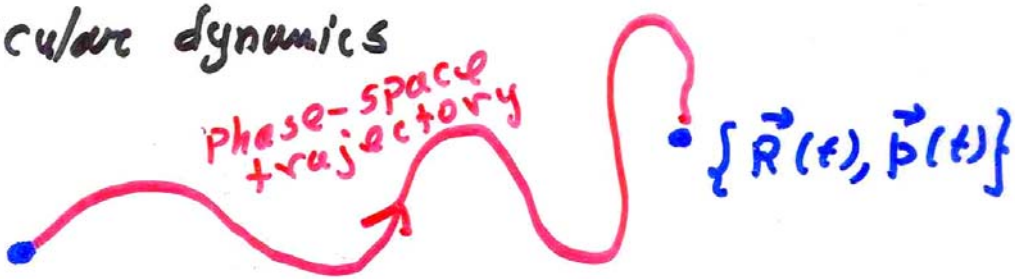

$\{\vec{R}(t_0), \vec{p}(t_0)\}$

↑ phase-space point

$$\{\quad(t)\} = e^{-iL(t-t_0)} \{\quad(t_0)\}$$

$L \Rightarrow$ Liouville operator

Hamiltonian $\mathcal{H}(\vec{R}(t), \vec{p}(t))$; Lagrangian $\mathcal{L}(\vec{R}(t), \dot{\vec{R}}(t))$

$$m_i \vec{a}_i = m_i \frac{d^2\vec{R}_i}{dt^2} = \vec{F}_i = -\vec{\nabla}_{\vec{R}_i} \Phi(\vec{R}_1, \ldots \vec{R}_N)$$

$\vec{F}_i = \sum_{j \neq i} \vec{f}_{ij}$ ex. pair-pot.

Born-Oppenheimer MD

BO-LSD-MD

Barnett, Landman; PRB 48, 2081('93)

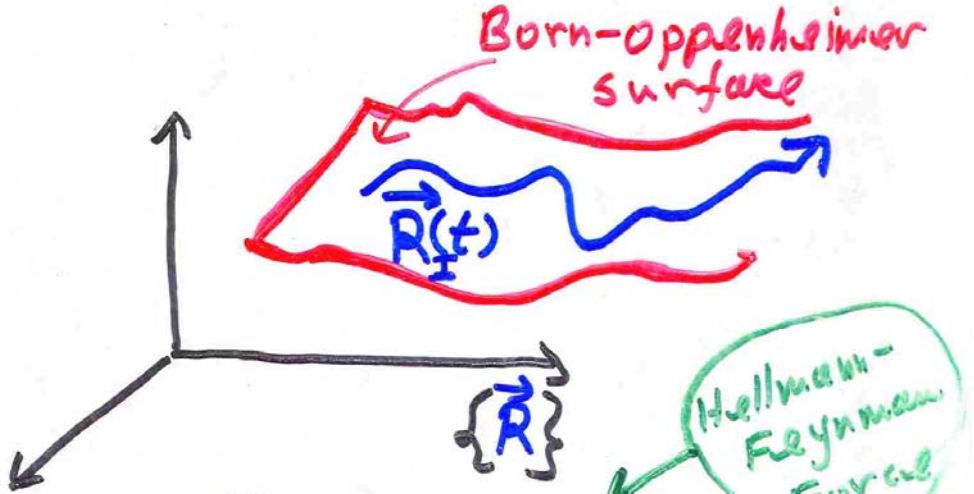

$$M_I \ddot{\vec{R}}_I = F_{el}\{\vec{R}, \vec{r}\} + F_{II}$$

$$-\nabla_{\vec{R}_I} E_{el}\{\vec{R}_I\}$$

Ion-Ion force

DFT: $E_{el}\{\vec{R}_I\} = \min_{\rho} E[\rho]$

Oxidative damage to DNA
Counter ion-assisted addition of water

**Robert N. Barnett, Angelo Bongiorno,
Charles L. Cleveland, Abraham Joy,
Uzi Landman, Gary B. Schuster**

(Science, 2005)

Error-prone replication of oxidatively damaged DNA by a high-fidelity DNA polymerase

Gerald W. Hsu[1], Matthias Ober[2], Thomas Carell[2] & Lorena S. Beese[1]

[1]*Department of Biochemistry, Duke University Medical Center, Durham, North Carolina 27710, USA*
[2]*Department of Chemistry and Biochemistry, Ludwig Maximilians University Munich, Butenandtstrasse 5-13, D 81377 Munich, Germany*

Aerobic respiration generates reactive oxygen species that can damage guanine residues and lead to the production of 8-oxoguanine (8oxoG), the major mutagenic oxidative lesion in the genome[1]. Oxidative damage is implicated in ageing[2] and cancer, and its prevalence presents a constant challenge to DNA polymerases that ensure accurate transmission of genomic information. When these polymerases encounter 8oxoG, they frequently catalyse misincorporation of adenine in preference to accurate incorporation of cytosine[3]. This results in the propagation of G to T transversions, which are commonly observed somatic mutations associated with human cancers[4,5]. Here, we present sequential snapshots of a high-fidelity DNA polymerase during both accurate and mutagenic replication of 8oxoG. Comparison of these crystal structures reveals that 8oxoG induces an inversion of the mismatch recognition mechanisms that normally proofread DNA, such that the 8oxoG·adenine mismatch mimics a cognate base pair whereas the 8oxoG·cytosine base pair behaves as a mismatch. These studies reveal a fundamental mechanism of error-prone replication and show how 8oxoG, and DNA lesions in general, can form mismatches that evade polymerase error-detection mechanisms, potentially leading to the stable incorporation of lethal mutations.

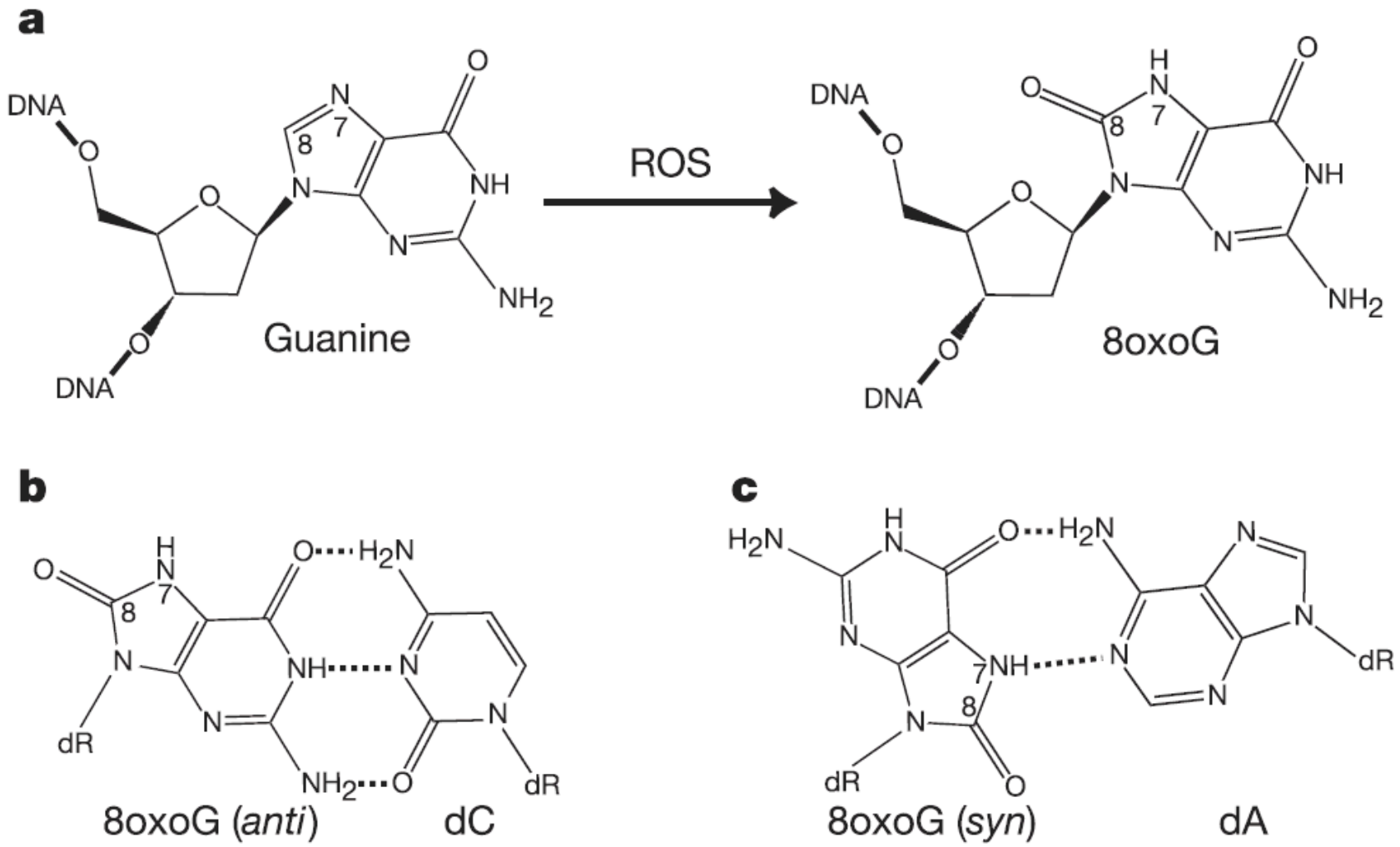

Figure 1 Modes of base pairing for 8oxoG. **a**, Oxidation of guanine at C8 by reactive oxygen species (ROS). **b**, 8oxoG in a Watson–Crick base pair with dC. Dashed lines indicate potential hydrogen bonds. **c**, 8oxoG (*syn*) in a Hoogsteen base pair with dA (*anti*).

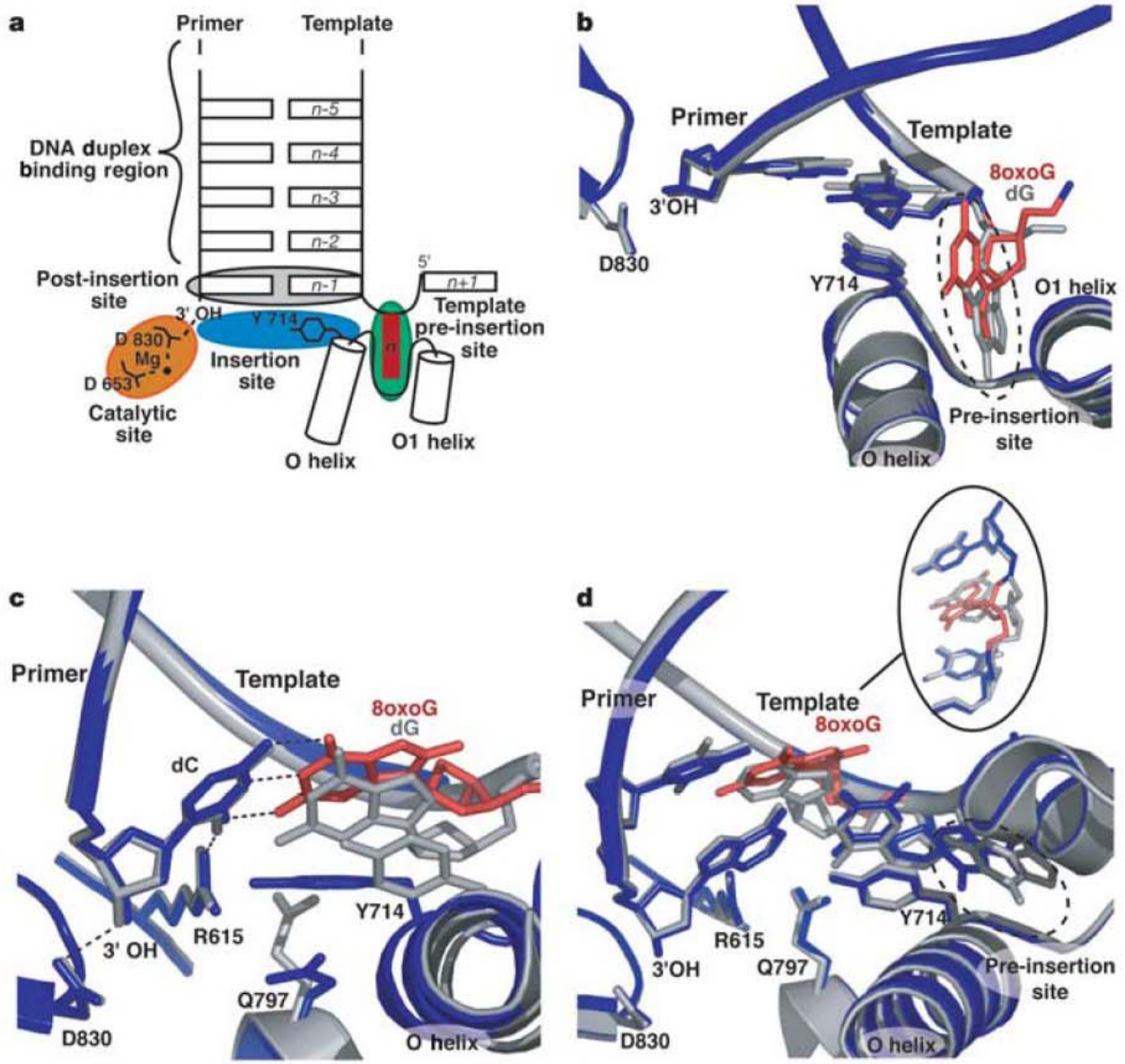

Figure 3 Accurate translesion replication of 8oxoG by BF in crystals. **a**, Schematic of BF active site. During replication, the template base (*n*, red) moves from the pre-insertion site to the post-insertion site to the DNA duplex binding region. **b**–**d**, Structures of accurate 8oxoG replication (blue) are superimposed with structures of unmodified guanine replication (grey). The 8oxoG template base (red) is shown at the pre-insertion site (**b**) before nucleotide incorporation, the post-insertion site (**c**) after dCTP incorporation, and the DNA duplex binding region (**d**) after extension of C·8oxoG.

Charge migration in DNA:

ion-gated transport

R.N. Barnett, C.L. Cleveland. A. Joy, Uzi Landman,

G.B. Schuster, Science *294*, 567 (2001)

School of Physics
Georgia Institute of Technology
Atlanta, Georgia USA

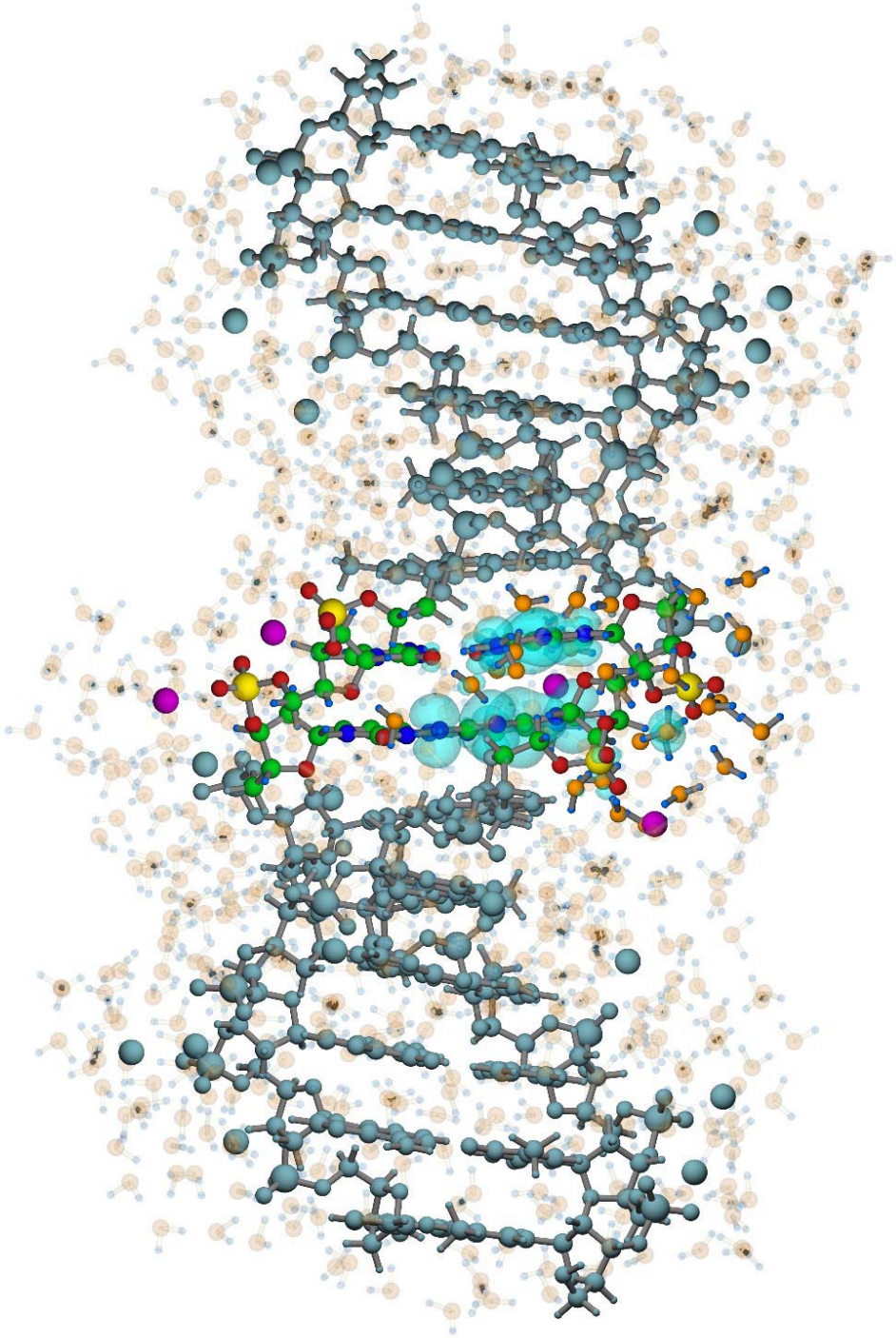

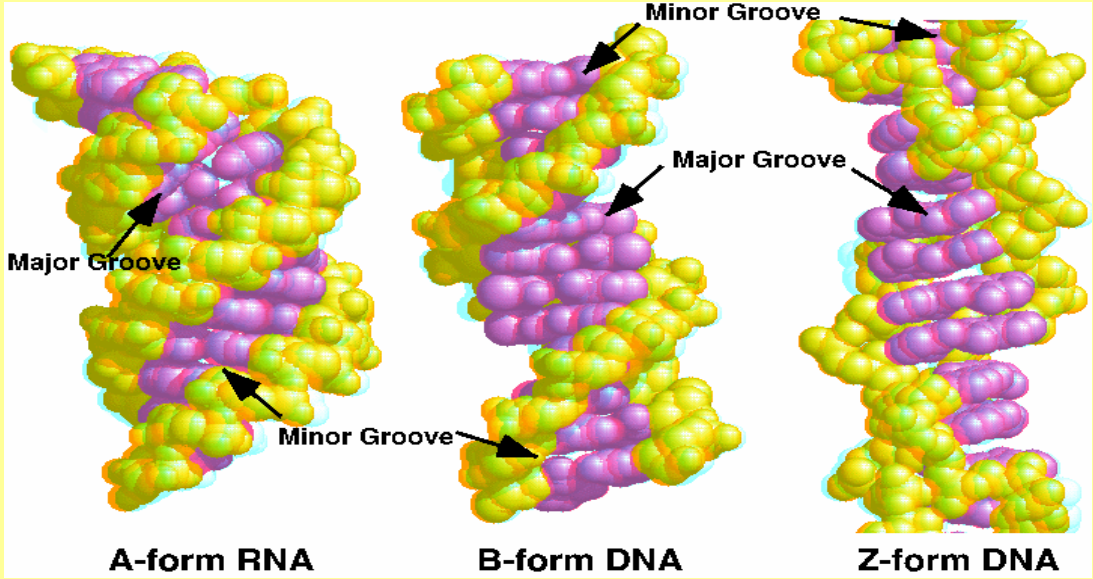

- **DNA: Vehicle for inheritance in cellular life.**
  - **Oxidative reactions damage DNA.**
  - **Un-repaired damage can cause mutations.**
- **DNA: Applications in nanotechnology.**
  - **One dimensional conductor.**
  - **Molecular machines.**
- **DNA: A unique medium for chemical study.**
  - **Self-organizing properties.**
  - **Well-defined global structure.**
  - **Synthetic and analytical methods.**

B-Form DNA

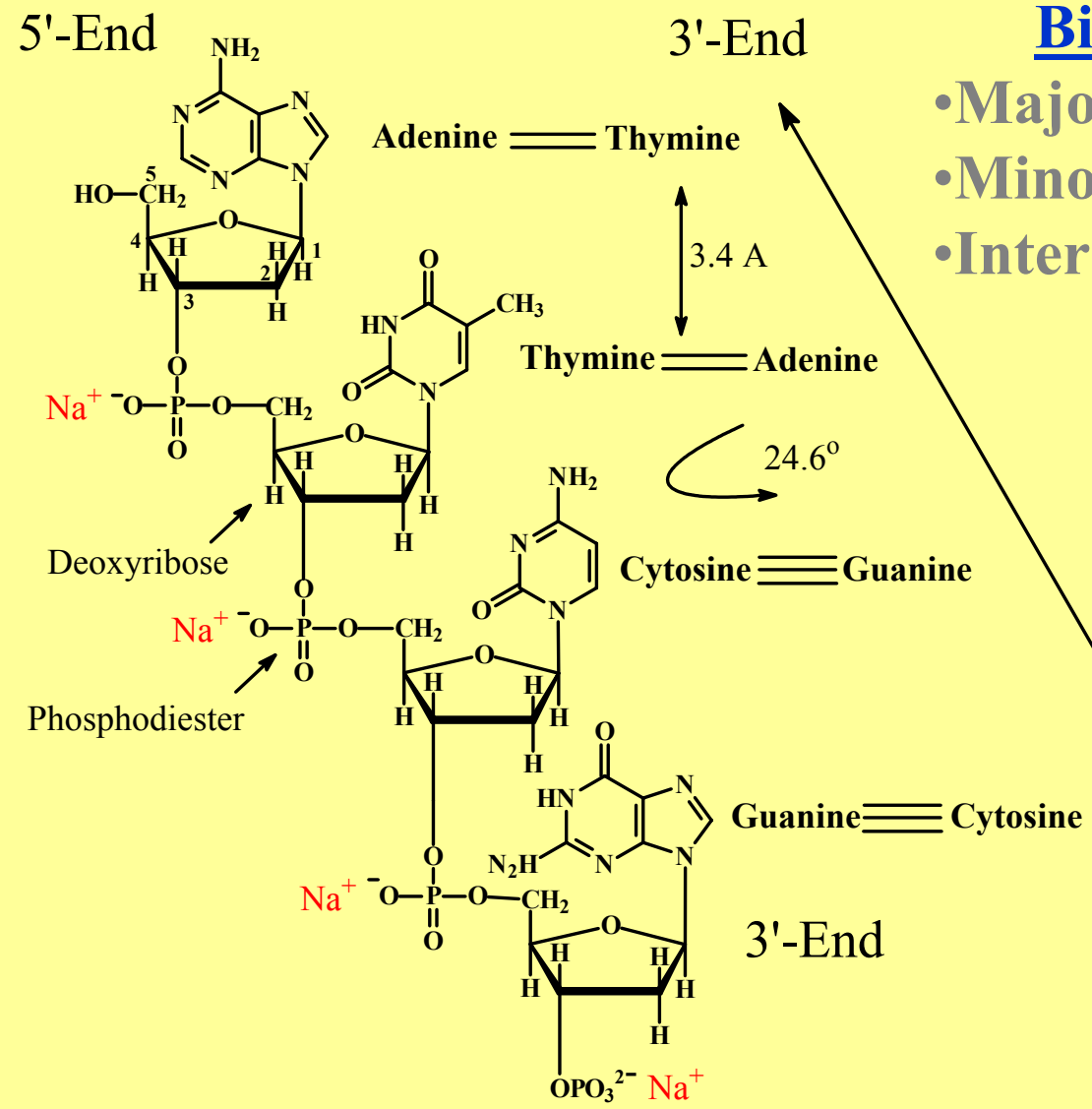

Binding

- Major Groove
- Minor Groove
- Intercalation

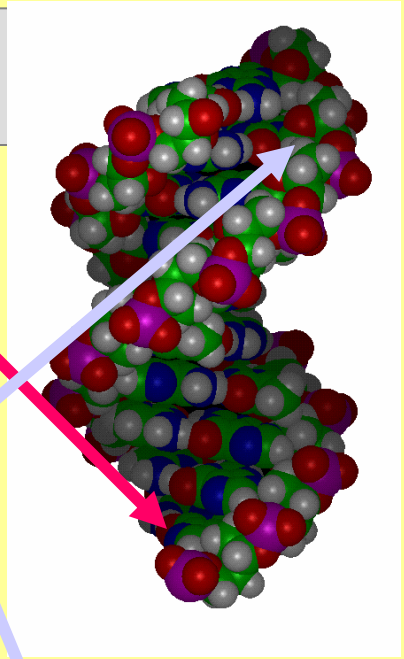

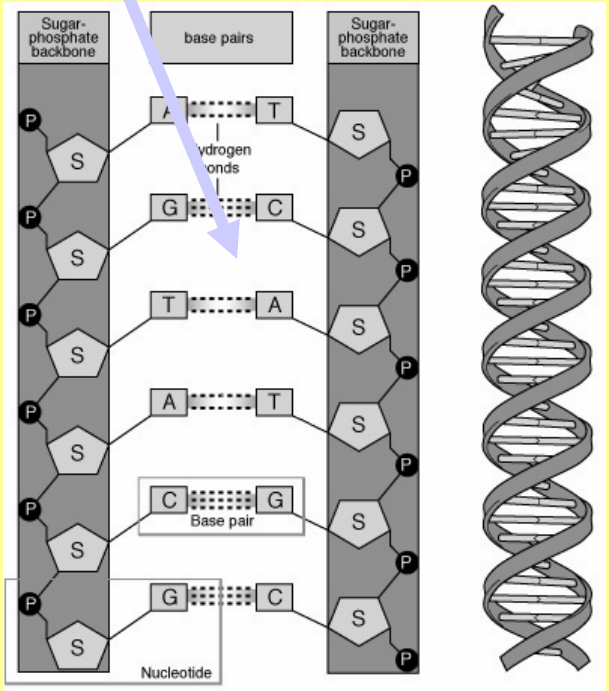

DNA Dynamics

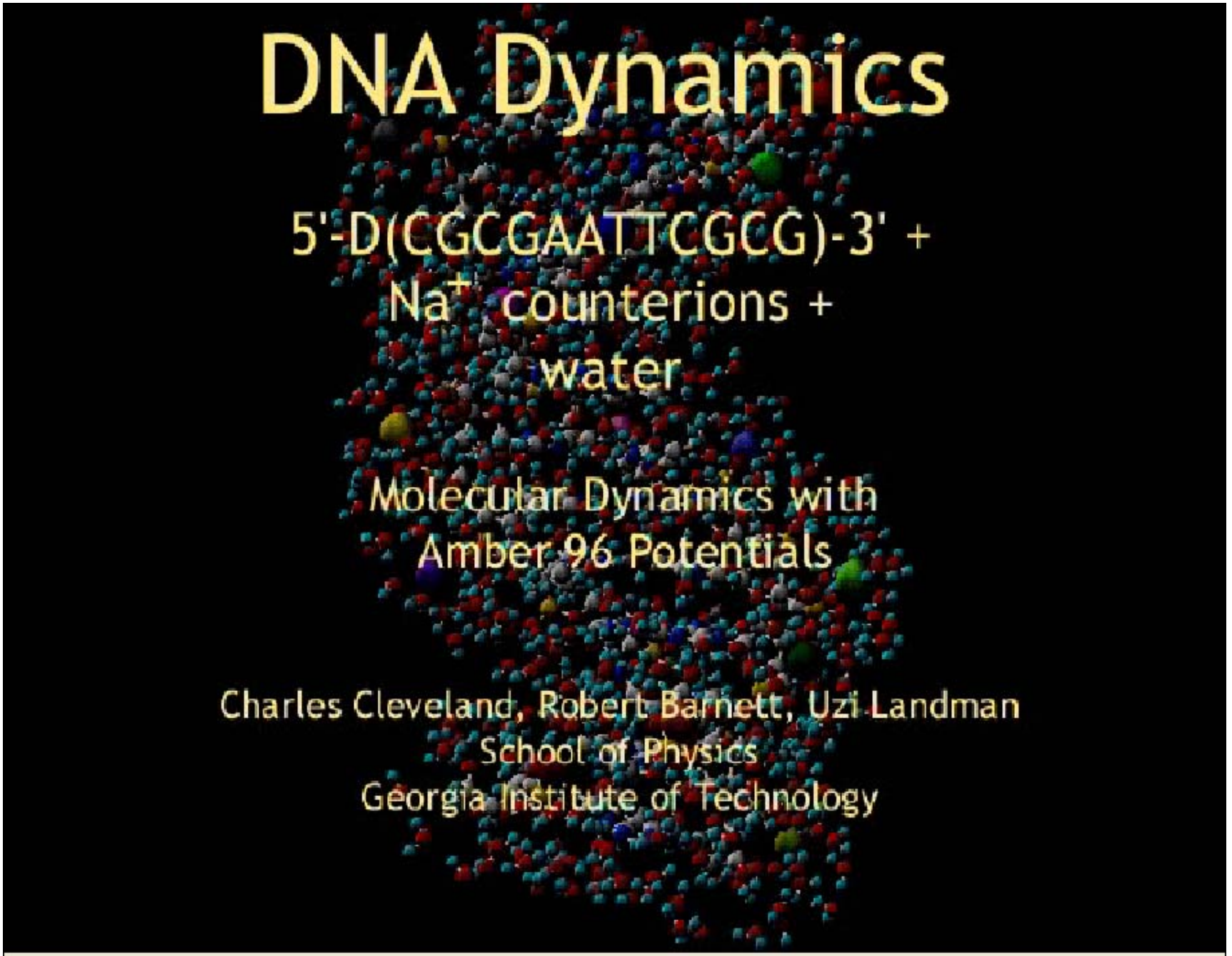

5'-D(CGCGAATTCGCG)-3' +
Na^+ counterions +
water

Molecular Dynamics with
Amber 96 Potentials

Charles Cleveland, Robert Barnett, Uzi Landman
School of Physics
Georgia Institute of Technology

Oxidative damage to DNA
Counter ion-assisted addition of water

**Robert N. Barnett, Angelo Bongiorno,
Charles L. Cleveland, Abraham Joy,
Uzi Landman, Gary B. Schuster**

(Science, 2005)

Error-prone replication of oxidatively damaged DNA by a high-fidelity DNA polymerase

Gerald W. Hsu[1], Matthias Ober[2], Thomas Carell[2] & Lorena S. Beese[1]

[1]*Department of Biochemistry, Duke University Medical Center, Durham, North Carolina 27710, USA*
[2]*Department of Chemistry and Biochemistry, Ludwig Maximilians University Munich, Butenandtstrasse 5-13, D 81377 Munich, Germany*

Aerobic respiration generates reactive oxygen species that can damage guanine residues and lead to the production of 8-oxoguanine (8oxoG), the major mutagenic oxidative lesion in the genome[1]. Oxidative damage is implicated in ageing[2] and cancer, and its prevalence presents a constant challenge to DNA polymerases that ensure accurate transmission of genomic information. When these polymerases encounter 8oxoG, they frequently catalyse misincorporation of adenine in preference to accurate incorporation of cytosine[3]. This results in the propagation of G to T transversions, which are commonly observed somatic mutations associated with human cancers[4,5]. Here, we present sequential snapshots of a high-fidelity DNA polymerase during both accurate and mutagenic replication of 8oxoG. Comparison of these crystal structures reveals that 8oxoG induces an inversion of the mismatch recognition mechanisms that normally proofread DNA, such that the 8oxoG·adenine mismatch mimics a cognate base pair whereas the 8oxoG·cytosine base pair behaves as a mismatch. These studies reveal a fundamental mechanism of error-prone replication and show how 8oxoG, and DNA lesions in general, can form mismatches that evade polymerase error-detection mechanisms, potentially leading to the stable incorporation of lethal mutations.

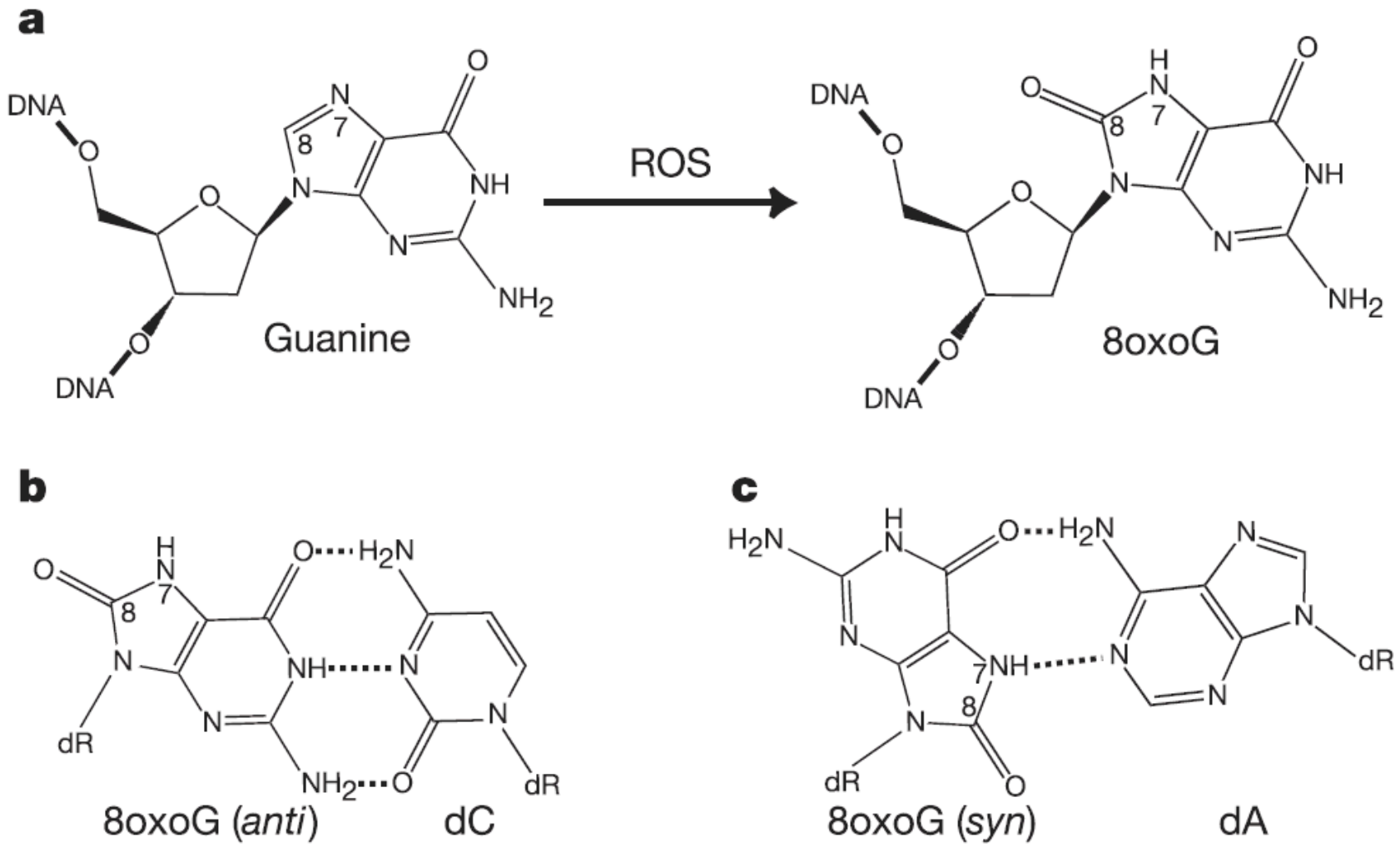

Figure 1 Modes of base pairing for 8oxoG. **a**, Oxidation of guanine at C8 by reactive oxygen species (ROS). **b**, 8oxoG in a Watson–Crick base pair with dC. Dashed lines indicate potential hydrogen bonds. **c**, 8oxoG (*syn*) in a Hoogsteen base pair with dA (*anti*).

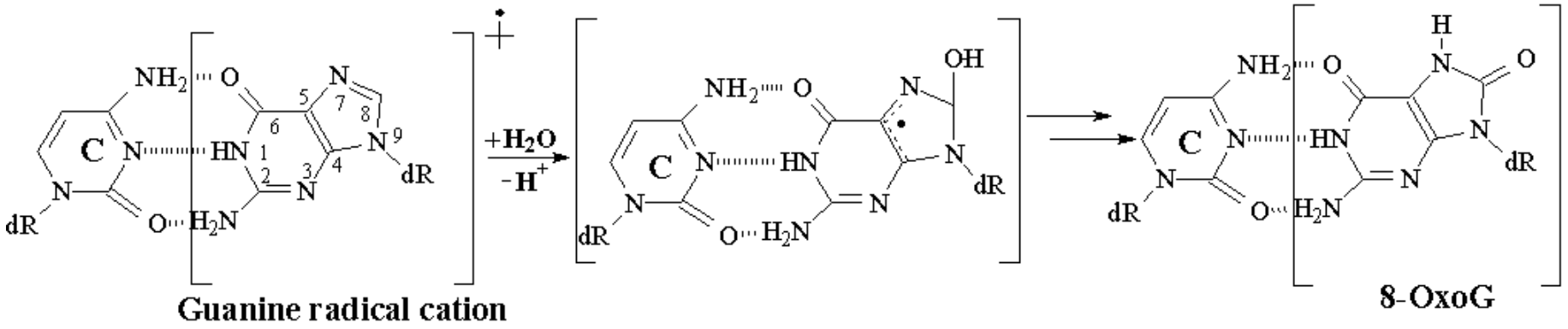
+H2O
-H+
Guanine radical cation
8-OxoG

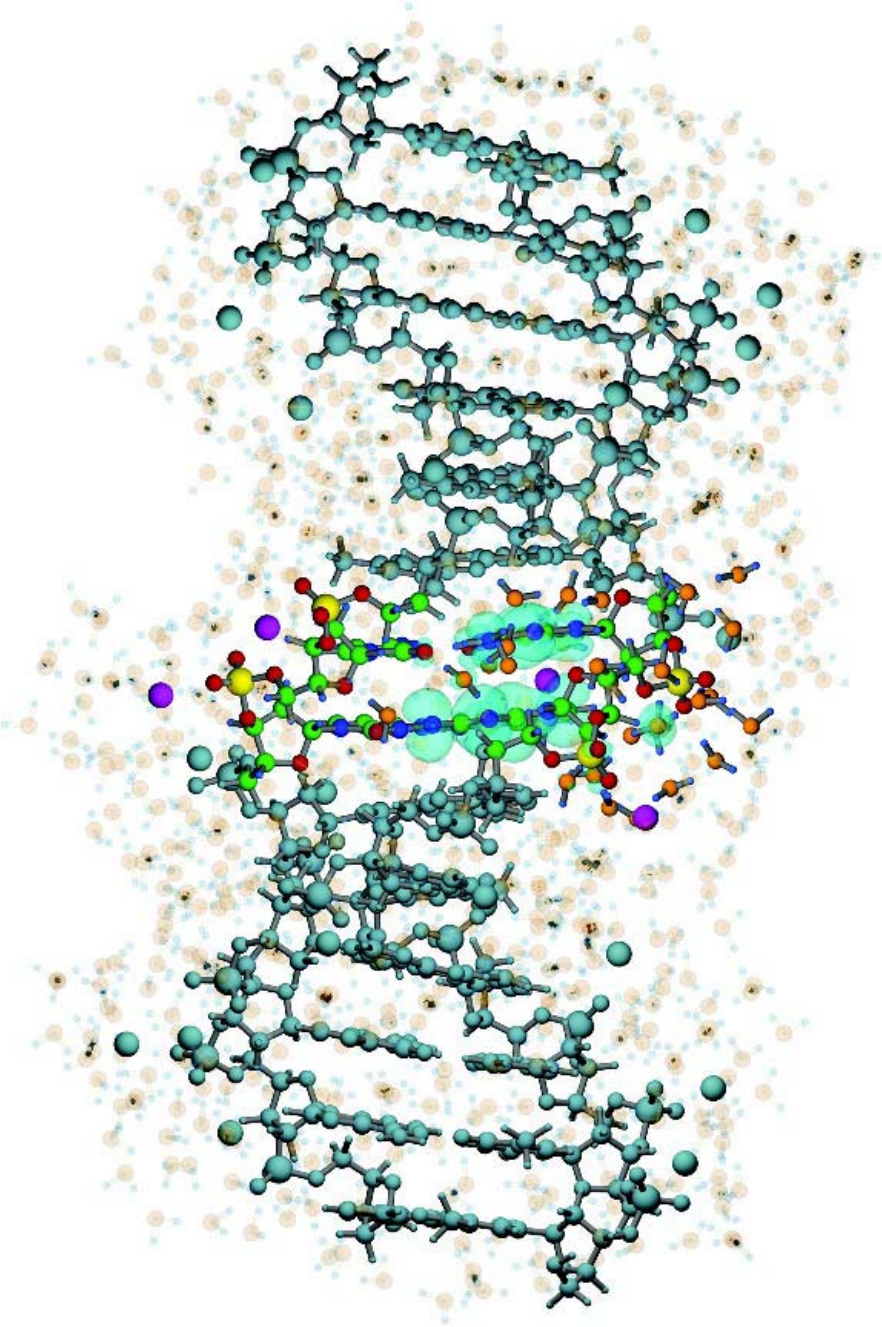

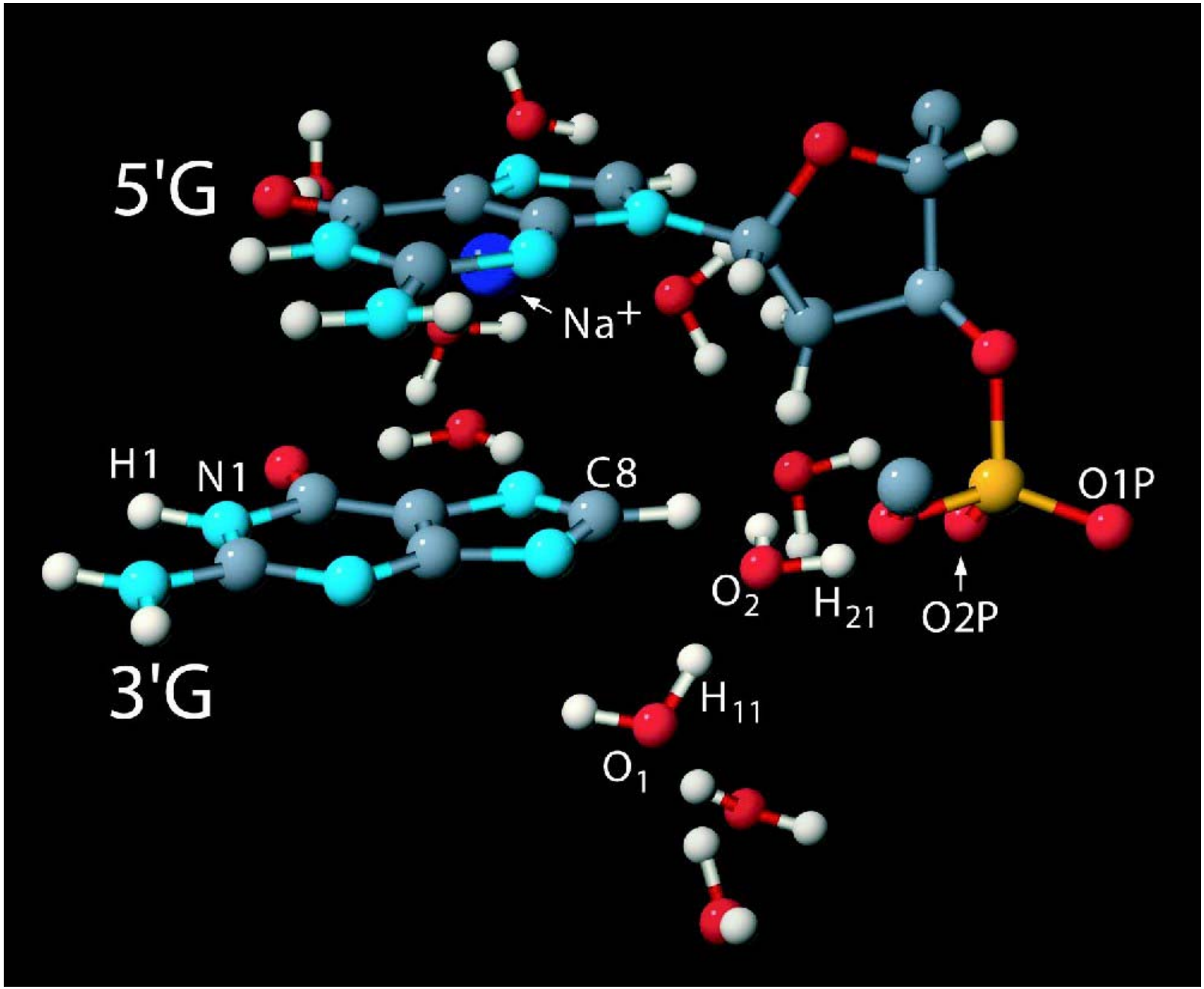
5'G
Na+
H1
N1
C8
O1P
O2
H21
O2P
3'G
H11
O1

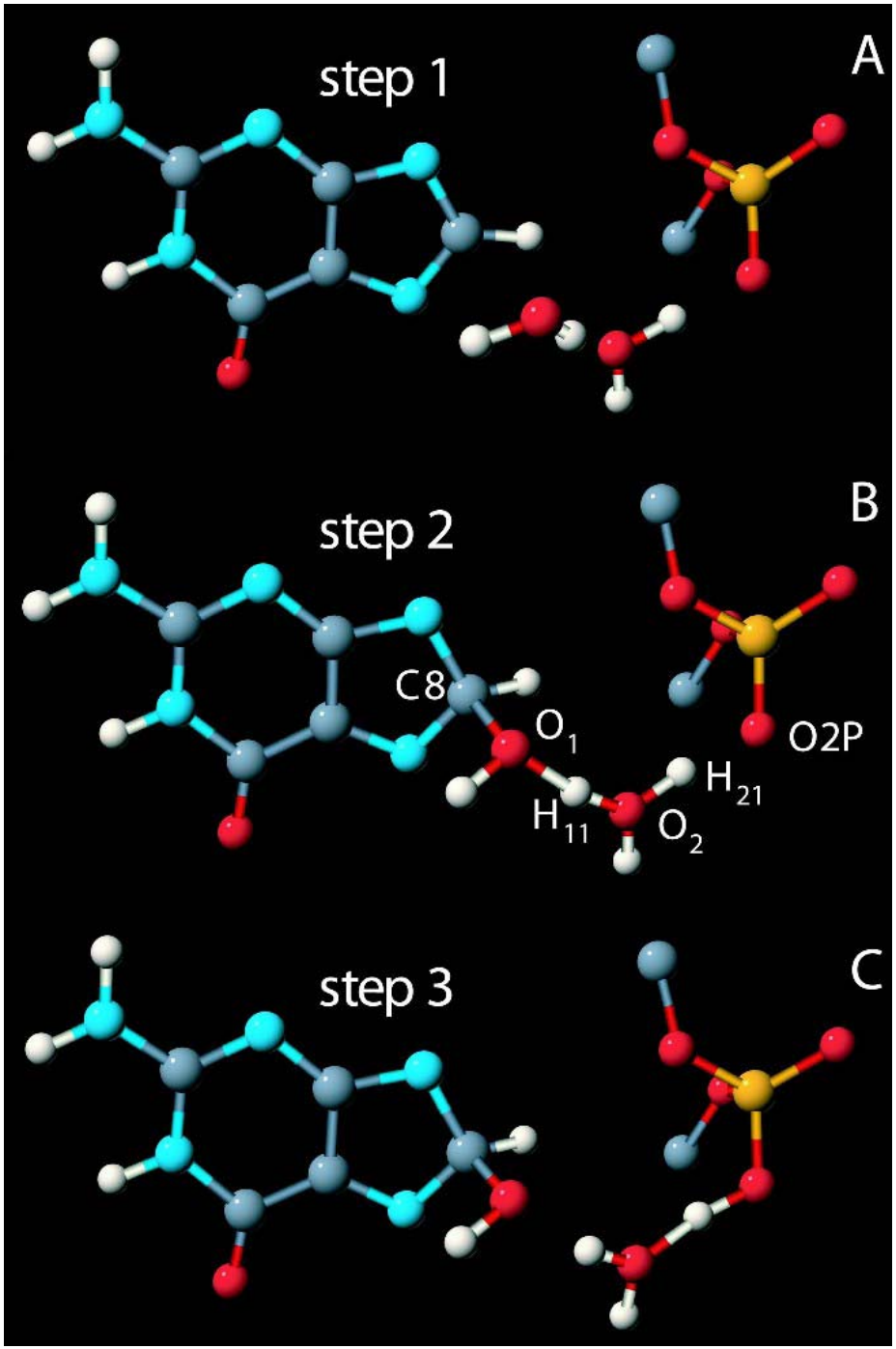
step 1
A
step 2
B
C8
O1
O2P
H21
H11
O2
step 3
C

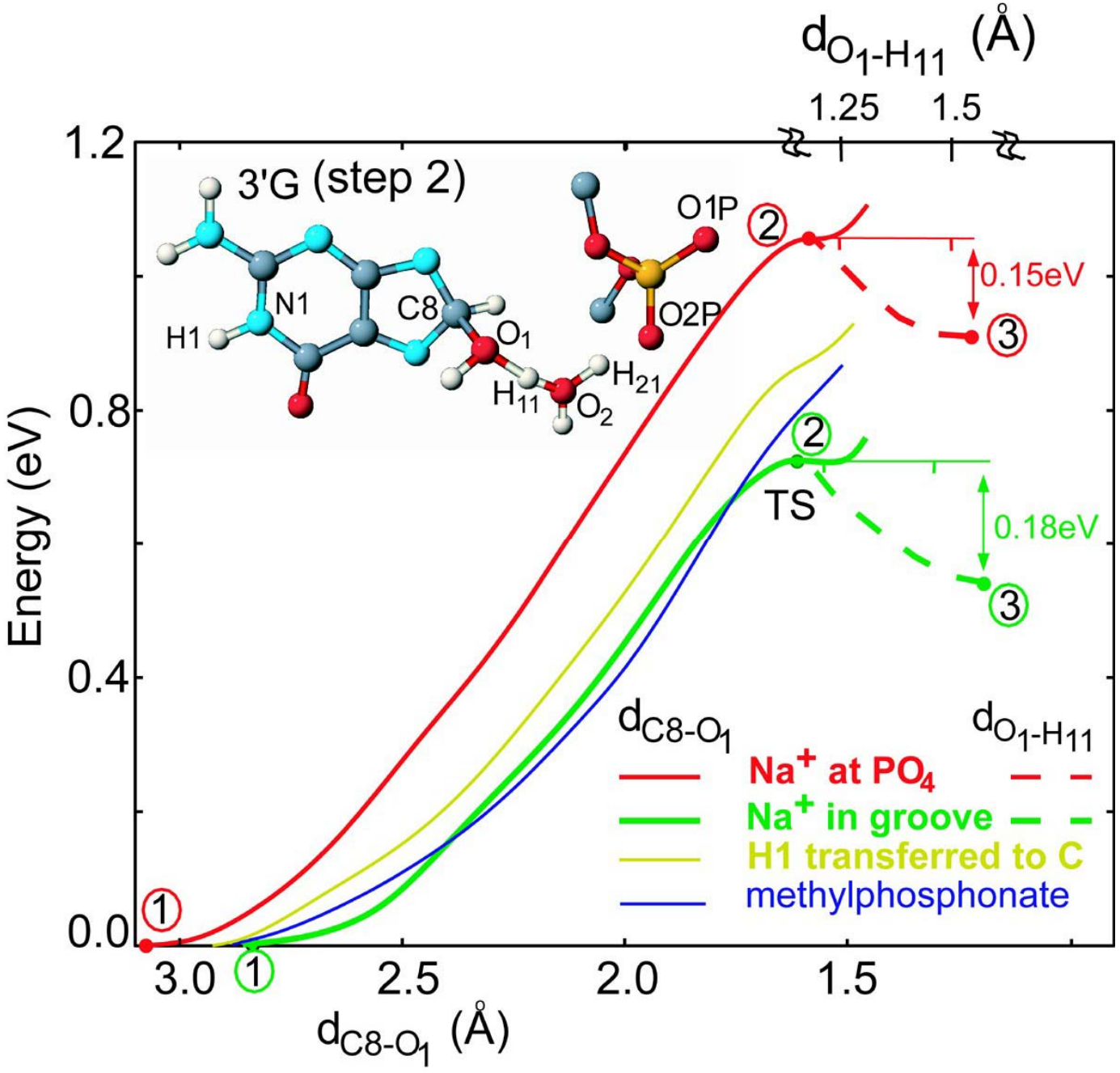
$d_{O_1-H_{11}}$ (Å)
1.25
1.5
1.2
0.8
0.4
0.0
Energy (eV)
3'G (step 2)
N1
H1
C8
O_1
H_{11}
O_2
H_{21}
O1P
O2P
2
3
0.15eV
TS
0.18eV
1
3.0
2.5
2.0
1.5
d_{C8-O_1} (Å)
d_{C8-O_1}
$d_{O_1-H_{11}}$
Na^+ at PO_4
Na^+ in groove
H1 transferred to C
methylphosphonate

AQ-DNA

d

5'-AQ A A G G_1 A A G G_2 A A G G_3 A A G G_4 A A G G_5 A T A T -3'

3'- T T C C T T C C T T C C T T C C T T C C T A T A -5'

a *b* *c*

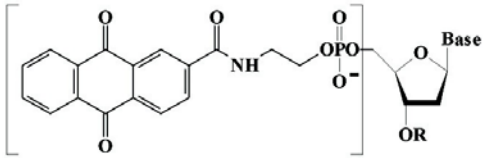

Anthraquinone– Linked DNA

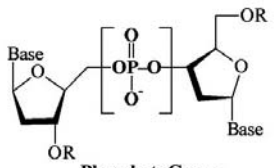

Phosphate Group

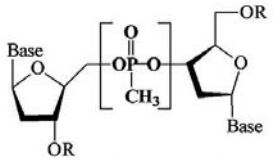

Methylphosphonate Group

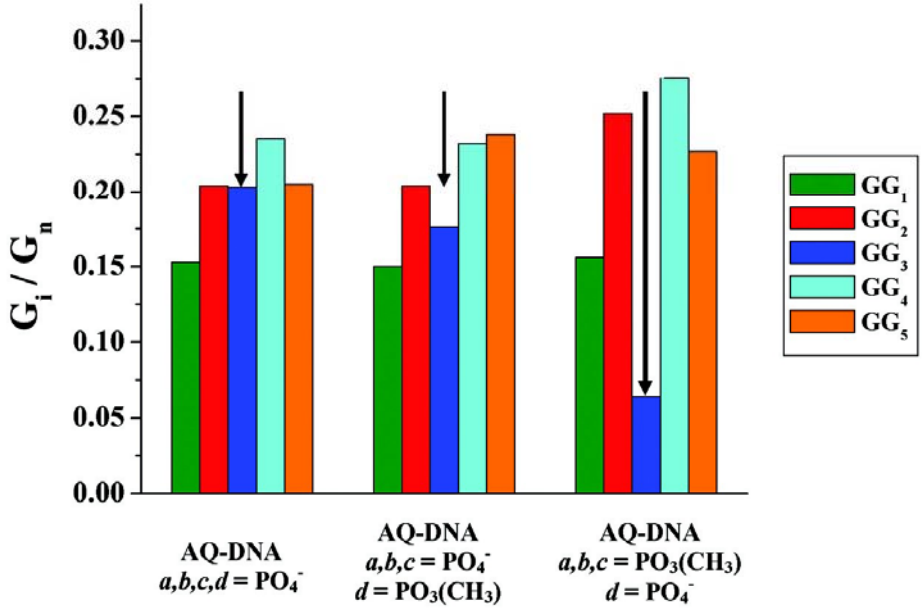

Nano-Scale Matter

Principles

- **Self-assembly** ("irrational" synthesis)
- **Self-selection**
  abundance, size (magic numbers), **shape**!!
- **Fluctuations**
- **Spontaneous Symmetry Breaking**

Emergent Phenomena

Phenomena which are not the properties of the individual elementary components BUT of the assembly of such components

⇨ Often accompanied by (Spontaneous Symmetry Breaking) Phenomena which are not evident (and are not part of) the formulation of the problem

Example:

$$H = \sum_{i} H(i) + \sum_{i,j} V(i,j) + \sum_{i,j,k} V(i,j,k)$$

Emergent Phenomena

The movement from low-level rules to higher-level sophistication

When agents residing on one scale start producing behavior that lies on a higher scale

Higher-level, large-scale, pattern arising out of local interactions between individual components

Ants → Colonies ; Urbanites → Cities
Atoms → Crystals ; Electrons → Wigner Crystallites

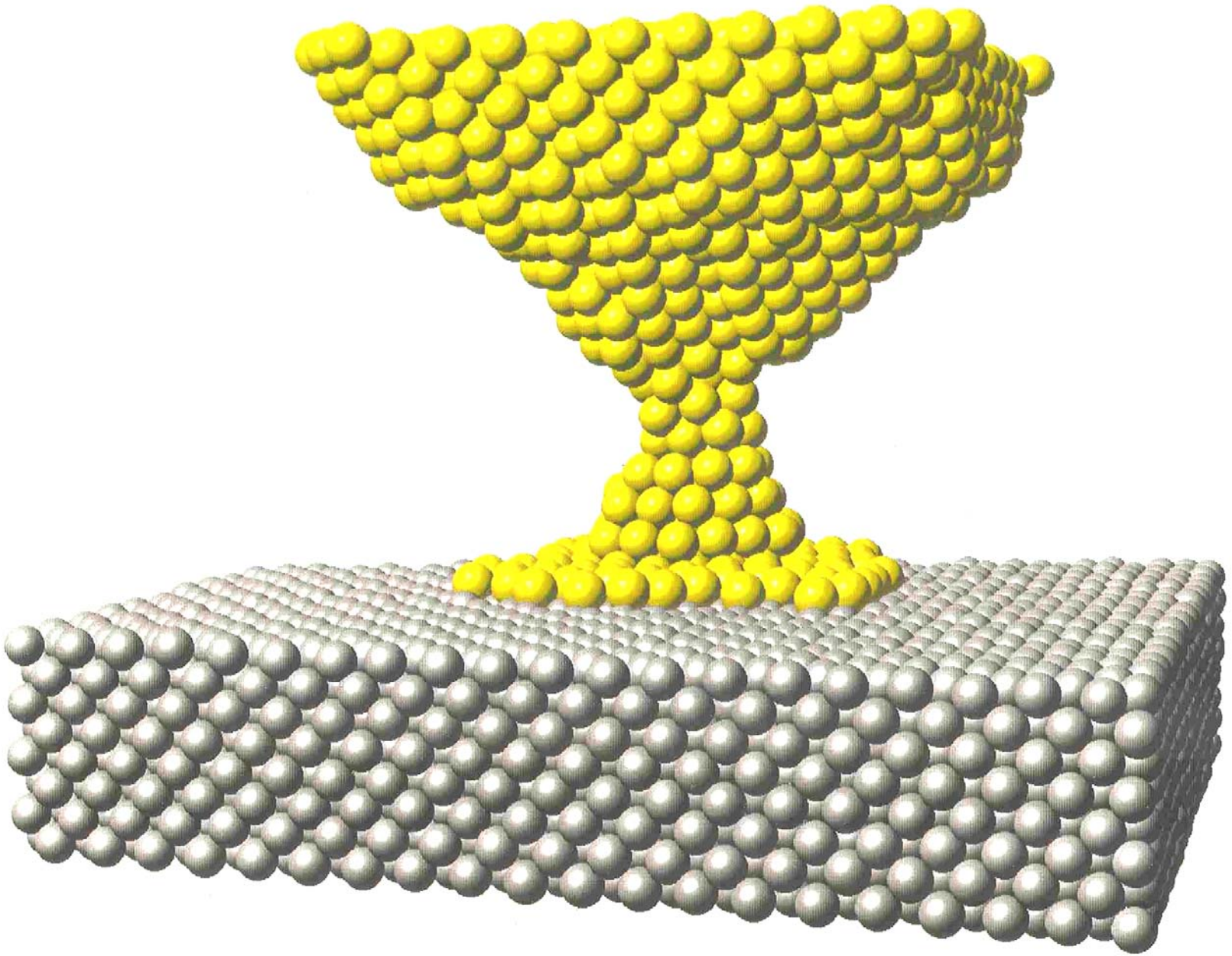

Luedtke + Landman JVST (1991); Science 248, 454 (1990)

SCIENCE Vol. 248, 454 (1990)

Atomistic Mechanisms and Dynamics of Adhesion, Nanoindentation, and Fracture

UZI LANDMAN, W. D. LUEDTKE, NANCY A. BURNHAM, RICHARD J. COLTON

Molecular dynamics simulations and atomic force microscopy are used to investigate the atomistic mechanisms of adhesion, contact formation, nanoindentation, separation, and fracture that occur when a nickel tip interacts with a gold surface. The theoretically predicted and experimentally measured hysteresis in the force versus tip-to-sample distance relationship, found upon approach and subsequent separation of the tip from the sample, is related to inelastic deformation of the sample surface characterized by adhesion of gold atoms to the nickel tip and formation of a connective neck of atoms. At small tip-sample distances, mechanical instability causes the tip and surface to jump-to-contact, which in turn leads to adhesion-induced wetting of the nickel tip by gold atoms. Subsequent indentation of the substrate results in the onset of plastic deformation of the gold surface. The atomic-scale mechanisms underlying the formation and elongation of a connective neck, which forms upon separation, consist of structural transformations involving elastic and yielding stages.

UNDERSTANDING THE ATOMISTIC MECHANISMS, ENERGETICS, and dynamics underlying the interactions and physical processes that occur when two materials are brought together (or separated) is fundamentally important to basic and applied problems such as adhesion (*1–7*), contact formation (*3–16*), surface deformations (*7, 16, 17–24*), materials elastic and plastic response characteristics (*17–24*), materials hardness (*25–27*), microindentation (*6, 10, 26–29*), friction and wear (*16, 19, 30–32*), and fracture (*33–34*). These considerations have motivated for over a century (*1, 3, 17–20*) extensive theoretical and experimental research endeavors of the above phenomena and their technological consequences. Most theoretical approaches to these problems, with a few exceptions (*7, 14–16*), have been anchored in continuum elasticity and contact mechanics (*17–25*). Similarly, until quite recently (*35–38*) experimental observations and measurements of surface forces and the consequent materials response to such interactions have been macroscopic in nature.

The everlasting quest to understand and observe natural phenomena on refined microscopic scales has led to the development of conceptual and technological devices allowing the interrogation of materials with increasing resolution. On the experimental front the developments of the surface force apparatus (SFA) (*36*), of scanning tunneling microscopy (STM) (*37*), and of the related atomic force microscopy (AFM) (*35*) broaden our perspectives and abilities to probe the morphology, electronic structure, and nature of interatomic forces in materials, as well as enhance our ability to manipulate materials on the atomic scale (*38*).

On the theoretical front, recent advances in the formulation and evaluation of the energetics and interatomic interactions in materials (*7, 39*), coupled with the development and implementation of computational methods and simulation techniques (*7, 40*), open new avenues for investigations of the microscopic origins of complex materials phenomena. In particular large-scale molecular dynamics computer simulations, which are in a sense computer experiments, where the evolution of a system of interacting particles is simulated with high spatial and temporal resolution by means of direct integration of the particles' equations of motion, have greatly enhanced our understanding of a broad range of materials phenomena.

Although our knowledge of interfacial processes occurring when two material bodies are brought together has significantly progressed since the original presentation by Heinrich Hertz before the Berlin Physical Society in January 1881 of his theory of the contact of elastic bodies (*17*), full microscopic understanding of these processes is still lacking. Moreover, it has been recognized that continuum mechanics is not fully applicable as the scale of the material bodies and the characteristic dimension of the contact between them are reduced (*24, 41*). Furthermore, it had been observed (*19, 27*) that the mechanical properties of materials exhibit a strong dependence on the size of the sample (small specimens appear to be stronger than larger ones). Since the junctions between contacting solids can be small, their mechanical properties may be drastically different from those of the same materials in their bulk form. Consequently, the application of the newly developed theoretical and experimental techniques to these problems promises to provide significant insights concerning the microscopic mechanisms and the role of surface forces in the formation of microcontacts and to enhance our understanding of fundamental issues pertaining to interfacial adherence, microindentation, structural deformations, and the transition from elastic to elastoplastic or fully developed plastic response of materials. Additionally, studies such as those described in this paper allow critical assessment of the range of validity of continuum-based theories of these phenomena and could inspire improved analytical formulations. Finally, knowledge of the interactions and atomic-scale processes occurring between small tips and materials surfaces, and their consequences, is of crucial importance to optimize, control, interpret, and design experiments employing the novel tip-based microscopies (*6, 7, 13, 14, 16, 32, 35–38, 42–47*).

U. Landman and W. D. Luedtke are in the School of Physics, Georgia Institute of Technology, Atlanta, GA 30332. N. A. Burnham and R. J. Colton are in the Surface Chemistry Branch, Code 6177, Naval Research Laboratory, Washington, DC 20375–5000.

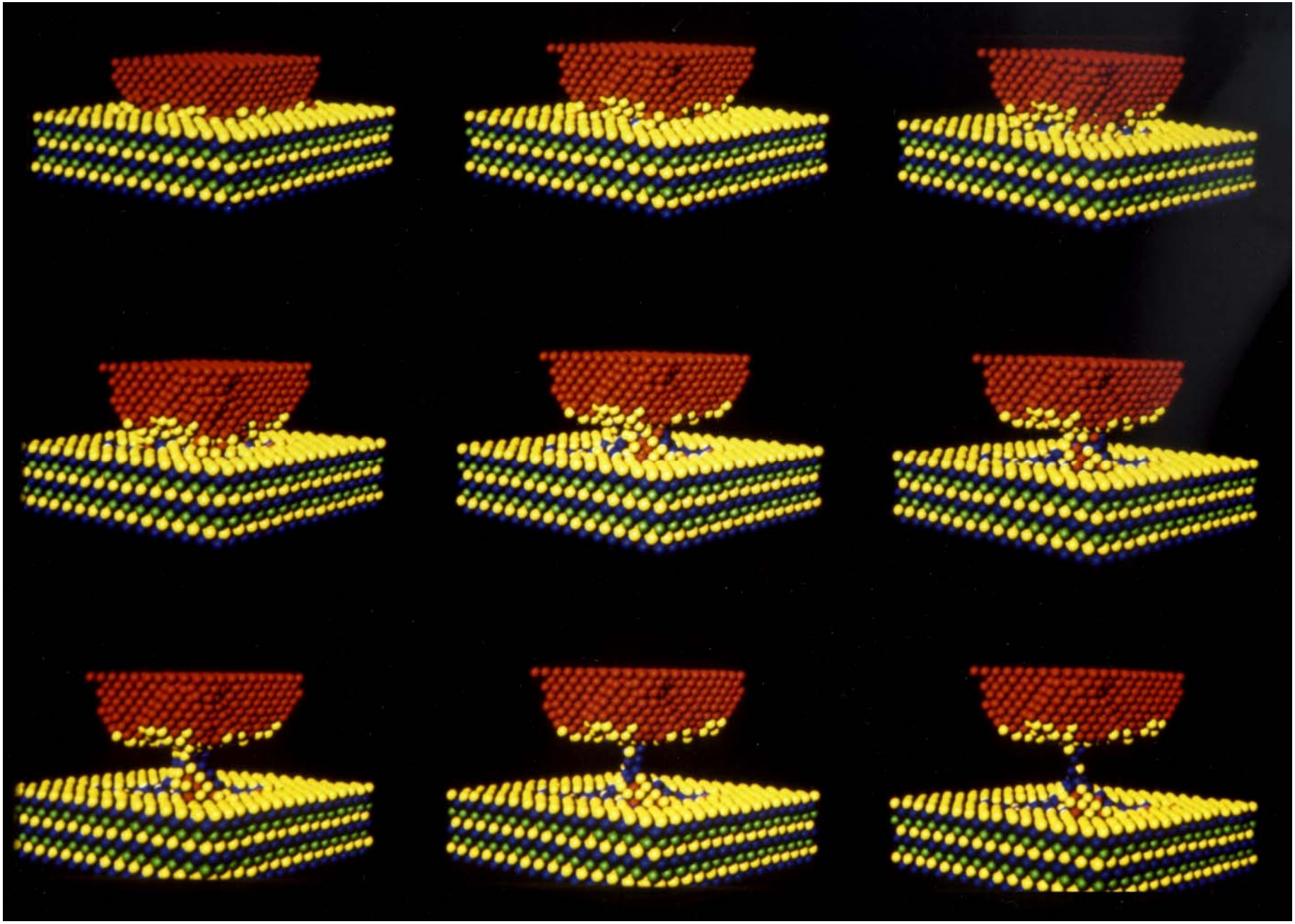

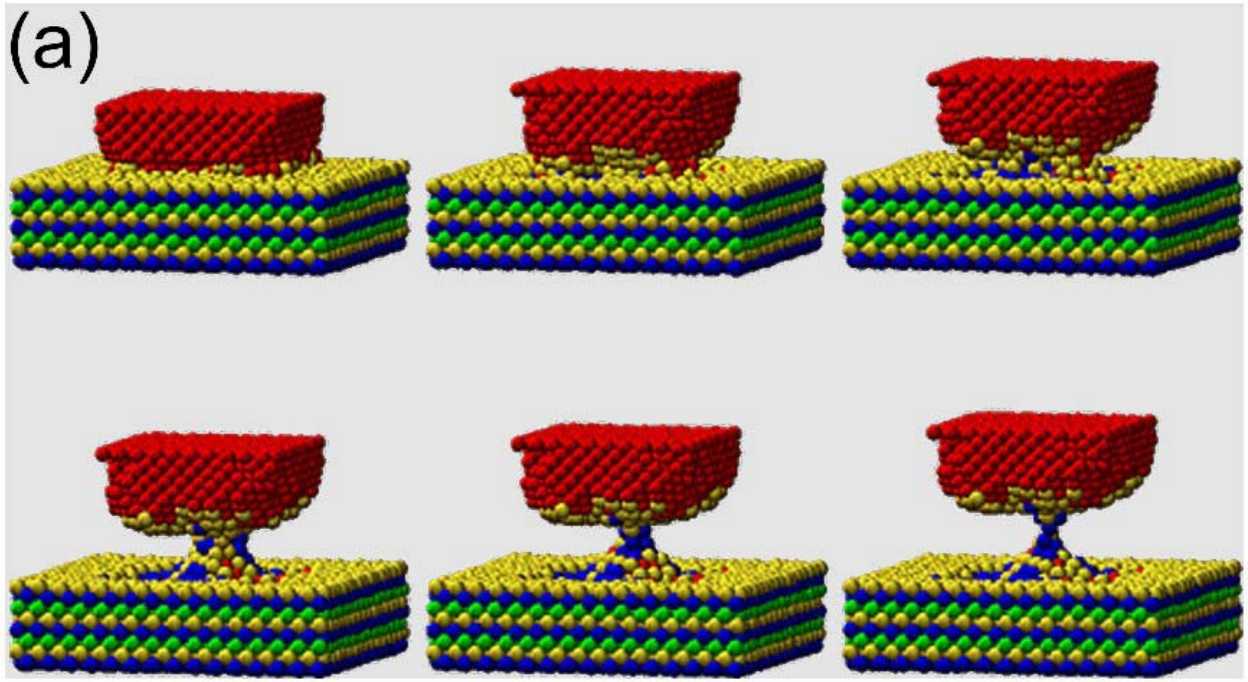
(a)

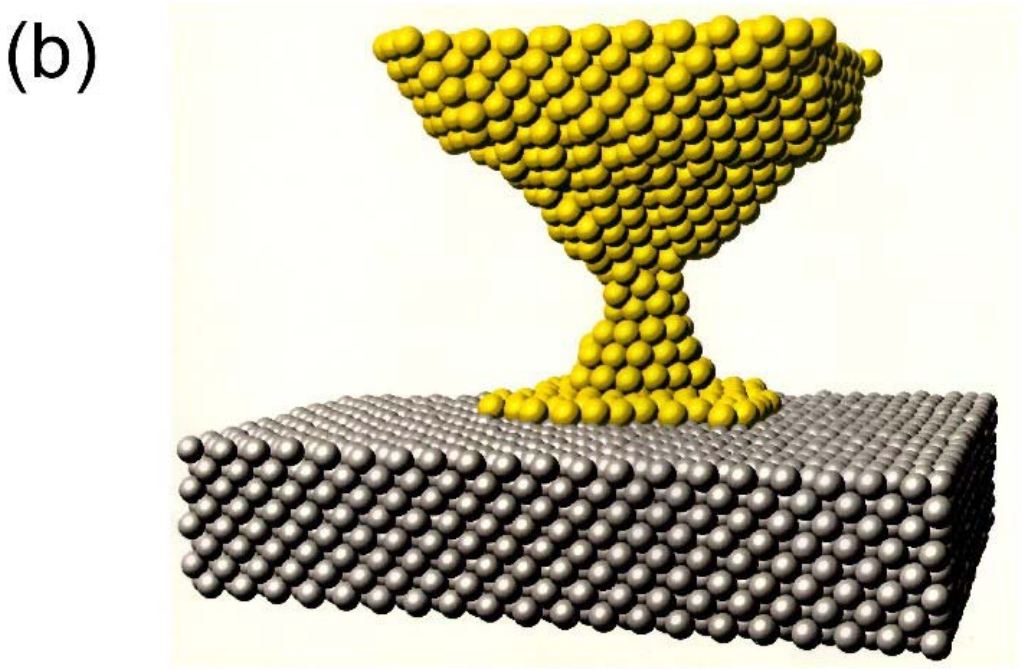
(b)

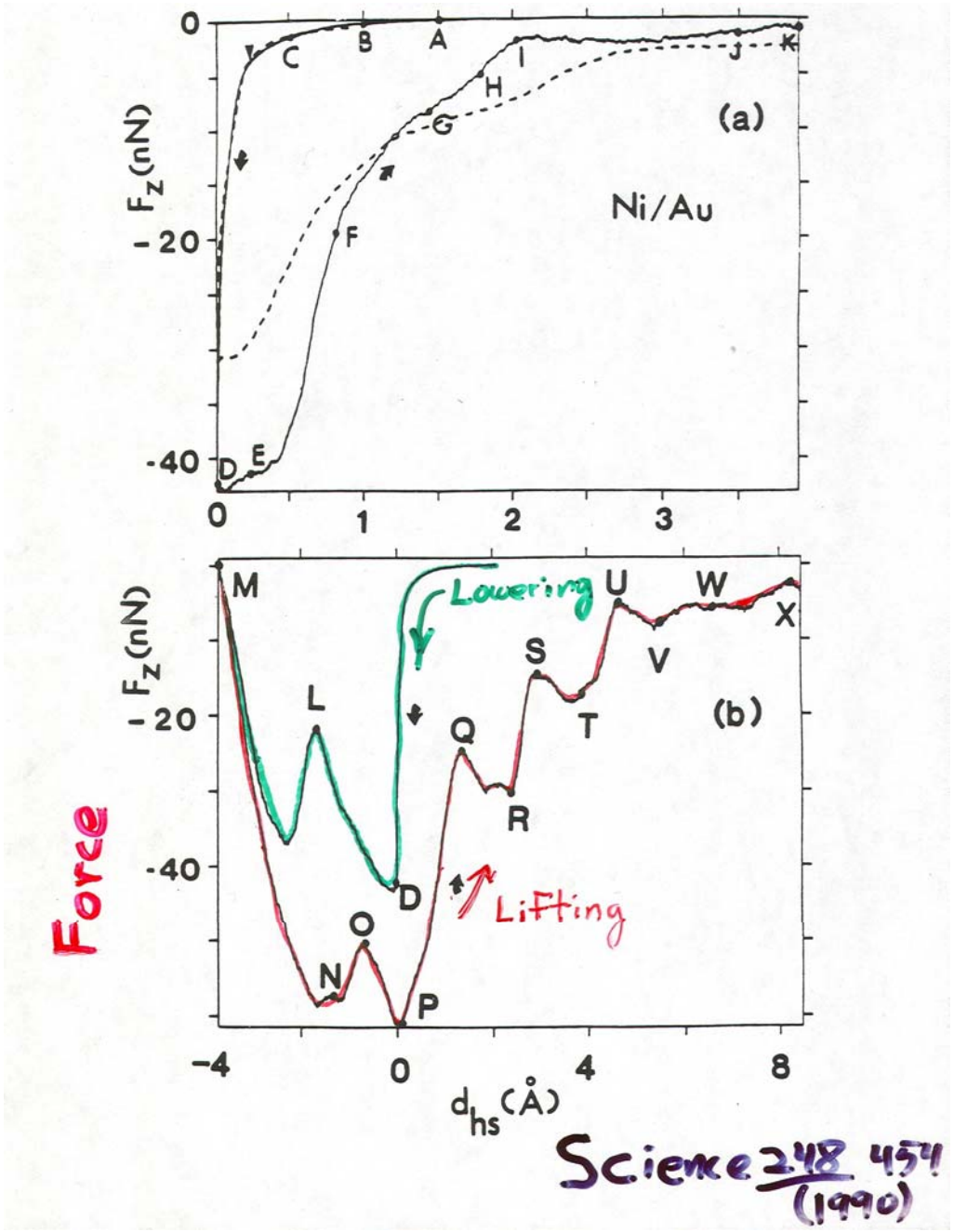

Science 248 454 (1990)

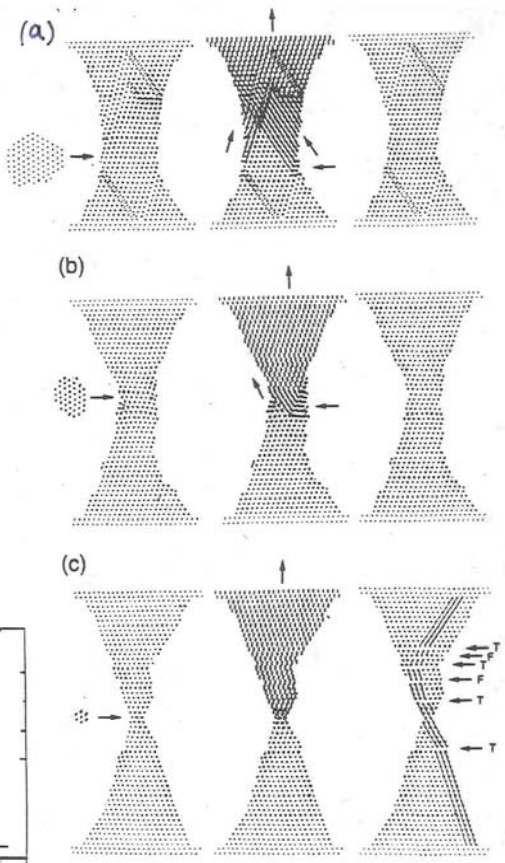

elongation force

33 component of stress tensor

electronic conductance

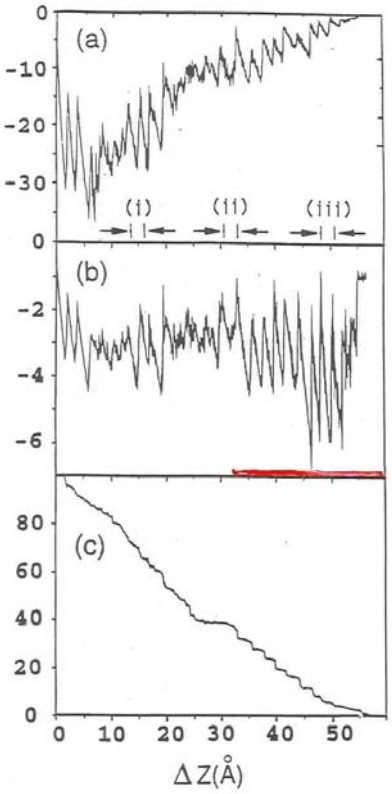

Landman et.al.
Langmuir 12, 4514 (1996)

Force and conductance measurements of gold nanowires.

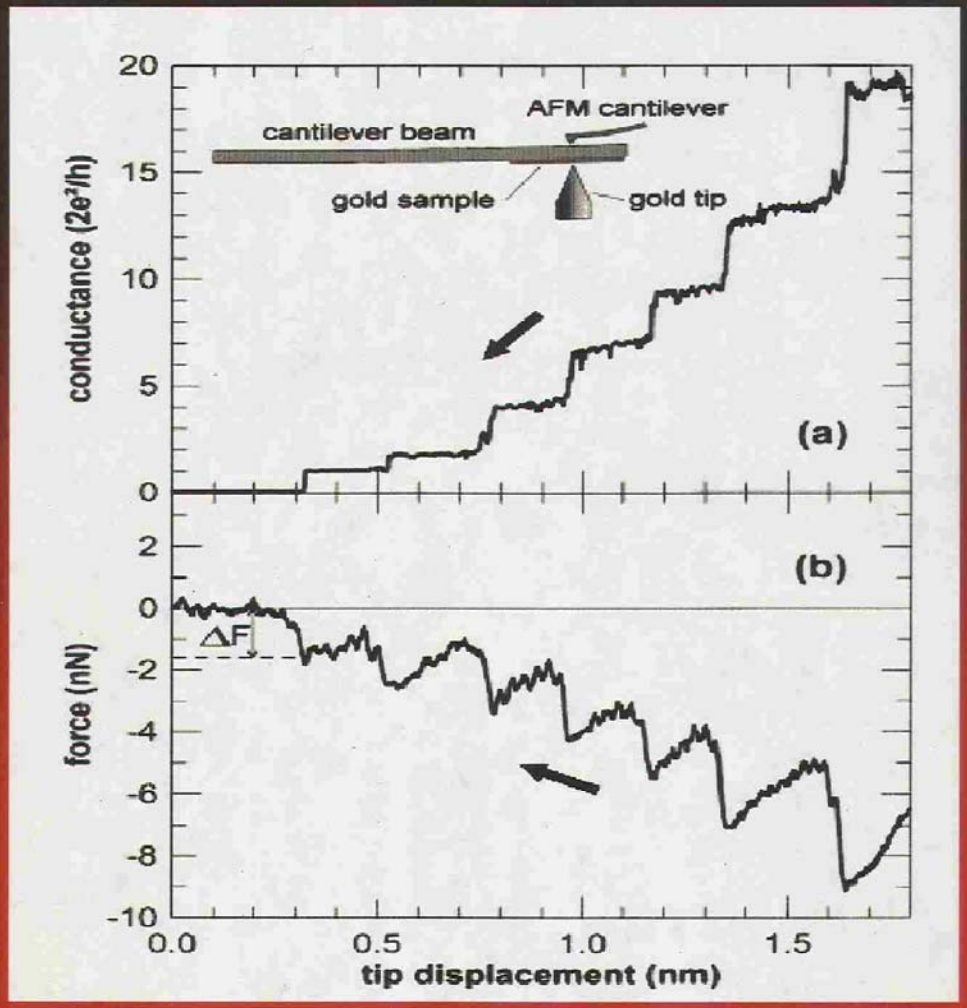

G. Rubio, N. Agrait and S. Vieira, Phys. Rev. Lett. 76, 2302 (1996).

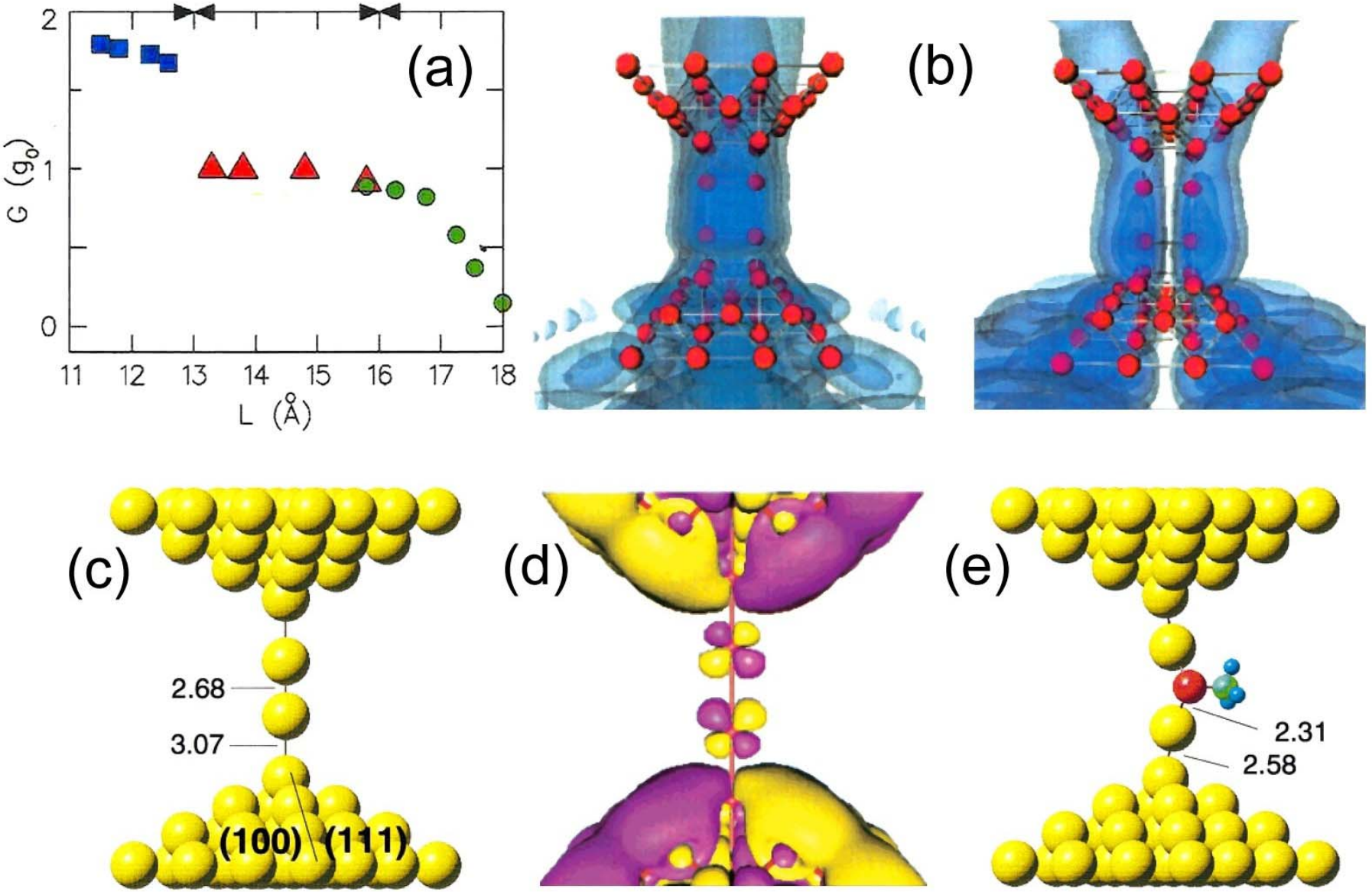
(a)
G (g0)
L (Å)
2
1
0
11
12
13
14
15
16
17
18
(b)
(c)
2.68
3.07
(100)
(111)
(d)
(e)
2.31
2.58

The Journal of
Physical Chemistry B
Volume 103 October 21, 1999 Number 42

ON THE WEB
pubs.acs.org/JPCB

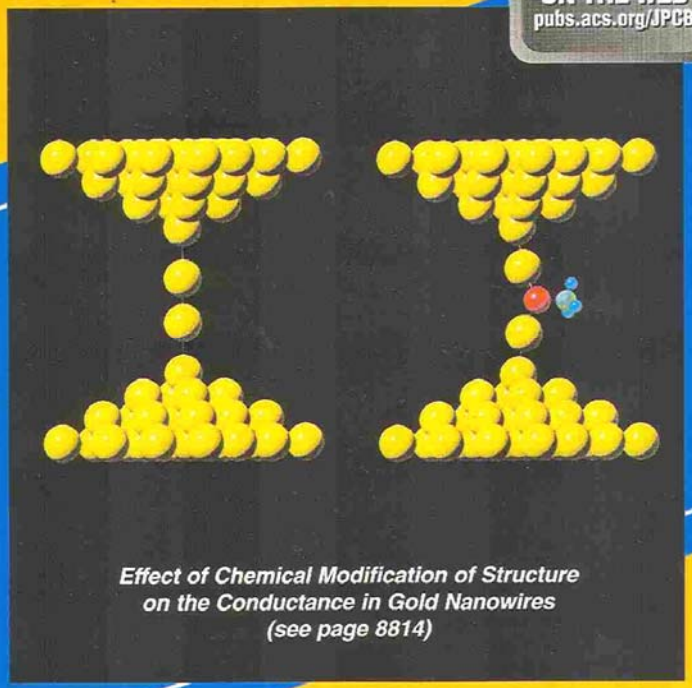

Effect of Chemical Modification of Structure on the Conductance in Gold Nanowires
(see page 8814)

CONDENSED MATTER, MATERIALS, SURFACES, INTERFACES, & BIOPHYSICAL

Häkkinen, Barnett, Landman

PUBLISHED WEEKLY BY THE AMERICAN CHEMICAL SOCIETY

TRIBOLOGY (Greek, tribos - rubbing)

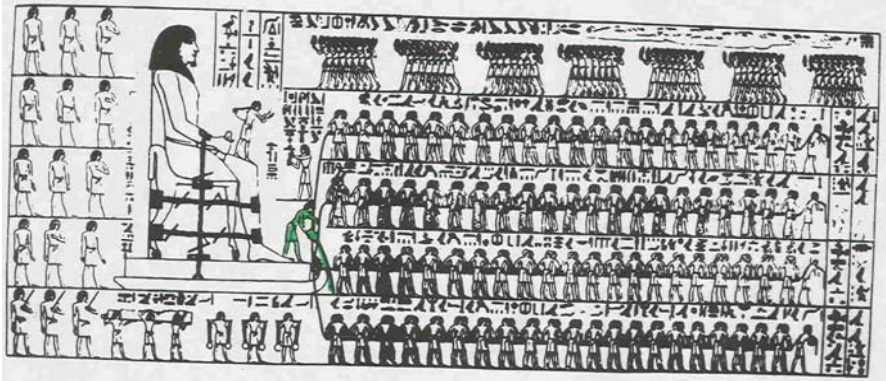

El Bersheh (c. 1900 B.C.)

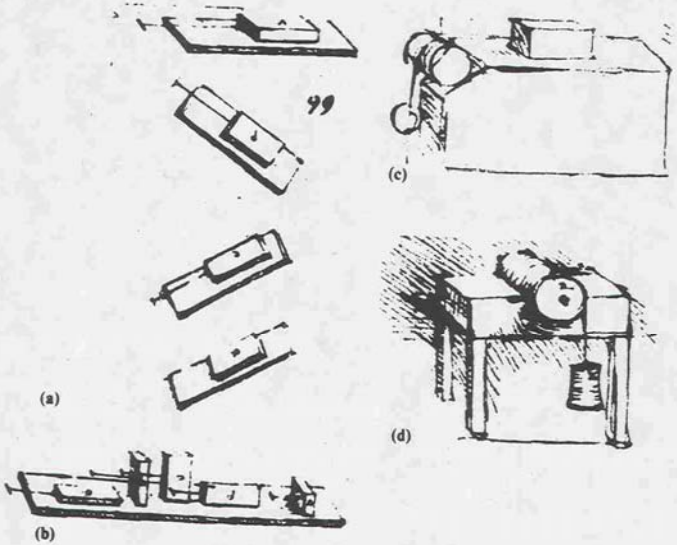

Leonardo da Vinci (1452 - 1519) (diaries)

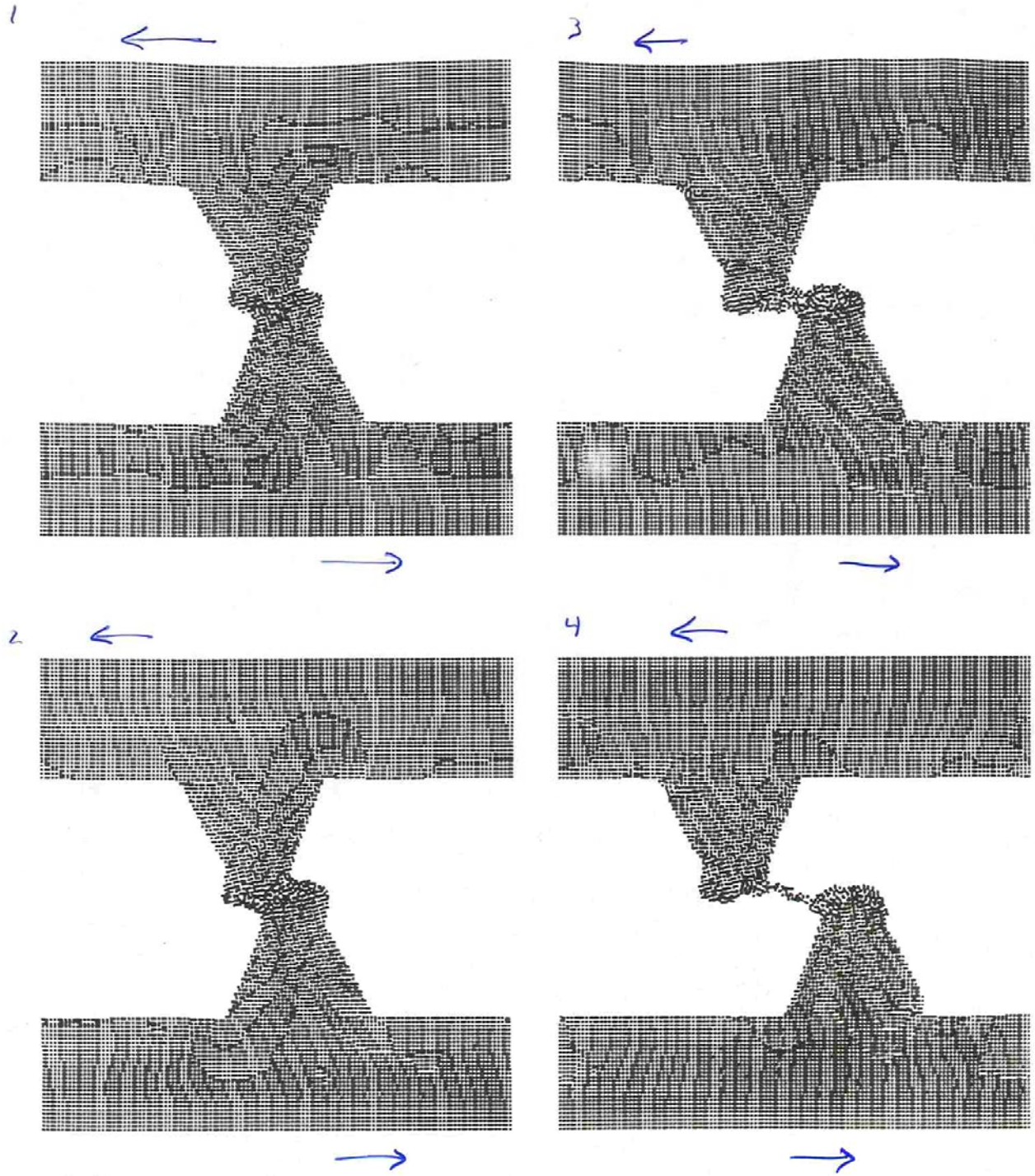
1
3
2
4

(Tabor + Bowden)

Friction is the force required to shear inter material junctions (+ plowing)

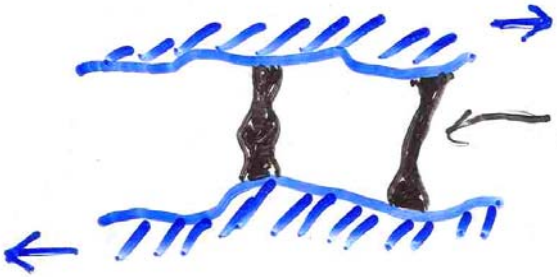

indeed: $A = \frac{L}{p}$

critical shear stress → $\sigma_c = F/A$

$F = (\sigma_c/p)\, L$

issues:

- Formation and properties of junctions
- How to inhibit junction formation (lubrication)

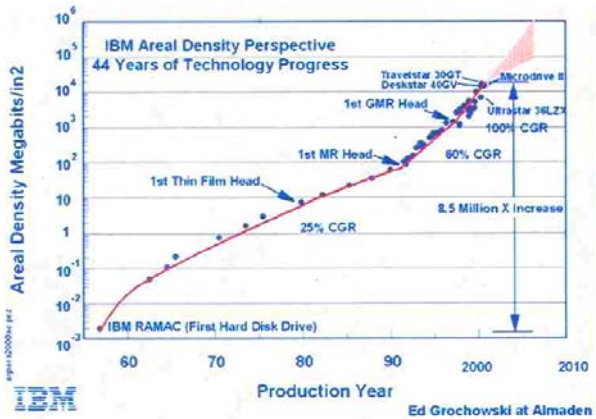
IBM Areal Density Perspective
44 Years of Technology Progress
Areal Density Megabits/in2
Production Year
IBM RAMAC (First Hard Disk Drive)
1st Thin Film Head
1st MR Head
1st GMR Head
25% CGR
60% CGR
100% CGR
8.5 Million X Increase
Ed Grochowski at Almaden

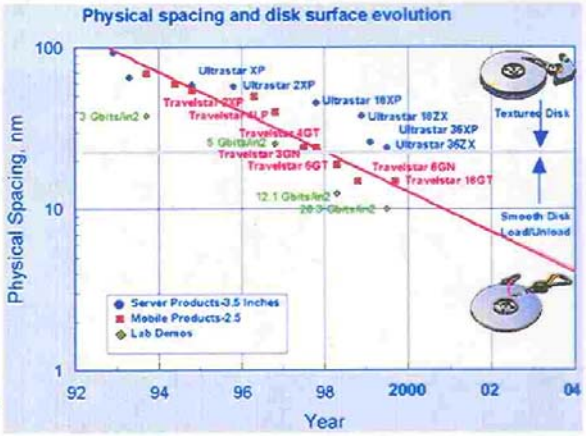
Physical spacing and disk surface evolution
Physical Spacing, nm
Year
Server Products-3.5 Inches
Mobile Products-2.5
Lab Demos
Textured Disk
Smooth Disk
Load/Unload

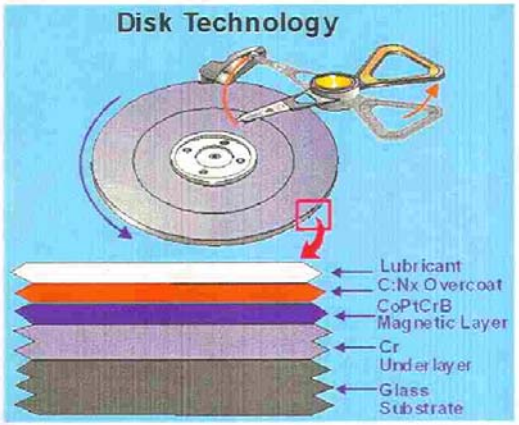
Disk Technology
Lubricant
C:Nx Overcoat
CoPtCrB
Magnetic Layer
Cr
Underlayer
Glass
Substrate

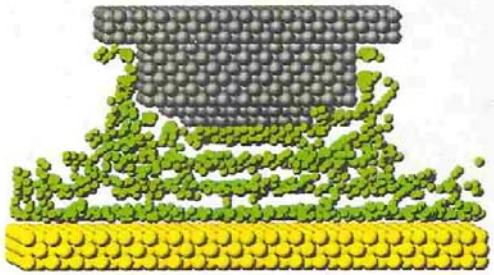

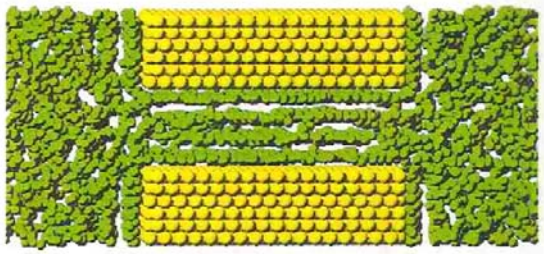

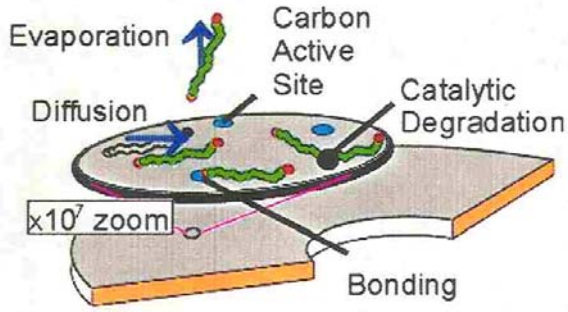
Evaporation
Carbon
Active
Site
Diffusion
Catalytic
Degradation
x10⁷ zoom
Bonding

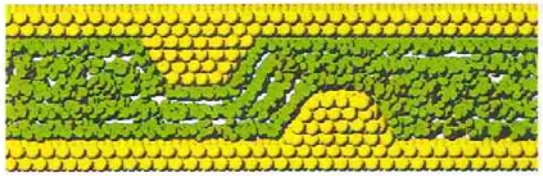

Highly Confined Classical and Quantum Liquids:
Nanojets, Nanotribology, and Quantum Dots

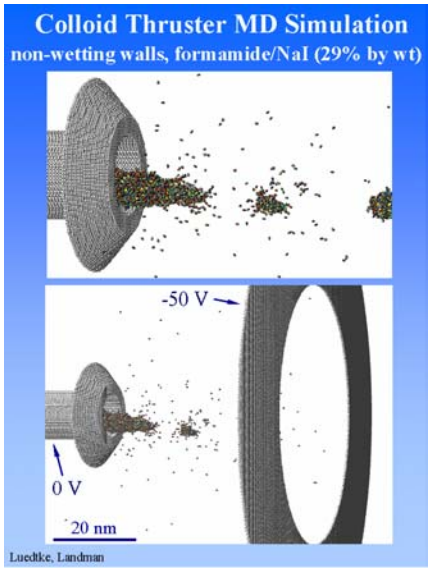

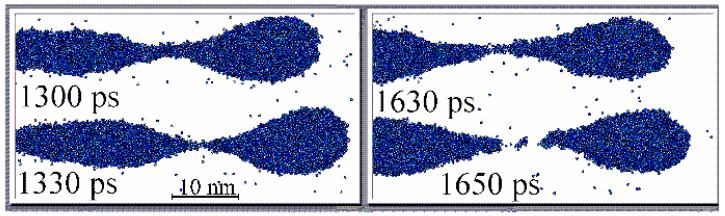

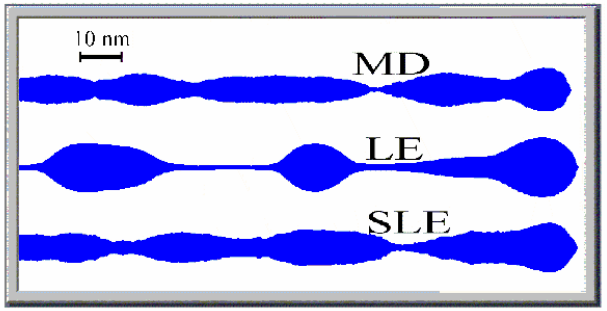

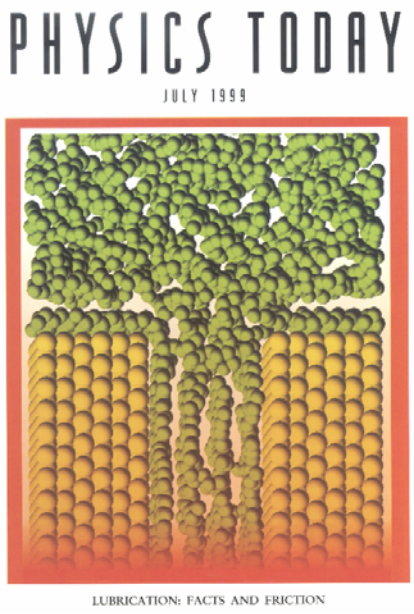

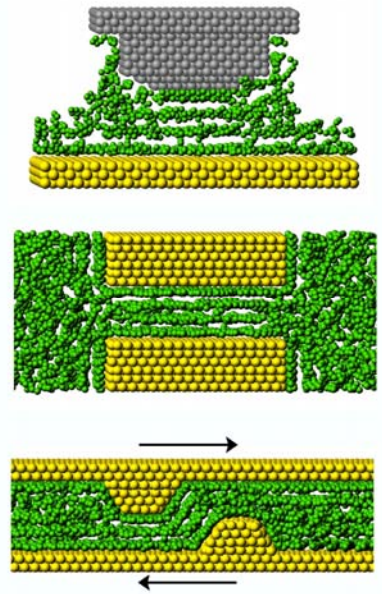

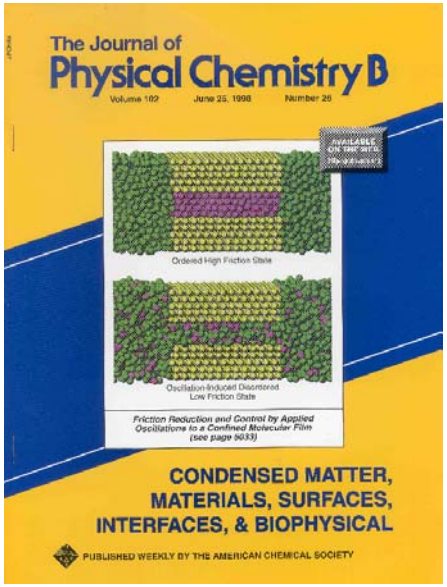

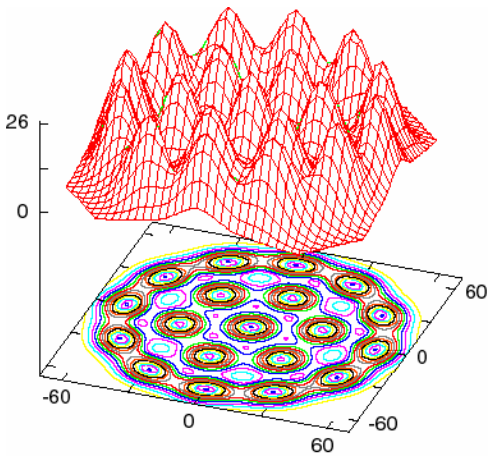

Electron Molecule
Wigner Crystallite

PHYSICS TODAY

JULY 1999

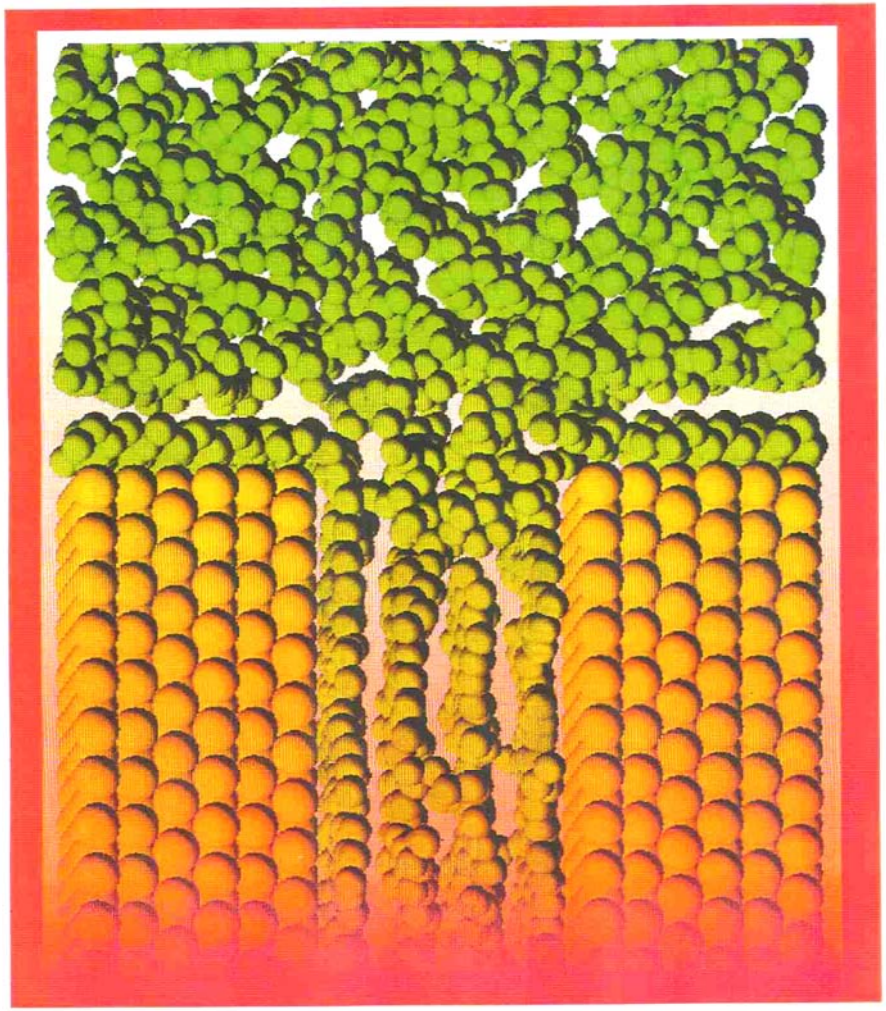

LUBRICATION: FACTS AND FRICTION

Gao, Luedtke, Landman

RSV = revised standard version KJV = King James Version

Deborah number

$$D = \tau_R / \tau_{exp} = \tau_R W_{drive}$$

Revised standard edition ↓ King James version ↓

	RSV	KJV
Judg 5:5.2	The **mountains** quaked before the LORD, yon Sinai before the LORD, the God of Israel.	The **mountains** melted from before the LORD, even that Sinai from before the LORD God of Israel.

"הרים נזלו מפני ה'"

שופטים ה':ה

(שירת דבורה)

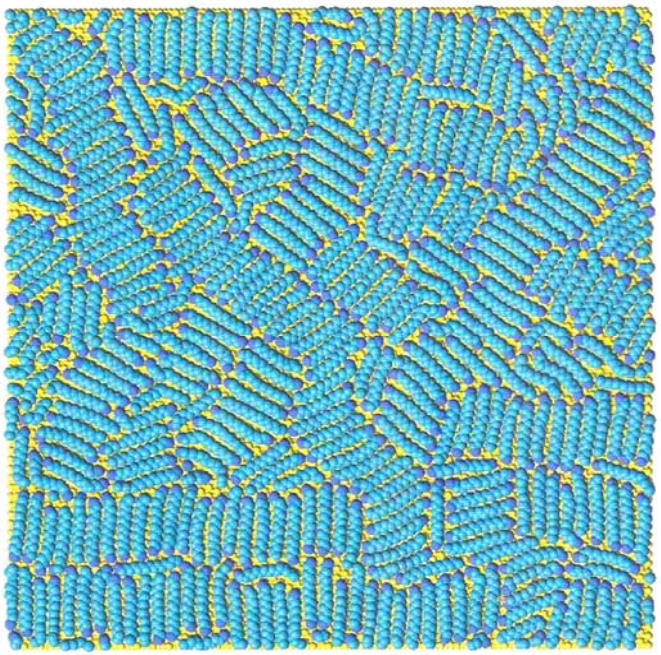

Flat

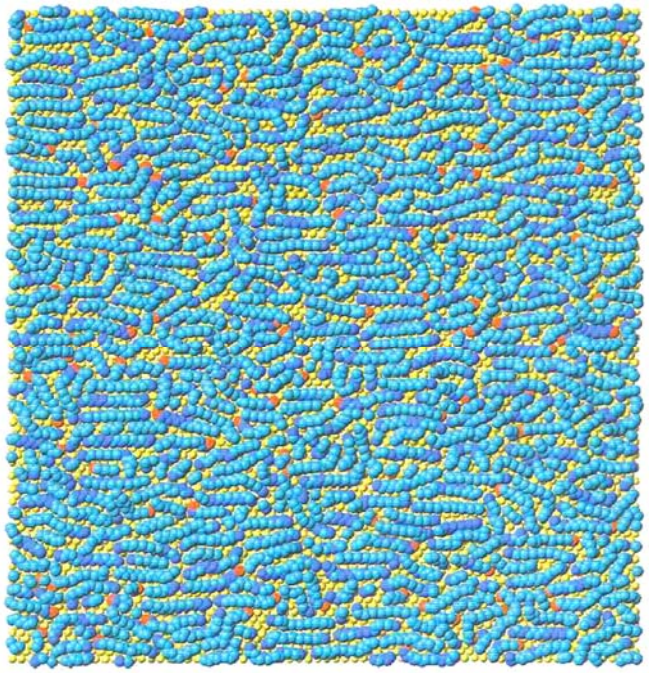

Rough

> -0.02 eV

-0.1 ~ -0.02 eV

-0.18 ~ -0.1 eV

< -0.18 eV

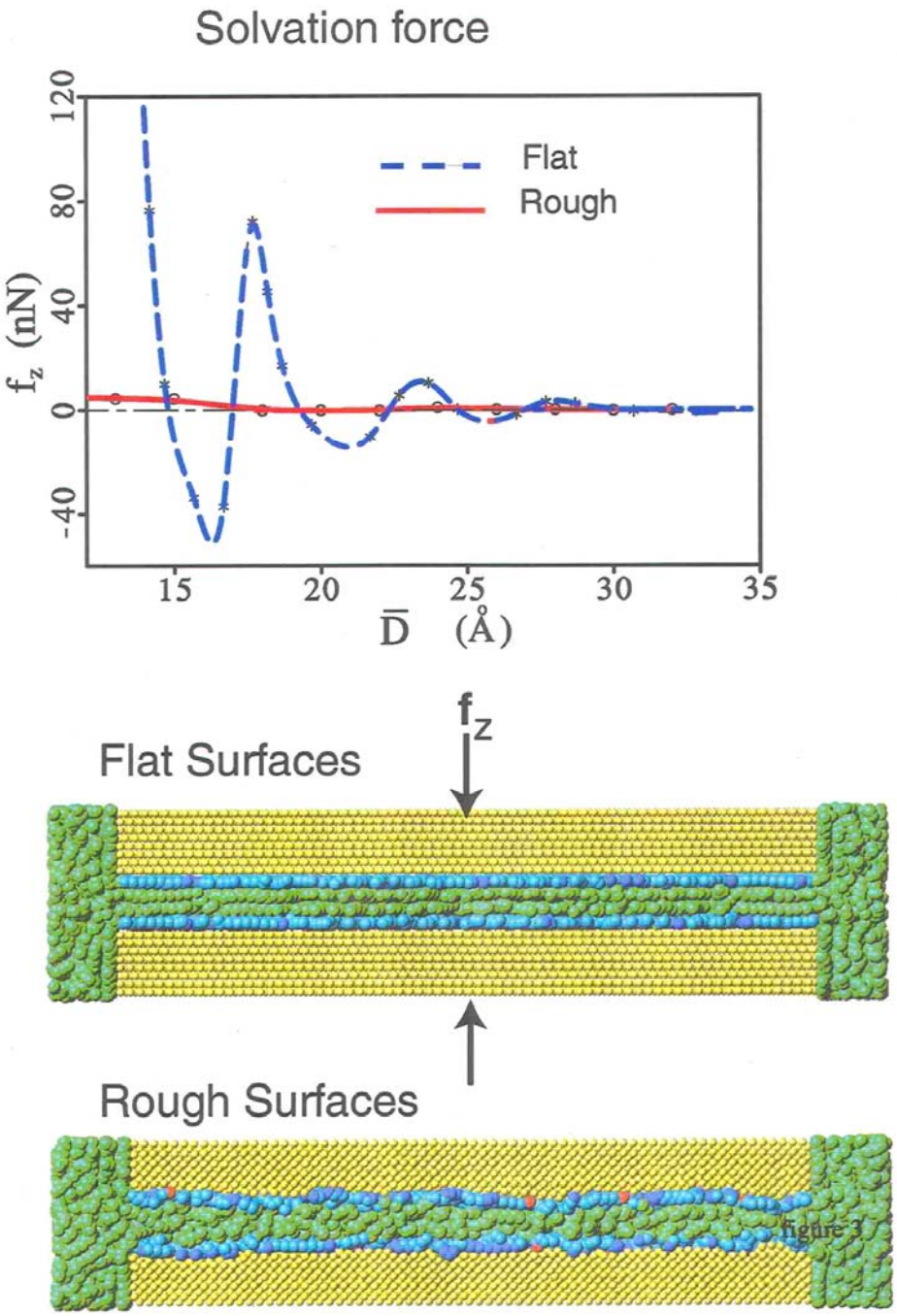
Solvation force
120
80
40
0
-40
f_z (mN)
Flat
Rough
15
20
25
30
35
$\bar{D}$ (Å)
f_z
Flat Surfaces
Rough Surfaces

figure 3

Friction Flicks

Computer animation offers insights into friction's molecular underpinnings

By JANET RALOFF

Landman's team provides a Cray supercomputer with a cast of characters whose personalities are determined by the physical and chemical forces that govern how they interact with their neighbors. Then the scientists set a theoretical stage and allow the simulated characters to improvise their way through a hypothetical scene.

A camera records the evolving choreography of these silent players — a complex drama simulating reactions on a scale beyond resolution by the human eye, motions that occur on stage sets measured in billionths of a meter. By replaying this drama over and over — some portions in frame-by-frame slow motion — tribologists are gleaning insights into how lubricants function.

Fiction? No, a number of researchers say. Indeed, Landman says, although the movie cannot yet quantitatively depict the real world, qualitatively "it's not far off."

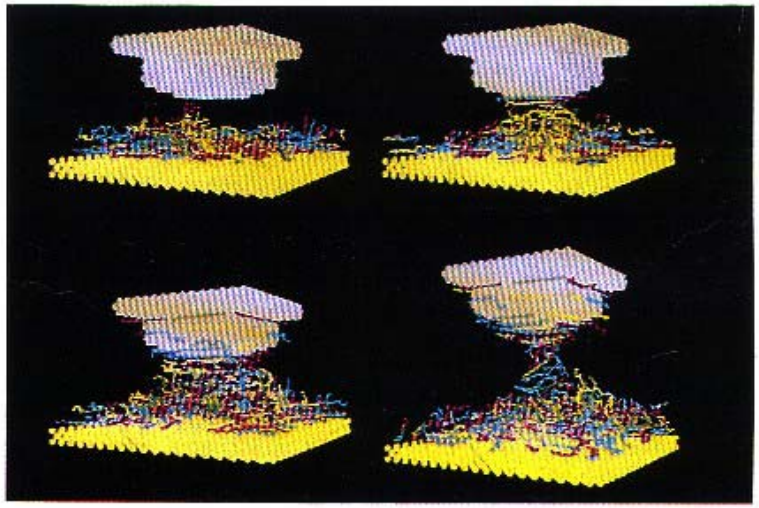

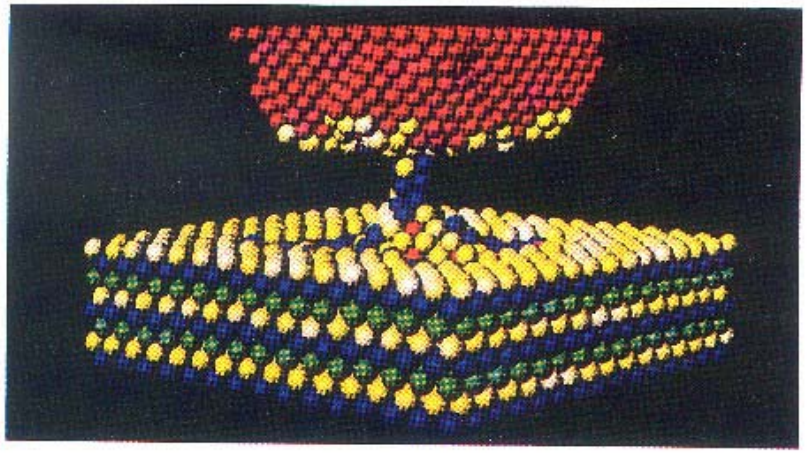

SCIENCE NEWS Vol 141, pp 360 – 362 (1992)

J. Gao, W. D. Luedtke, U. Landman
J. Phys. Chem. B 102, 5033 ('98)

JPCHAx

The Journal of Physical Chemistry B

Volume 102 June 25, 1998 Number 26

AVAILABLE ON THE WEB
http://pubs.acs.org

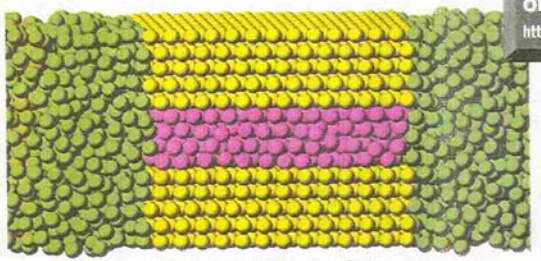

Ordered High Friction State

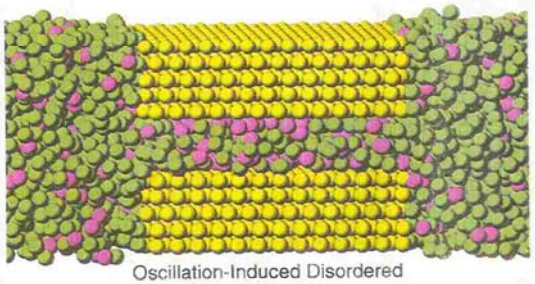

Oscillation-Induced Disordered Low Friction State

Friction Reduction and Control by Applied Oscillations to a Confined Molecular Film
(see page 5033)

CONDENSED MATTER, MATERIALS, SURFACES, INTERFACES, & BIOPHYSICAL

PUBLISHED WEEKLY BY THE AMERICAN CHEMICAL SOCIETY

Friction Control in Thin-Film Lubrication

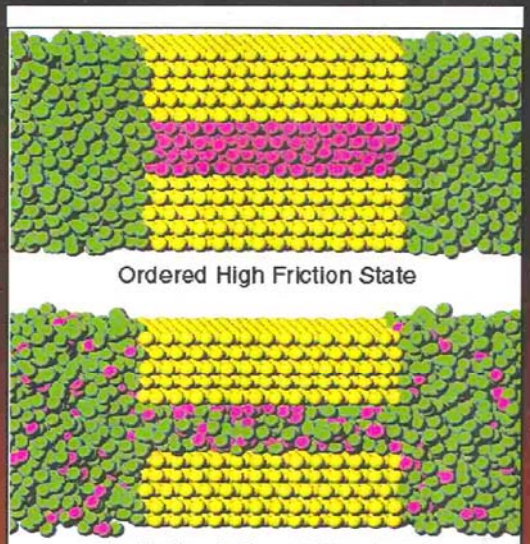

Ordered High Friction State

Oscillation-Induced Disordered
Low Friction State

Friction Reduction and Control by Applied
Oscillations to a Confined Molecular Film

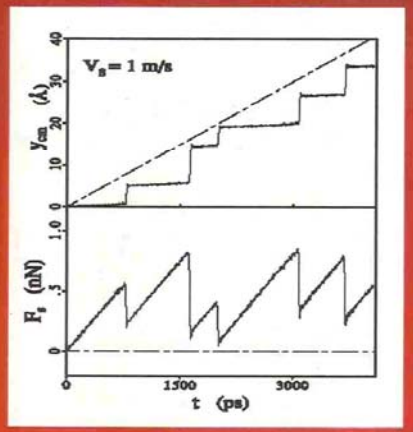

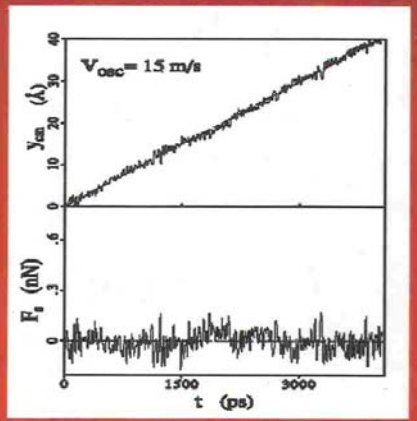

Jianping Gao, W.D. Luedtke, and Uzi Landman,

J. Phys. Chem B, **102**, 5033 (1998)

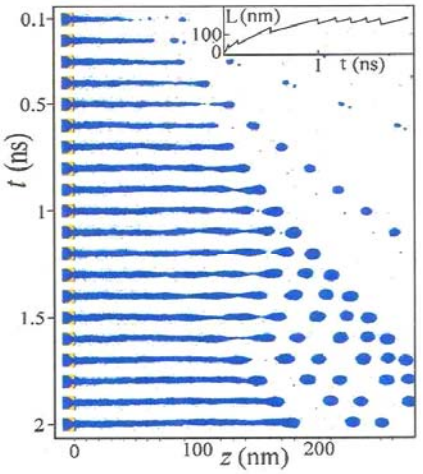
L (nm)
100
0
t (ns)
0.1
0.5
1
1.5
2
t (ns)
0
100
z (nm)
200

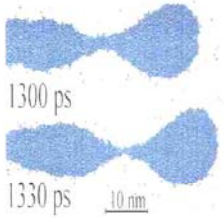
1300 ps
1330 ps
10 nm

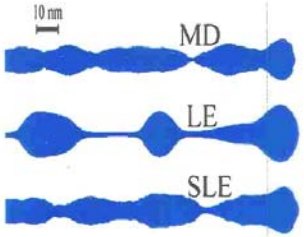
10 nm
MD
LE
SLE


Science

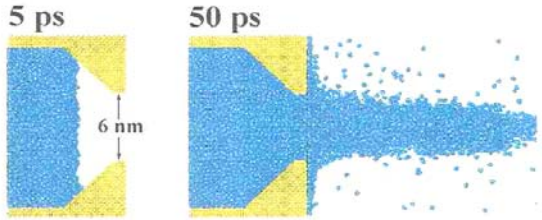
5 ps
50 ps
6 nm

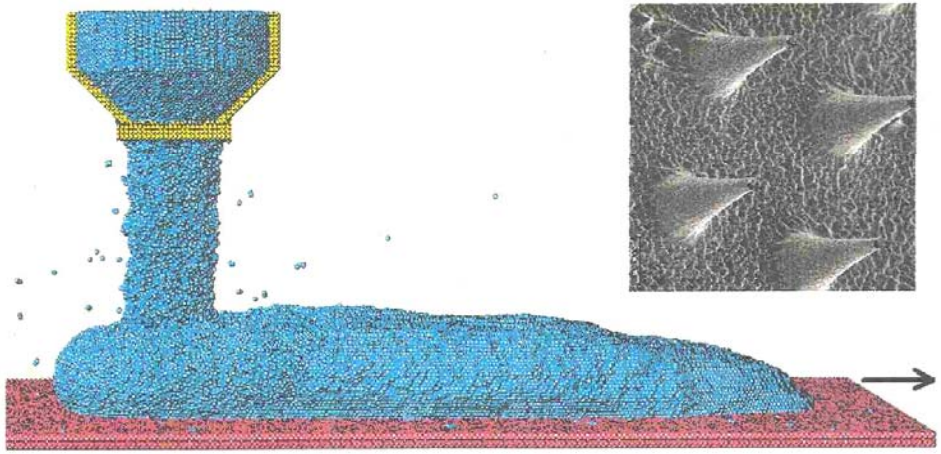

AMERICAN ASSOCIATION FOR THE ADVANCEMENT OF SCIENCE

SCIENCE

8 JULY 1994 $6.00
VOL. 265 • PAGES 157–288

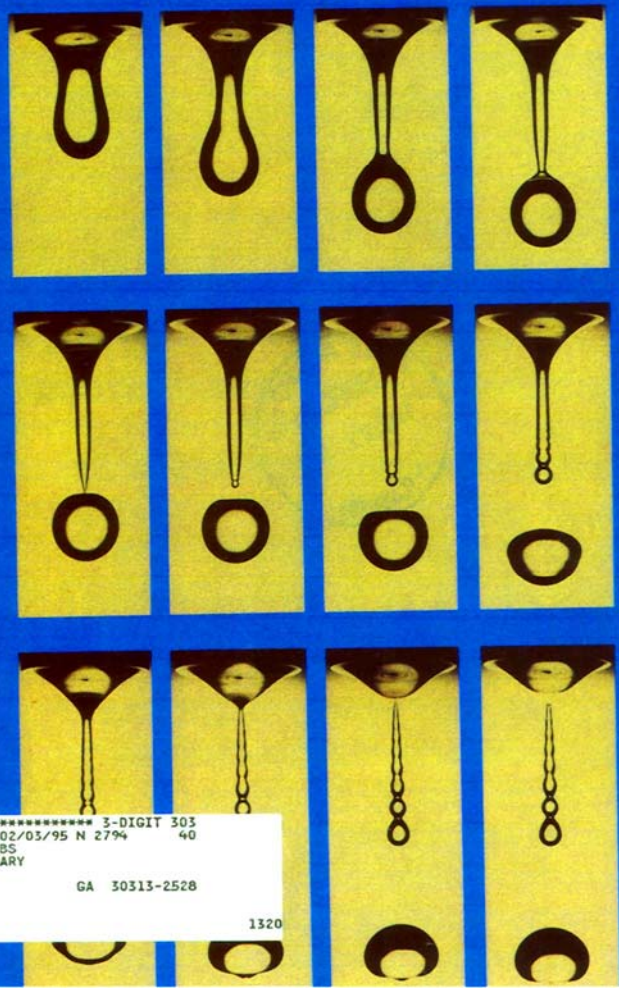

Physical Review Focus

Two Fluid Drop Snap-Off Problem: Experiments and Theory
Itai Cohen, Michael P. Brenner, Jens Eggers, and Sidney R. Nagel
Phys. Rev. Lett. **83**, 1147 (9 August 1999)

Watching the Faucet Drip

11 August 1999

When the faucet drips, most people call the plumber or get out their tools, but some physicists are content to study the phenomenon instead. The equations describing the pinch-off of a drop of water are so difficult mathematically that they've only recently been solved. The problem is of interest in fields as disparate as black holes and ink jet printers. According to the 9 August *PRL*, a drop's break-off point exhibits fractal properties--a slice through it looks the same at any time if you rescale the axes. The authors confirmed that theoretical prediction with their own version of a dripping faucet where drops of one type of fluid drip through a different fluid.

Understanding the way fluid flows break into drops is useful for industry, in such areas as the mixing of chemicals and designing ink-jet printers, but the mathematics goes beyond these direct applications. At the moment of pinch-off, parts of the equations become infinite in a way that appears in other areas of physics, such as fluid turbulence, star formation, and the gravity around black holes. Sidney Nagel of the University of Chicago and his colleagues hope that studying this simple and controllable system will provide insights into these other problems as well.

Nagel and his colleagues have previously observed liquids of different viscosities dripping through air, but in those experiments they could never directly verify one of the most interesting predictions from theory. According to simulations, a snapshot of the pinch-off zone taken at any time during the process should look like one at any other time, except for a rescaling of the axes--a property called self-similarity.

In their latest experiments, the team trained their high-speed video camera on a nozzle dripping glycerin/water mixtures through silicone and other oils. University of Chicago team member Itai Cohen says one motivation for these experiments for him was the beauty of the slowed-down action. "If you've ever looked at a lava lamp [fluid] snapping off, it's just really pretty," he says. The researchers managed to overlay profiles of the budding drop from three different times within the final 50 ms

Phys. Rev. Lett. 83, 1147 (1999)

Physicist's lava lamp. Glycerin drips through a viscous oil, showing the details of pinching off in slow motion.

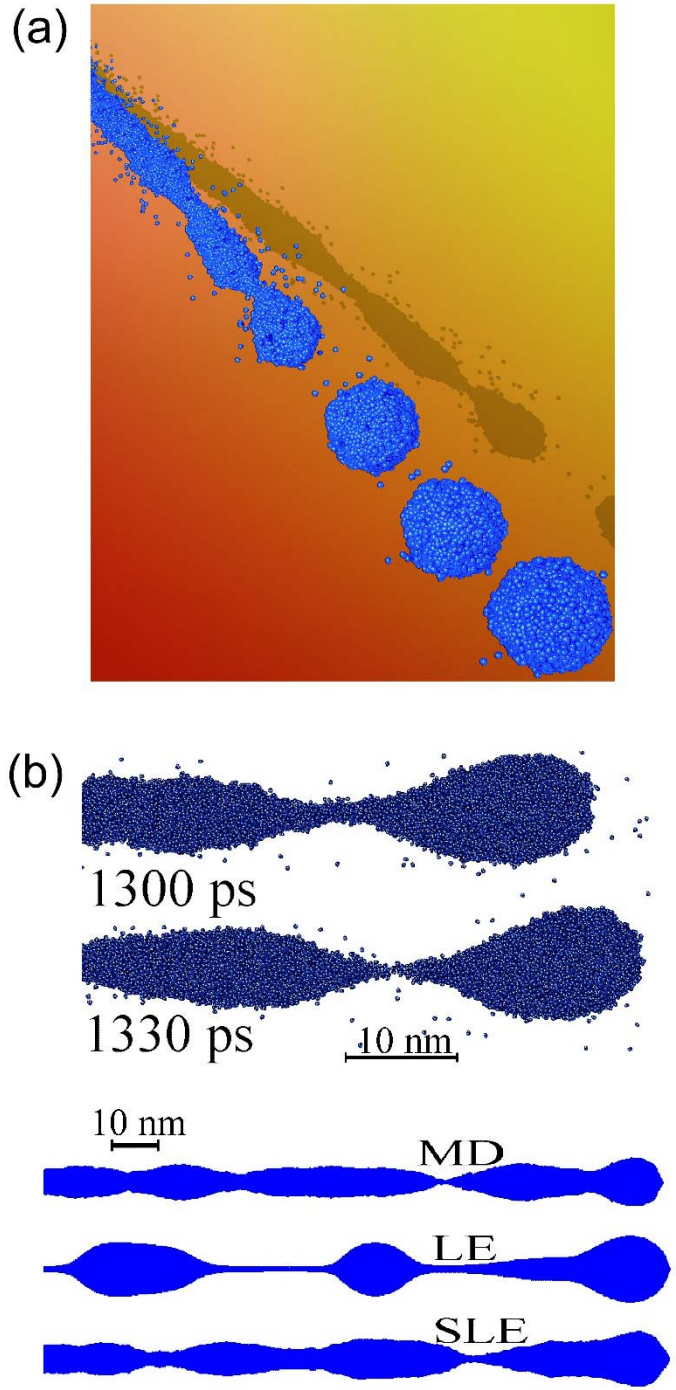
(a)
(b)
1300 ps
1330 ps
10 nm
10 nm
MD
LE
SLE

Breakup in MD:

- double-cone neck

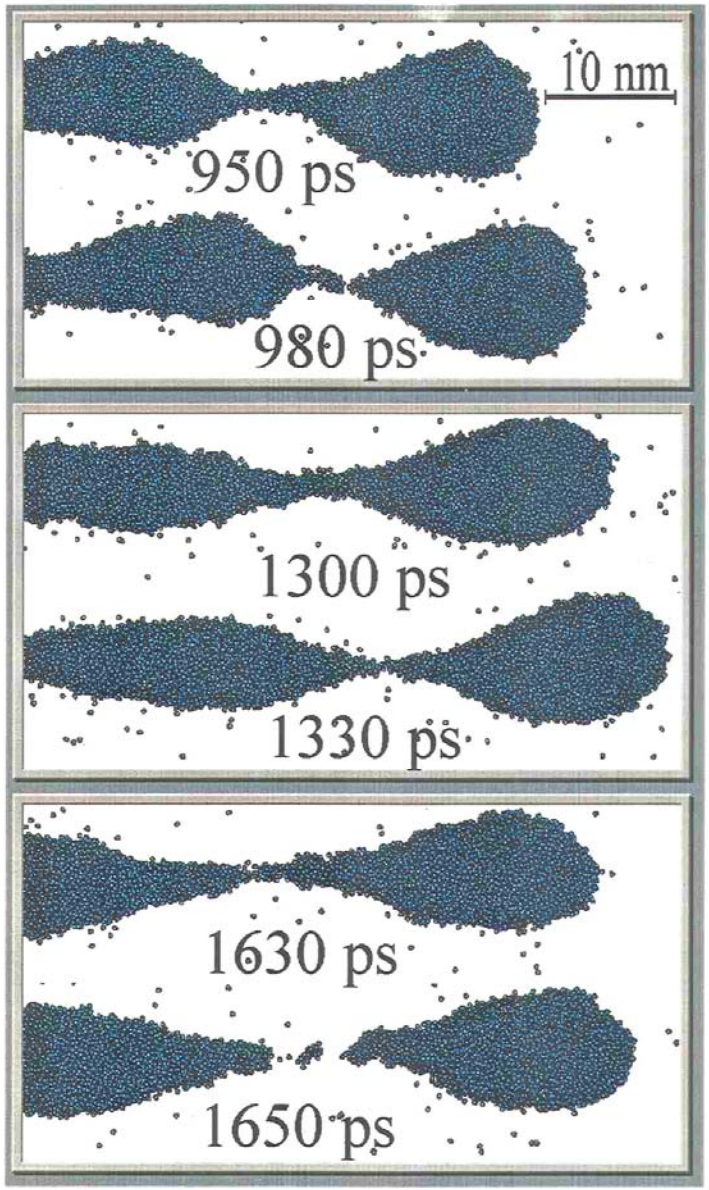

WHEN

EACH

ATOM

COUNTS

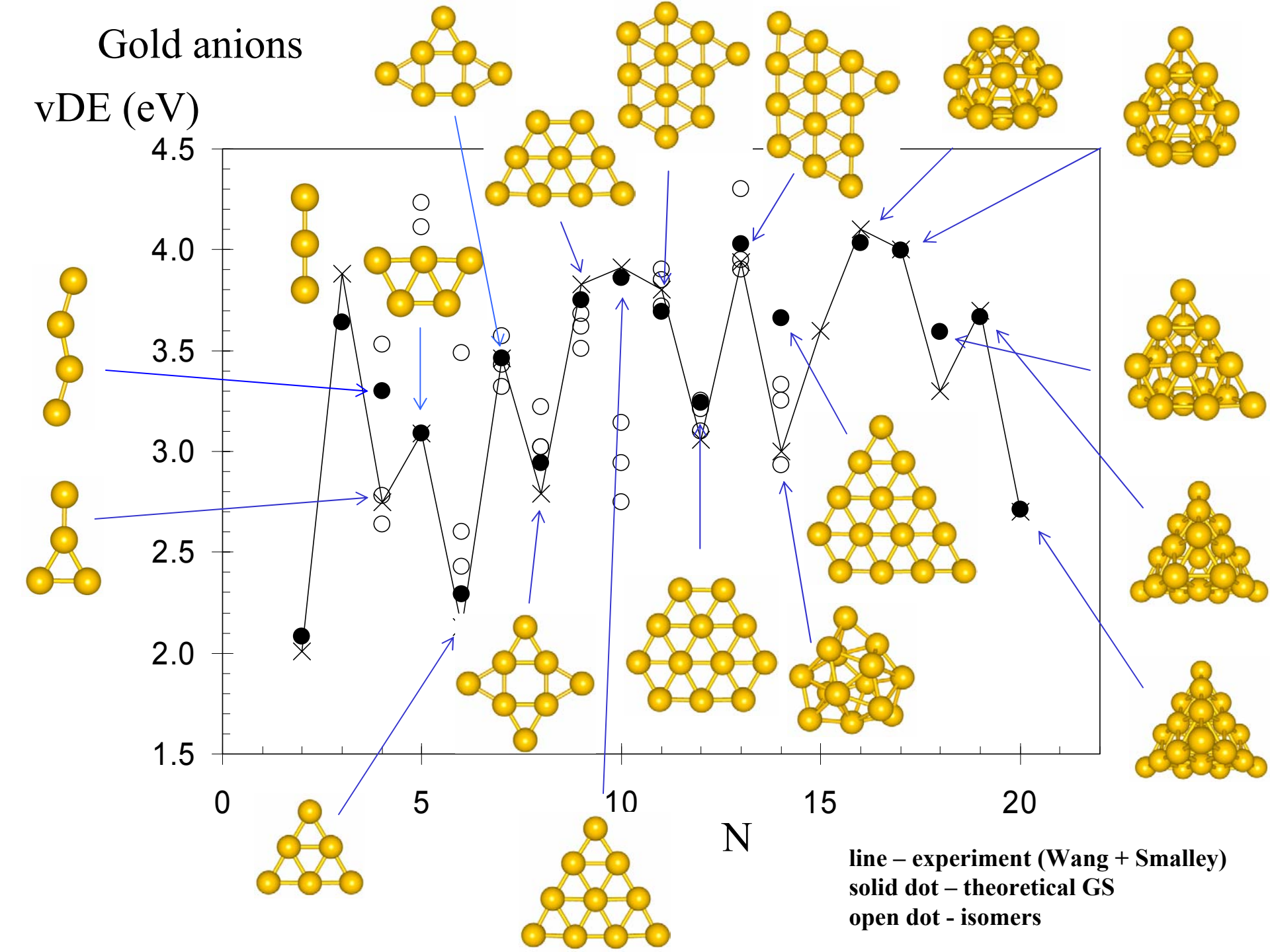
Gold anions
vDE (eV)
4.5
4.0
3.5
3.0
2.5
2.0
1.5
0
5
10
15
20
N
line – experiment (Wang + Smalley)
solid dot – theoretical GS
open dot - isomers

When gold is not noble : Nanoscale gold catalysis

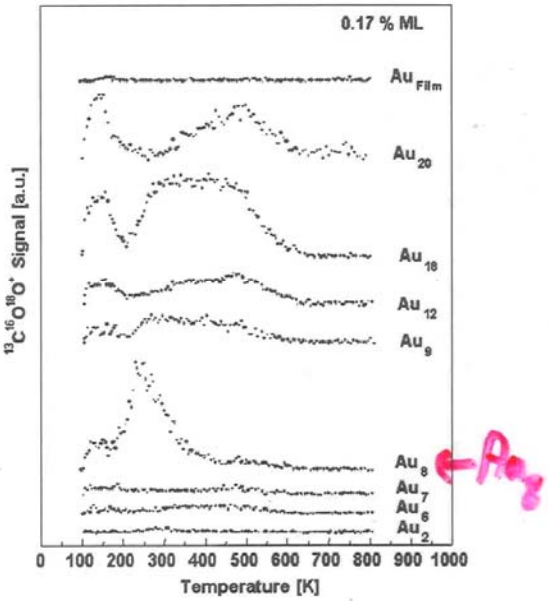

$$CO + \tfrac{1}{2}\,O_2 \xrightarrow{Au_n/MgO} CO_2$$

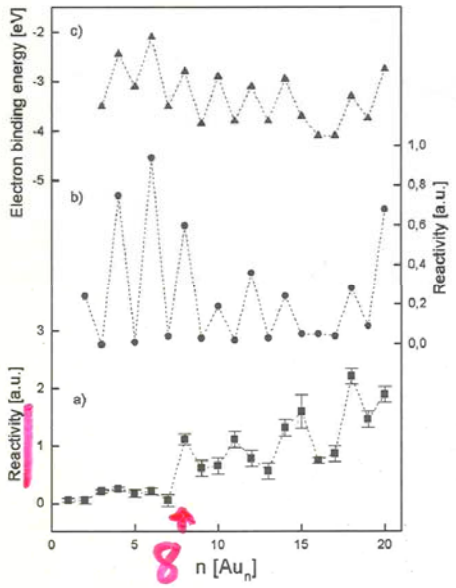

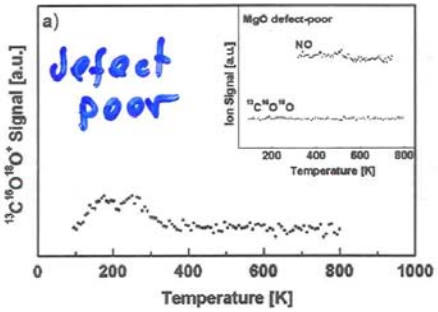

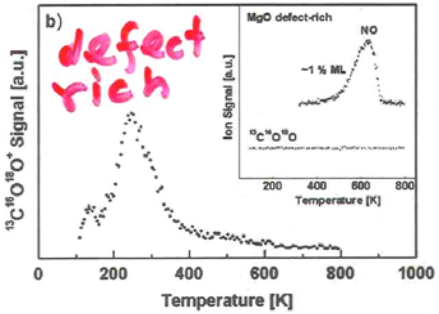

Gold Cluster as a Catalyst for CO oxidation reaction

Supported gold cluster : Au_n/MgO(FC)–

Sanchez, et. al. JPC A 103 9573 (1999)

Au_n on defect-rich MgO (100), 8≤n ≤20 :

Low temperature combustion of CO

↳ **oxygen vacancy F-centers**

Au_n on defect-poor MgO (100) :

Very small combustion of CO

Electron transfer from F-Center to gold cluster plays an essential role in the activation of gold clusters as catalysts for CO combustion.

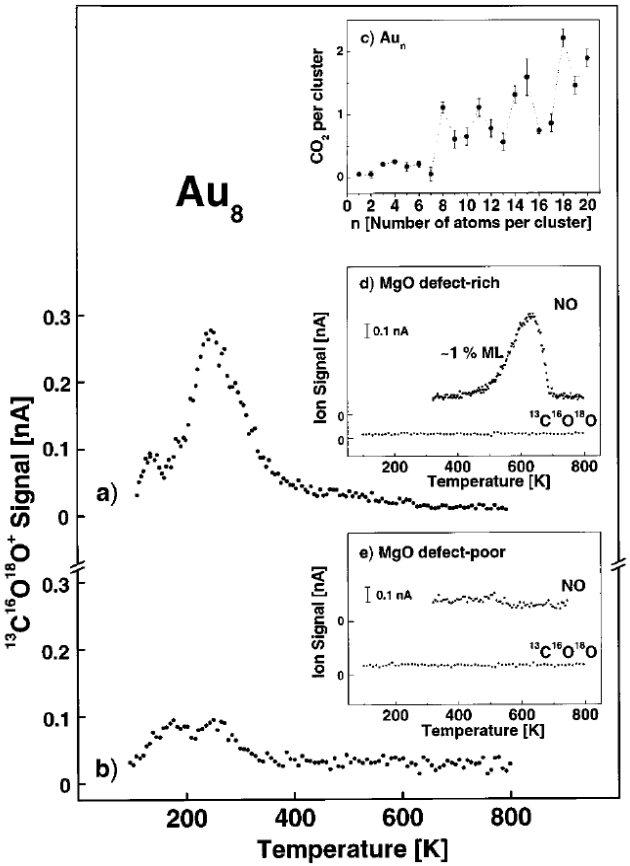

Au_2^- in gas phase : predicted theoretically as a catalyst for CO oxidation and later confirmed experimentally.

Häkkinen and Landman, JACS 123 9704 (2001)

Oxidation of CO on Au_n (n = 2-20) bound to Defect-Rich MgO(100) Surfaces

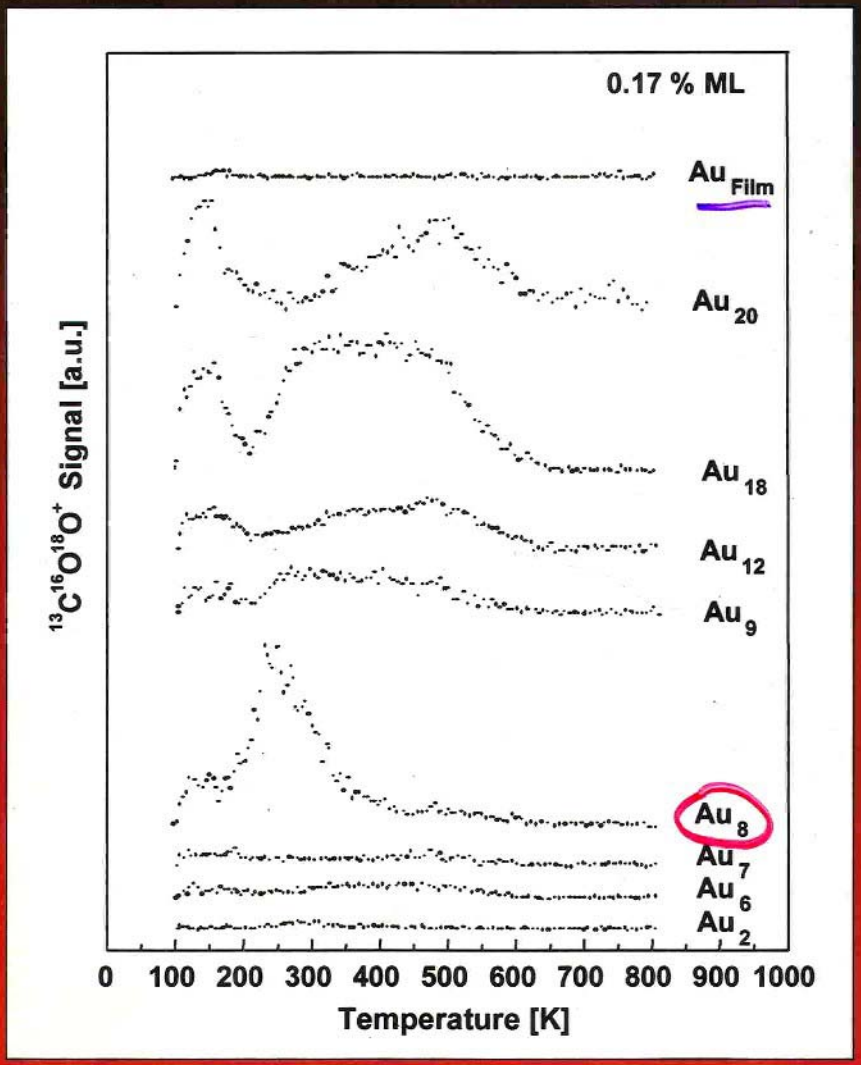

Adsorption of Au_8 on MgO without/with F-Center

Au8/MgO

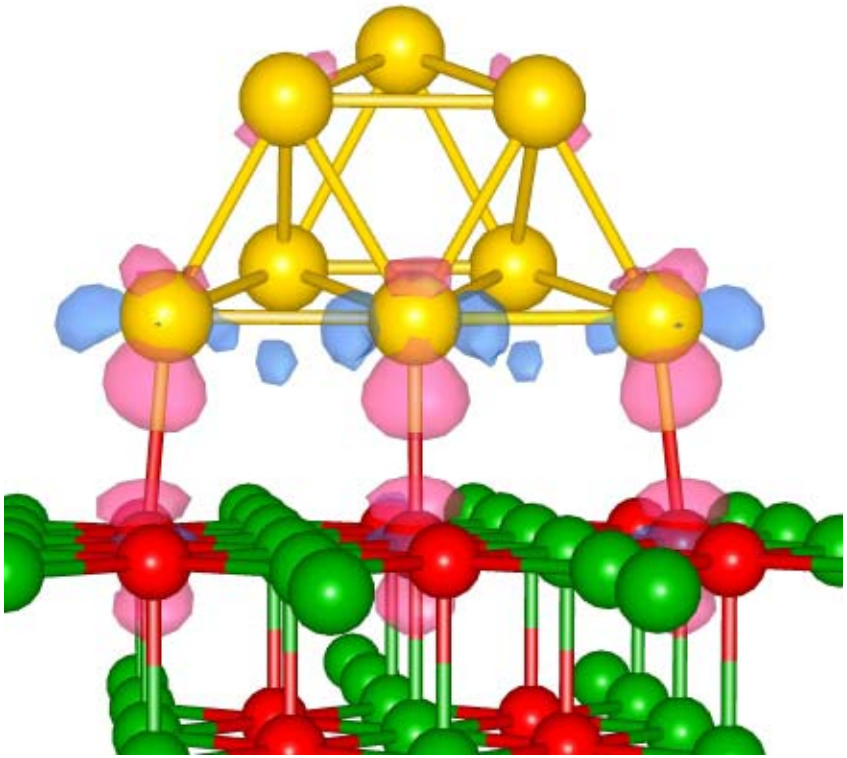

$BE_{Au_8} = 1.22\ \text{eV}$

$\delta\rho = \rho[\text{Au}_8/\text{MgO}] - (\rho[\text{Au}_8] + \rho[\text{MgO}])$

$\delta\rho > 0$

$\Delta Q(\text{Au}_8/\text{MgO}) = 0.82e$

Au8/MgO(FC)

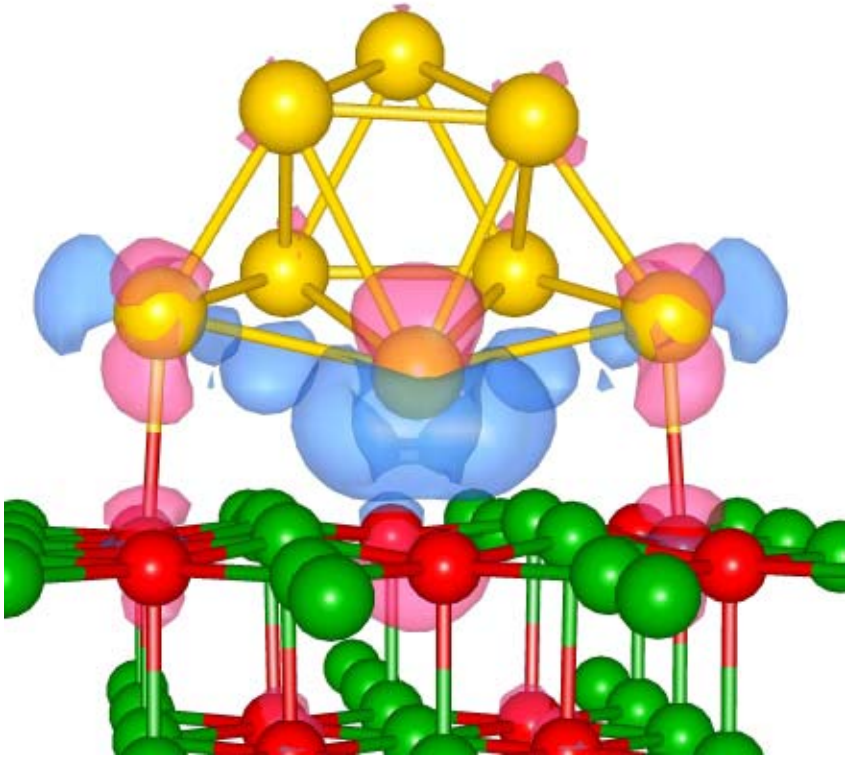

$BE_{Au_8} = 3.44\ \text{eV}$

$\delta\rho = \rho[\text{Au}_8/\text{MgO(FC)}] - (\rho[\text{Au}_8] + \rho[\text{MgO(FC)}])$

$\delta\rho < 0$

$\Delta Q(\text{Au}_8/\text{MgO(FC)}) = 1.44e$

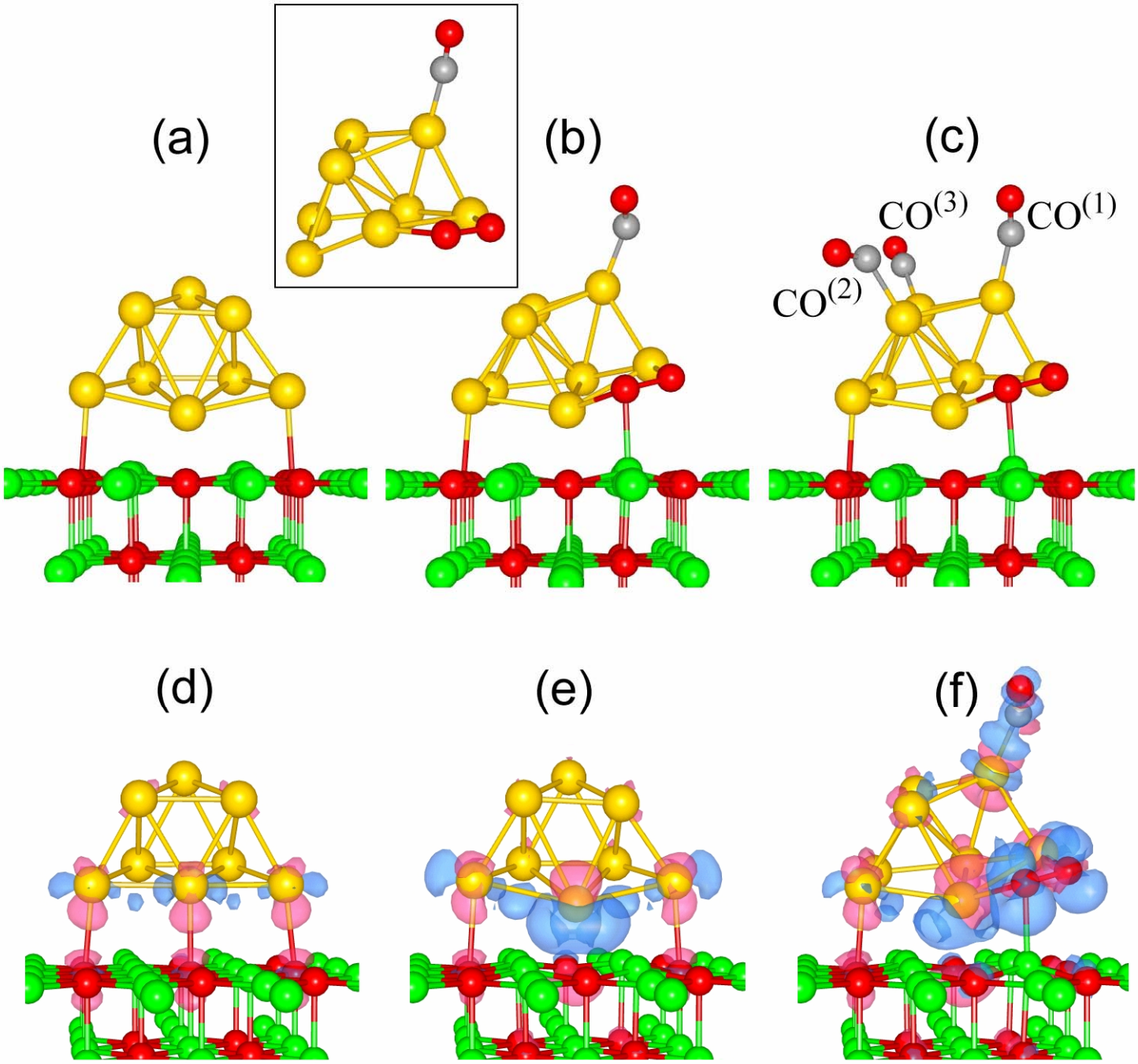
(a)
(b)
(c)
CO(3)
CO(1)
CO(2)
(d)
(e)
(f)

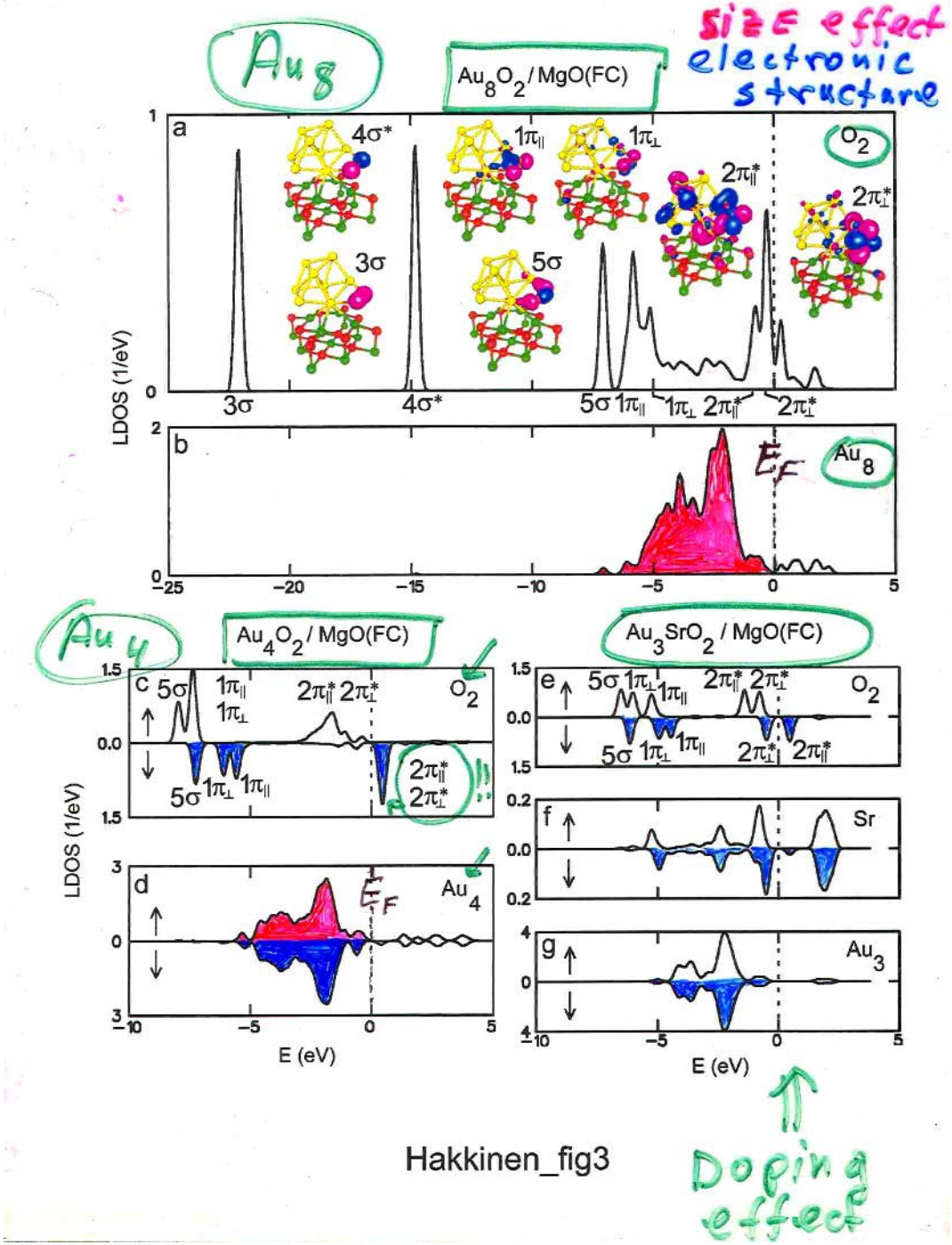
Au8
Au8O2 / MgO(FC)
size effect
electronic
structure
a
4σ*
3σ
1π||
1π⊥
5σ
2π||*
O2
2π⊥*
LDOS (1/eV)
3σ
4σ*
5σ 1π||
1π⊥ 2π||*
2π⊥*
b
EF
Au8
Au4
Au4O2 / MgO(FC)
Au3SrO2 / MgO(FC)
c
5σ
1π||
1π⊥
2π||* 2π⊥*
O2
2π||*
2π⊥*
!!
d
EF
Au4
e
5σ 1π⊥ 1π||
2π||* 2π⊥*
O2
f
Sr
g
Au3
E (eV)
Hakkinen_fig3
Doping
effect

Heiz, Schneider et.al. (Expt).
A. Sanchez et.al J. Phys. Chem. A103, 9573(99)

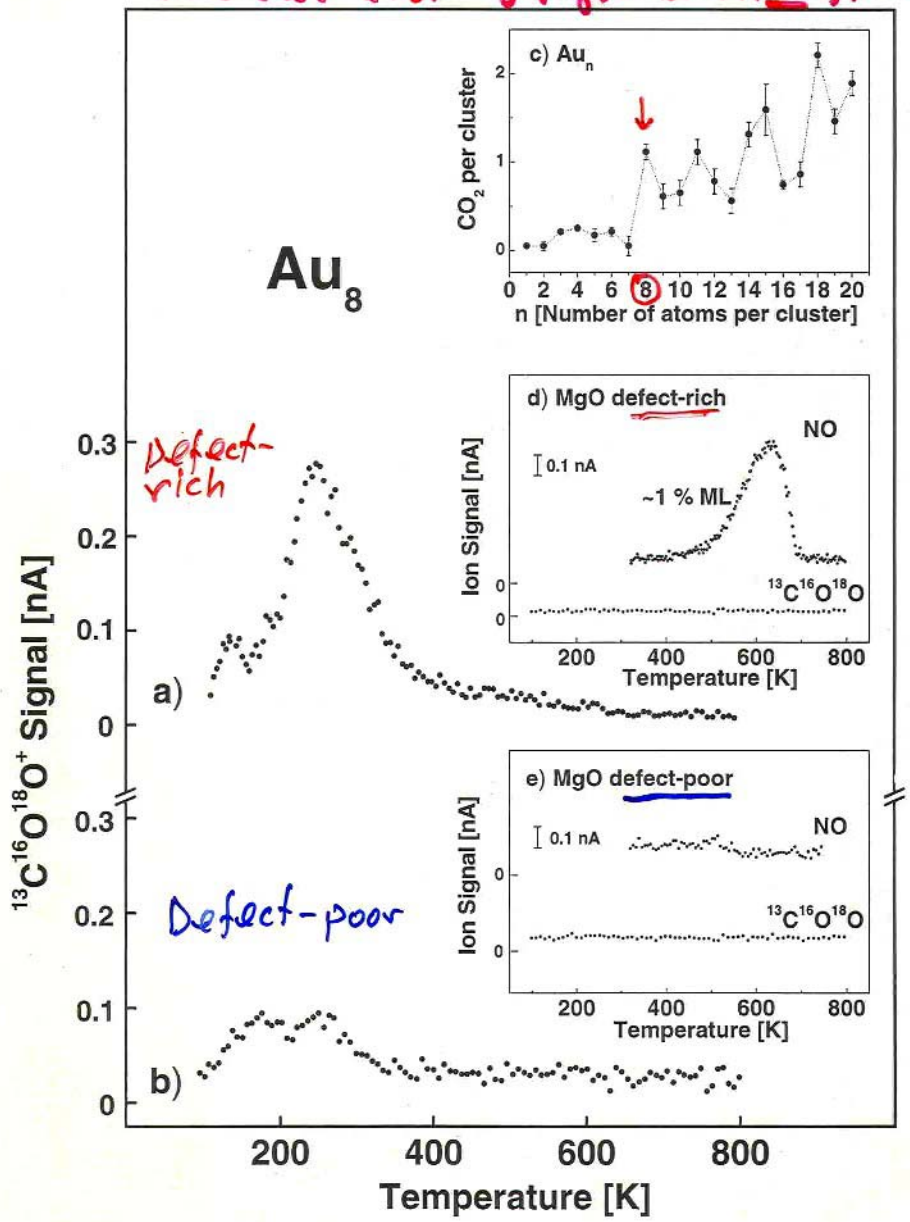

Figure 1

Vital Role of Moisture in the Catalytic Activity of Supported Gold Nanoparticles**

Masakazu Daté, Mitsutaka Okumura, Susumu Tsubota, and Masatake Haruta*

Why can inert gold become catalytically active only when dispersed in the form of nanoparticles?—This simple question has attracted growing interest in the field of not only catalytic and industrial chemistry,[1–4] but also cluster and theoretical science.[5–7] To answer this question, CO oxidation has been intensively studied as a model reaction.[8–14] The reaction is known to be greatly influenced by moisture in the reactant gas.[10,15] However, only a few recent studies discuss the reaction mechanisms taking water into account.[16,18] Even in these studies on the effect of moisture, for practical reasons, the addition of water vapor has been examined only at high concentrations.

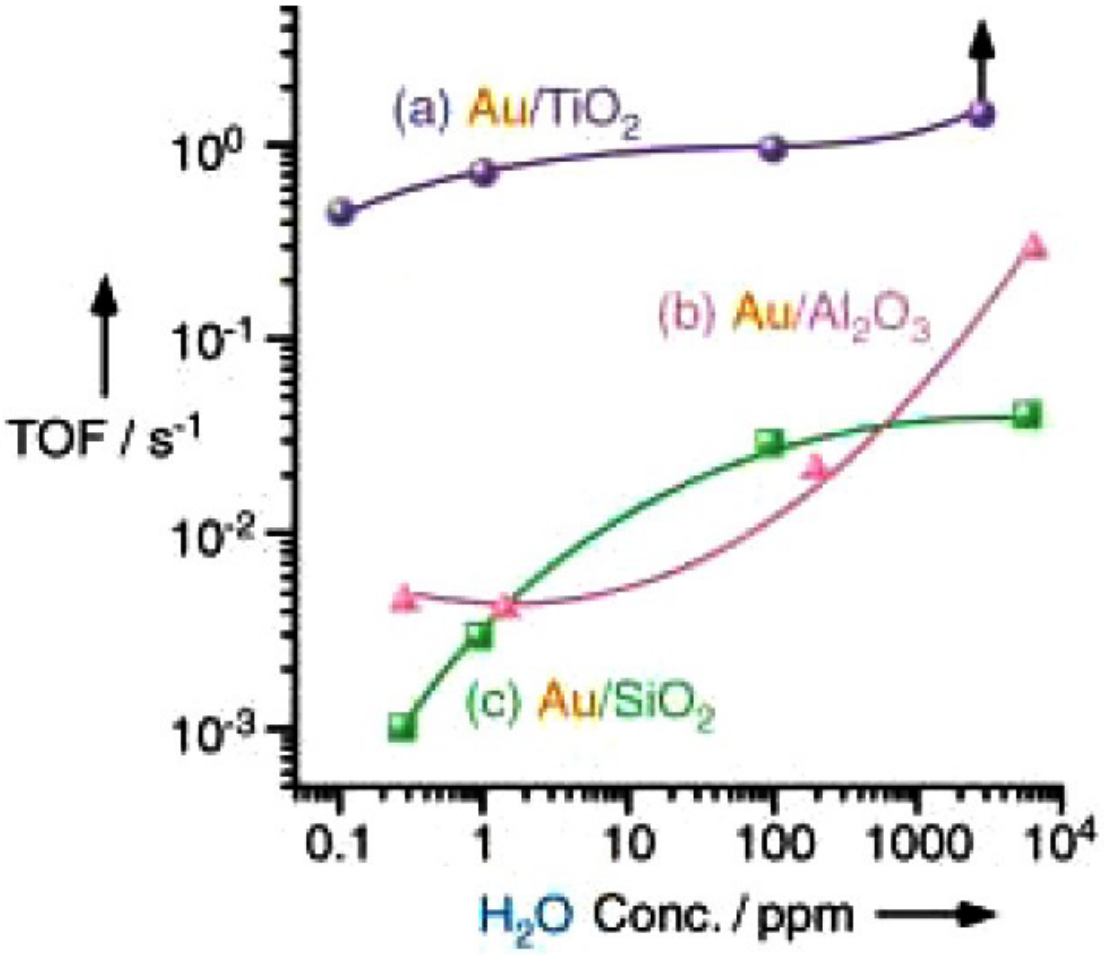

Figure 2. Turnover frequencies per surface gold atom at 273 K for CO oxidation over a) Au/TiO_2, b) Au/Al_2O_3 and c) Au/SiO_2 as a function of moisture concentration. Upright arrow indicates the saturation of CO conversion.

$$CO + H_2O \not\longrightarrow CO_2 + H_2 \quad (1)$$

$$O_2(p) + H_2O(s) \longrightarrow O^*(p) + 2OH(p) \quad (2a)$$

$$2OH(p) \longrightarrow O^*(p) + H_2O(s) \quad (2b)$$

$$CO(Au) + O^*(p) \longrightarrow COO(p) \longrightarrow CO_2(g) \quad (3)$$

$$CO_3(p) + H_2O(s) \longrightarrow CO_3H(p) + OH(p) \quad (4a)$$

$$CO_3H(p) \longrightarrow CO_2(g) + OH(p) \quad (4b)$$

$$CO(Au) + O_2(p) \longrightarrow CO_3(p) \quad (5a)$$

$$COO(p) + O^*(p) \longrightarrow CO_3(p) \quad (5b)$$

Scheme 1. Possible reaction steps at around the perimeter interfaces between gold and oxide support. (p), (s) and (Au) represent the adsorption at the perimeter interfaces, support surfaces, and Au surfaces, respectively, while (g) denotes the gas phase. O* indicates the activated oxygen species.

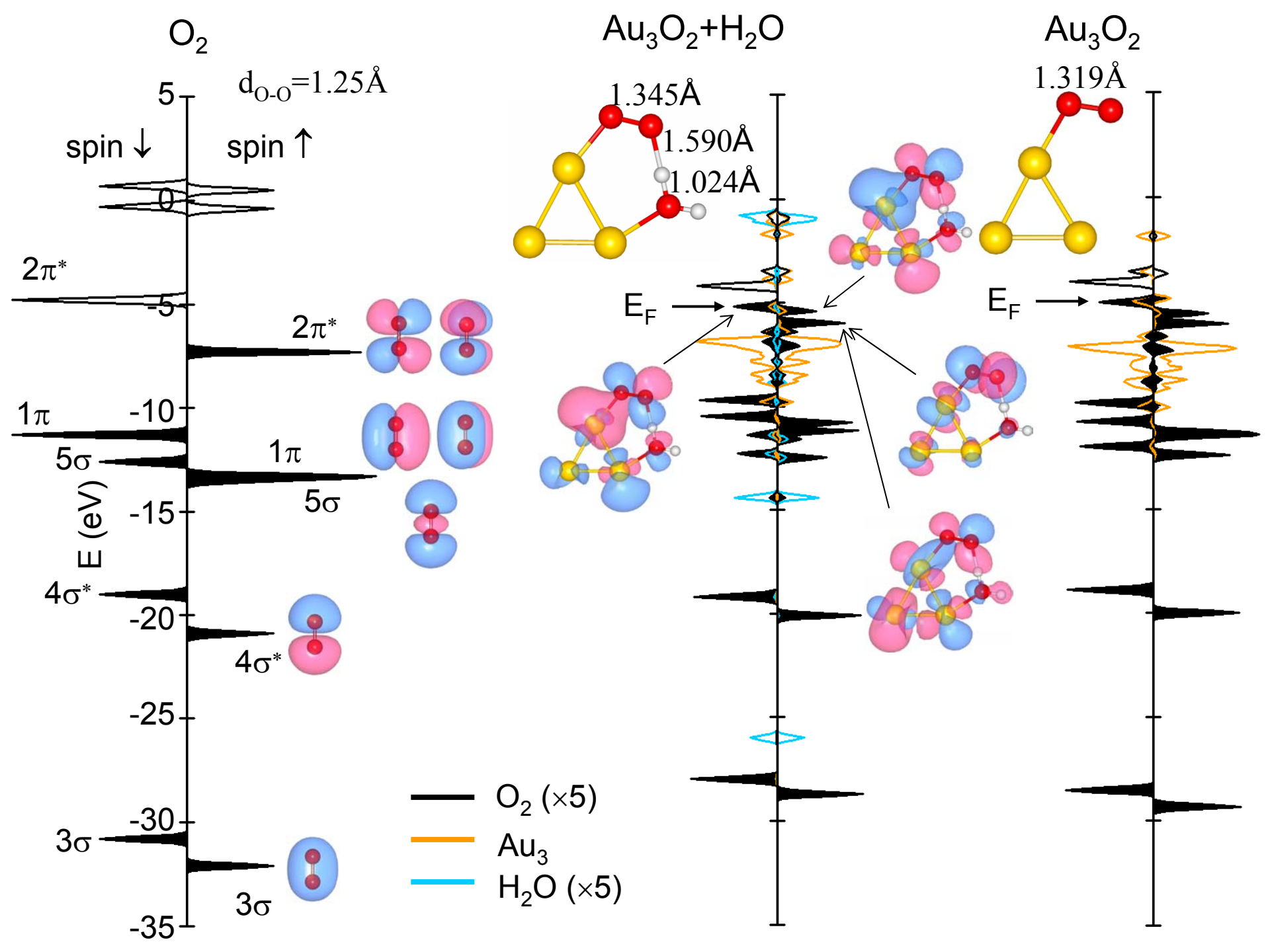
O2
d O-O=1.25Å
Au3O2+H2O
1.345Å
1.590Å
1.024Å
Au3O2
1.319Å
spin ↓
spin ↑
5
0
-5
-10
-15
-20
-25
-30
-35
E (eV)
2π*
1π
5σ
4σ*
3σ
E F
E F
O2 (×5)
Au3
H2O (×5)

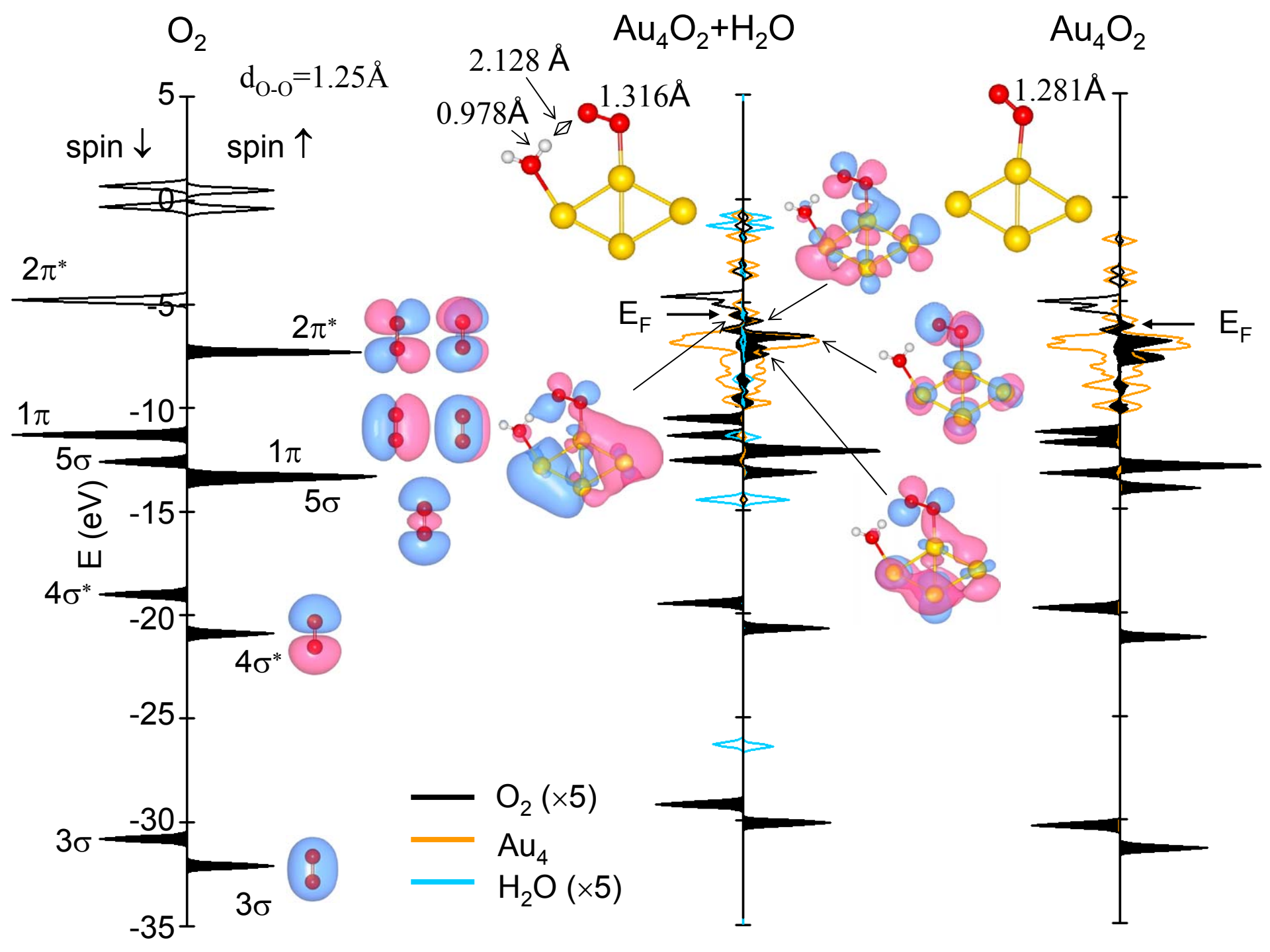
O2
d O-O=1.25Å
Au4O2+H2O
2.128 Å
0.978Å
1.316Å
Au4O2
1.281Å
spin ↓
spin ↑
5
0
-5
-10
-15
-20
-25
-30
-35
E (eV)
2π*
1π
5σ
4σ*
3σ
E F
E F
O2 (×5)
Au4
H2O (×5)

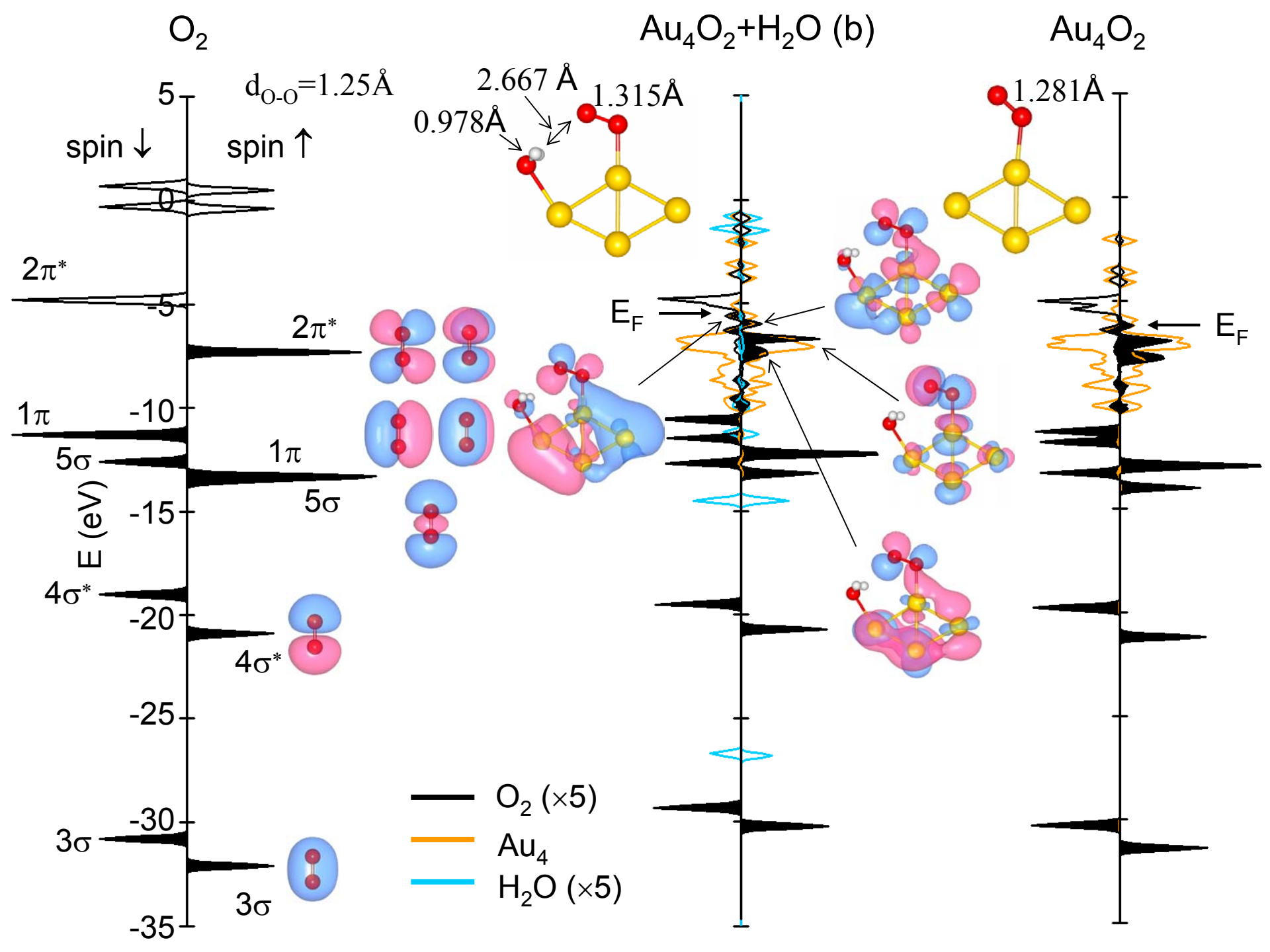
O2
Au4O2+H2O (b)
Au4O2
d O-O=1.25Å
2.667 Å
1.315Å
0.978Å
1.281Å
spin ↓
spin ↑
5
0
-5
-10
-15
-20
-25
-30
-35
E (eV)
2π*
1π
5σ
4σ*
3σ
E F
O2 (×5)
Au4
H2O (×5)

TABLE I. Energies (in eV) for the adsorption and coadsorption of O_2 and H_2O on free (Au_8 and Au_{30}) clusters and on a gold octamer supported on MgO(100), i.e. Au_8/MgO. In the case of the Au_8/MgO system, results are given for both the adsorption on the top-facet of the gold cluster cluster (-T) and at the peripheral interface of the cluster with the substrate (-P).

	O_2	H_2O	O_2-H_2O
Au_8	unbound	~0.3	0.4–0.9
Au_{30}	≤0.4	0.3–0.6	0.7–0.9
Au_8/MgO-T	≤0.1	0.2–0.3	0.5–1.2
Au_8/MgO-P	0.3–0.8	0.4–0.6	1.3–2.1

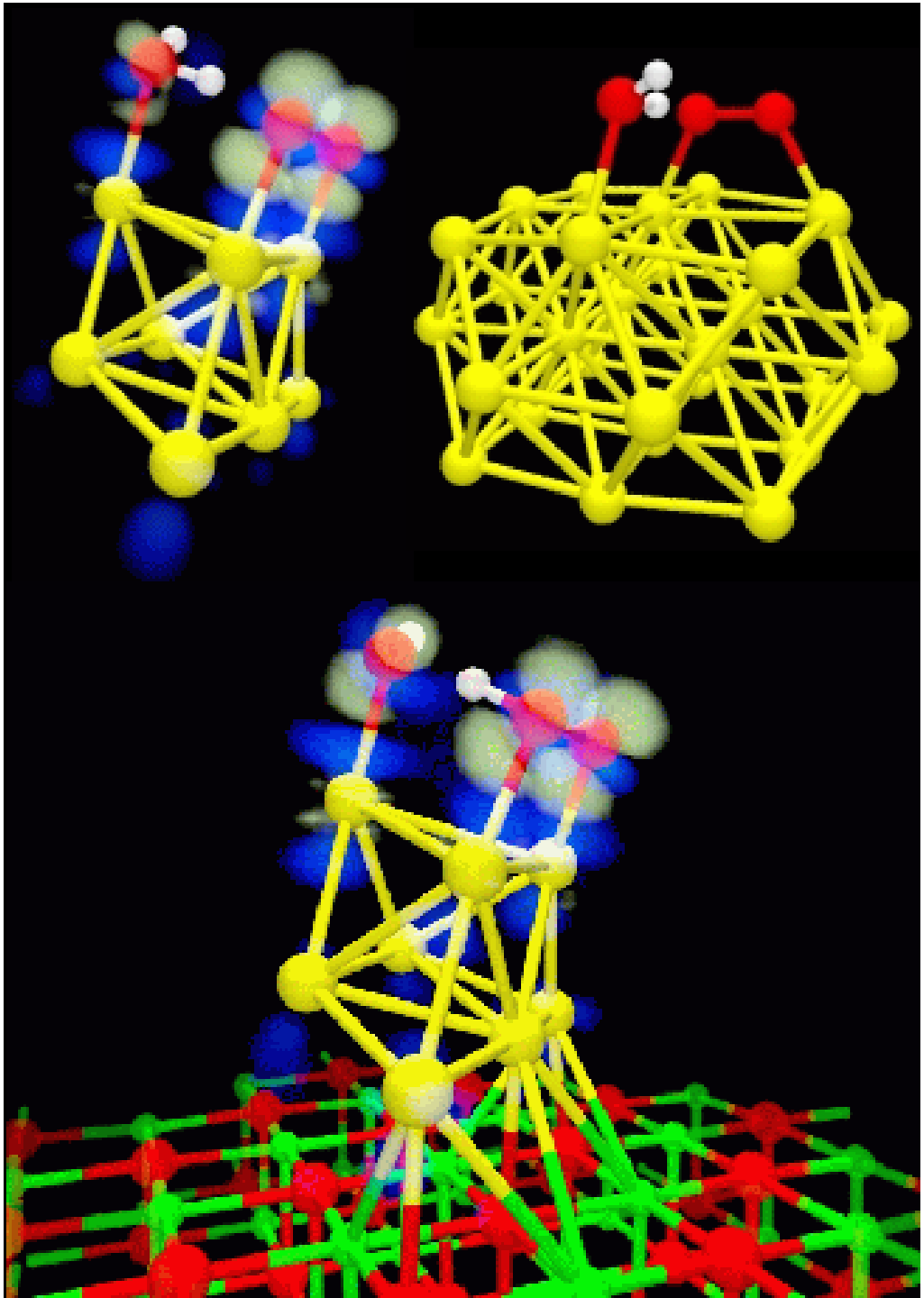

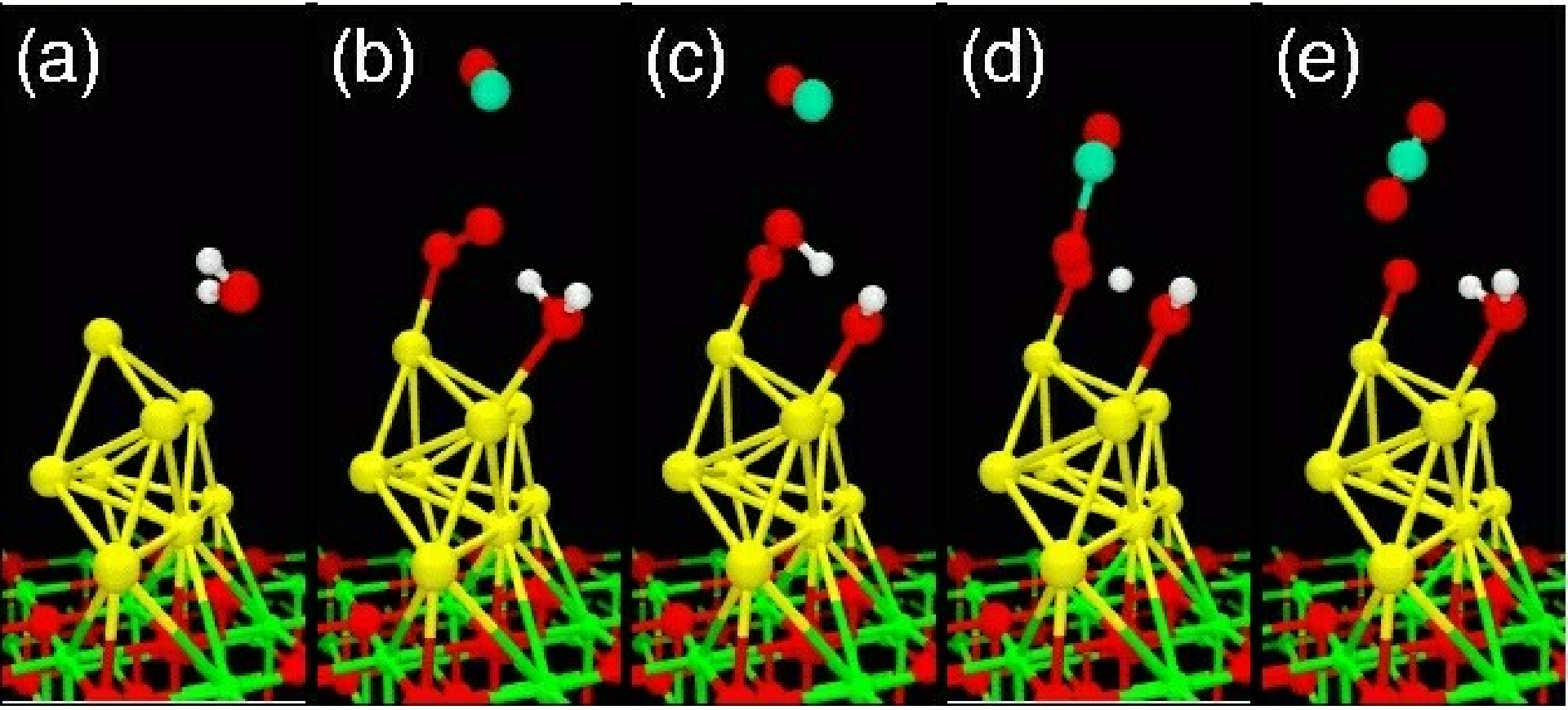
(a)
(b)
(c)
(d)
(e)

Low-temperature Average Magnetic Moment per Atom in Metal Clusters

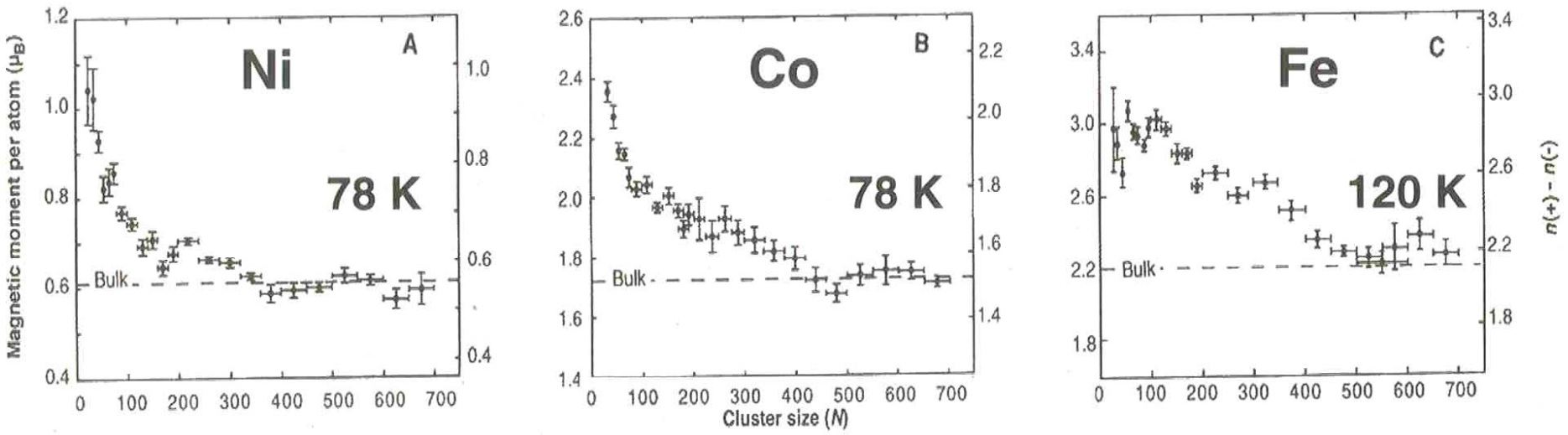

I.M. L. Billas, A. Chatelain, and W. A. de Heer, Science **265,** 1682 (1994)

Pd_N clusters

M. Moseler
H. Häkkinen
R.N. Barnett
U. Landman

■ anion
□ neutral

• Phys. Rev. Lett. (2001) 86, 2545 ('01)

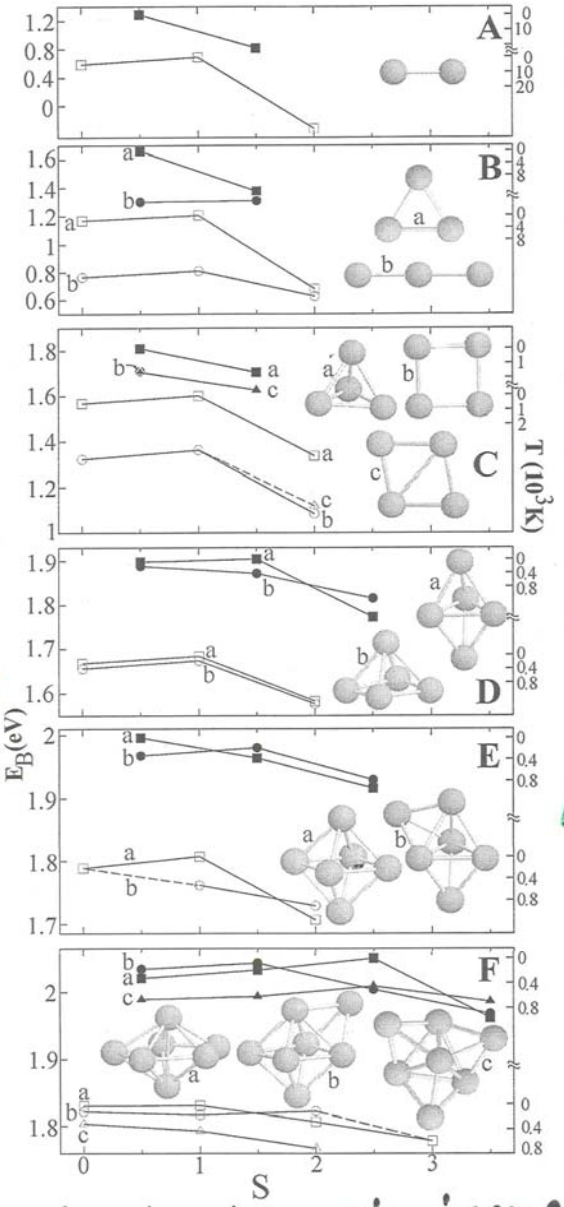

structural + spin isomers

Pd_{13}

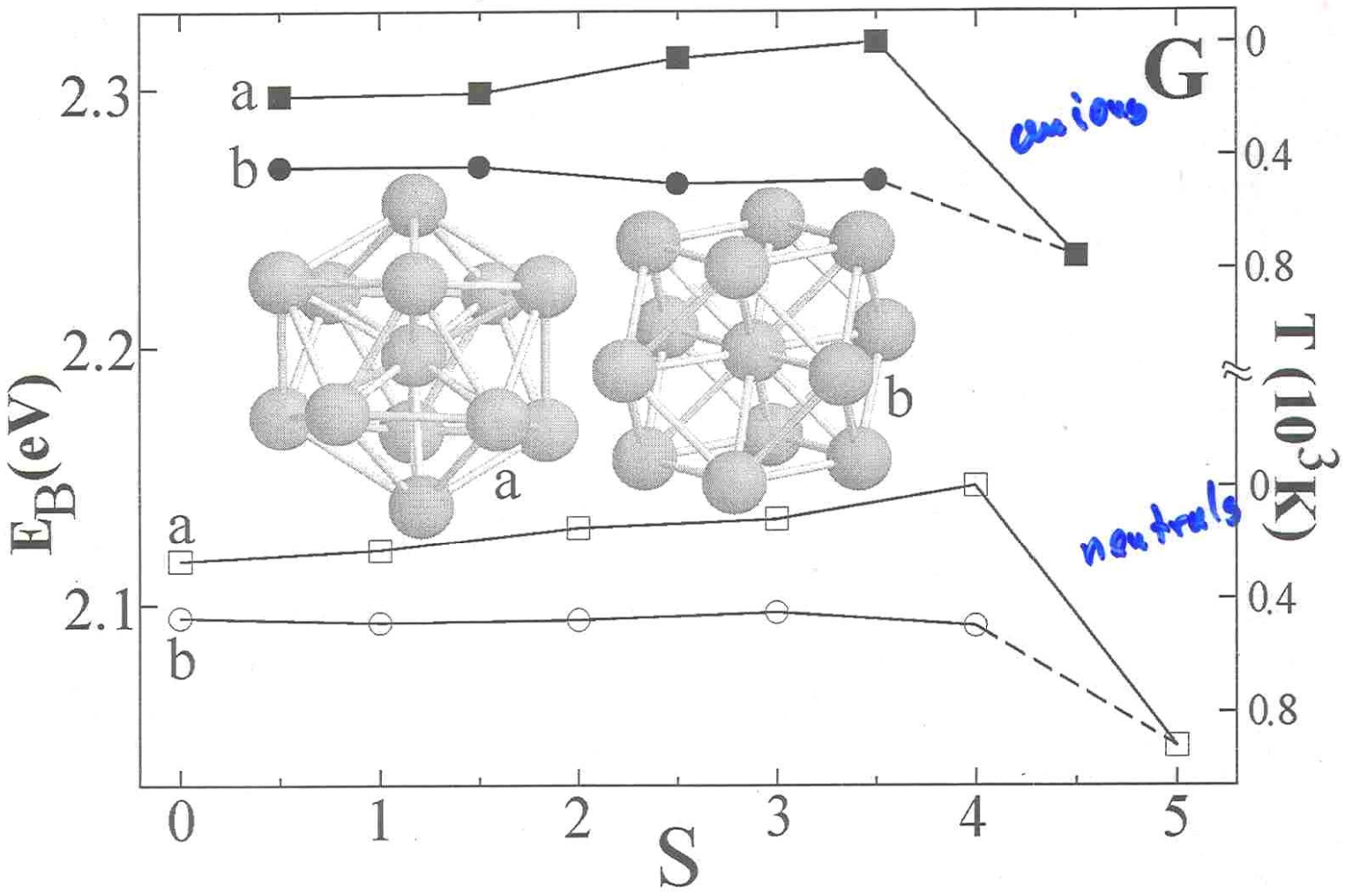
2.3
2.2
2.1
E_B(eV)
a
b
a
b
a
b
cations
G
neutrals
0
0.4
0.8
0
0.4
0.8
T (10^3K)
0
1
2
3
4
5
S

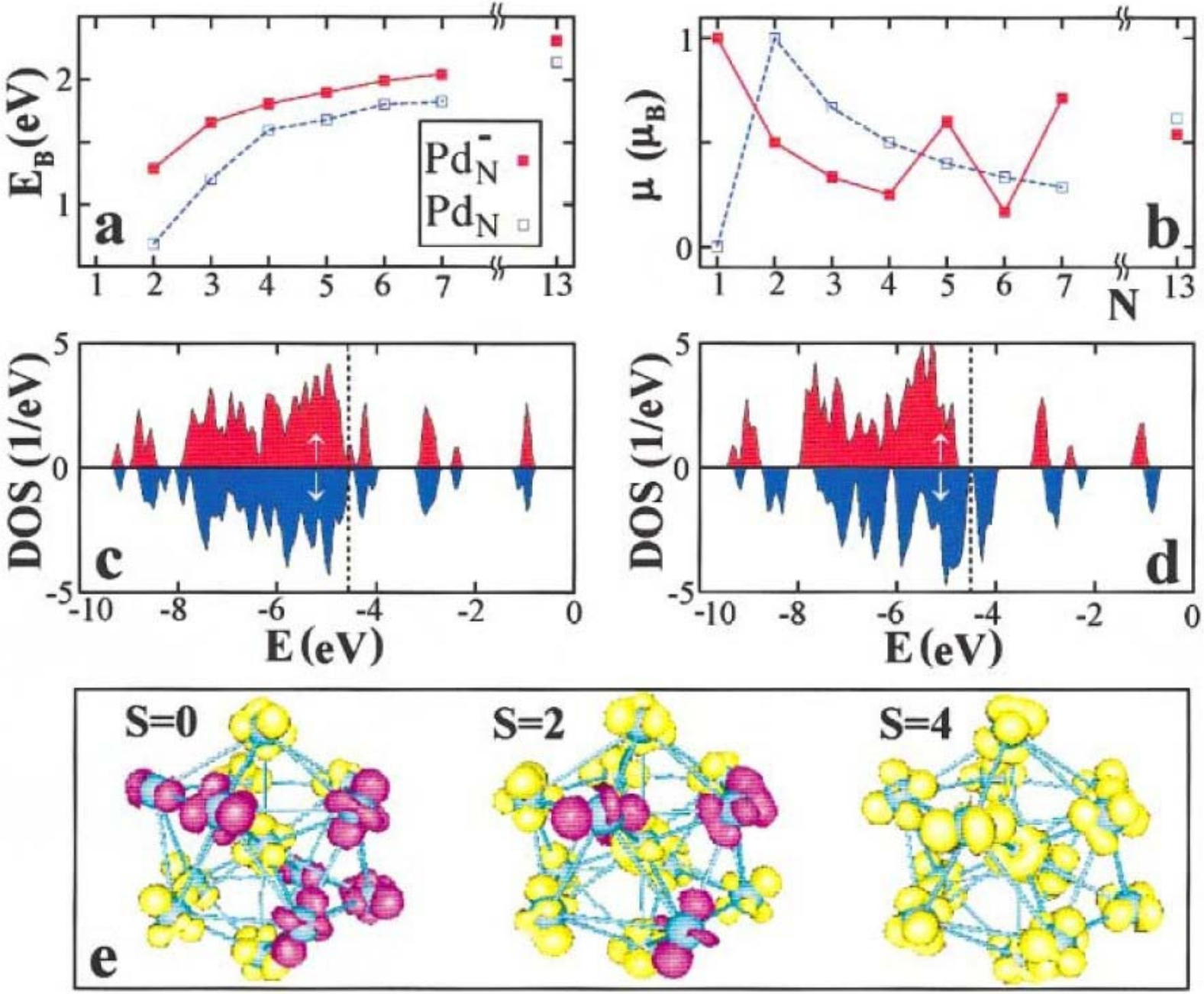
a
E_B(eV)
Pd_N^-
Pd_N
b
μ (μ_B)
N
c
DOS (1/eV)
E (eV)
d
DOS (1/eV)
E (eV)
e
S=0
S=2
S=4

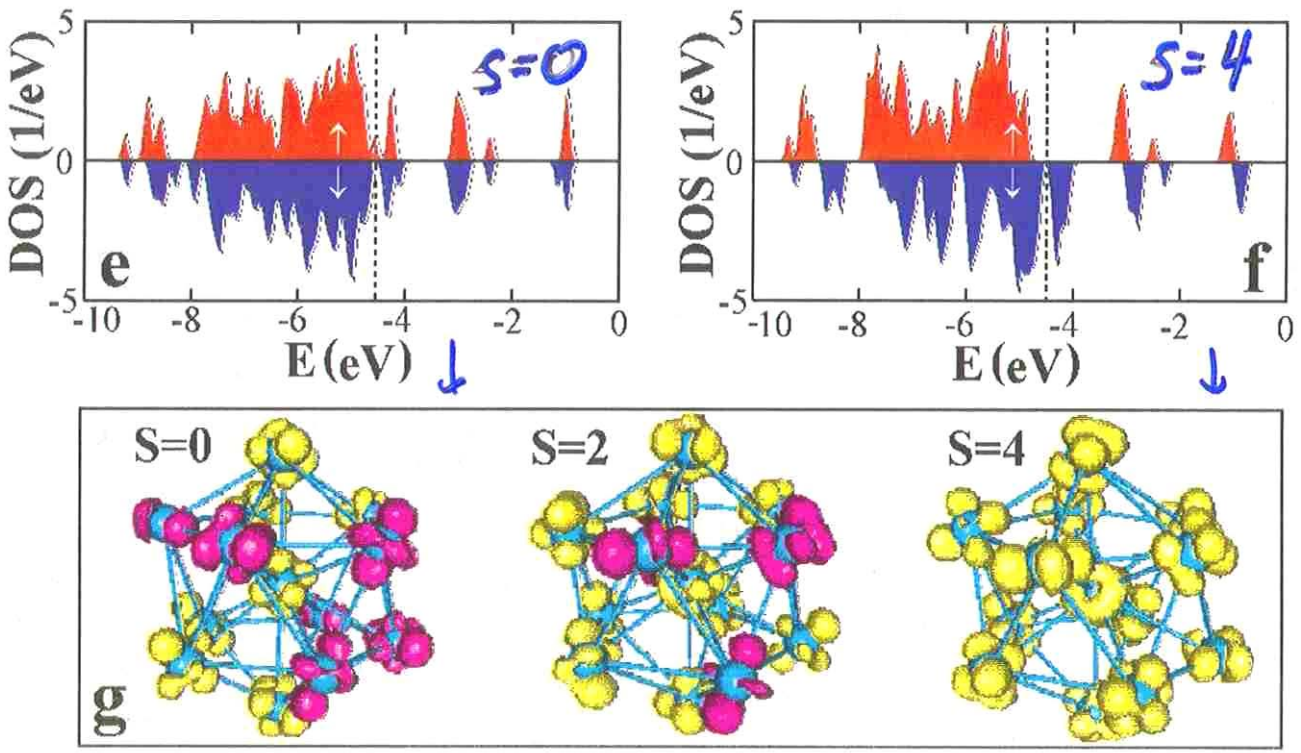

← ground-state

Moseler, Hakkinen, Landman PRL 86, 2545 ('01)

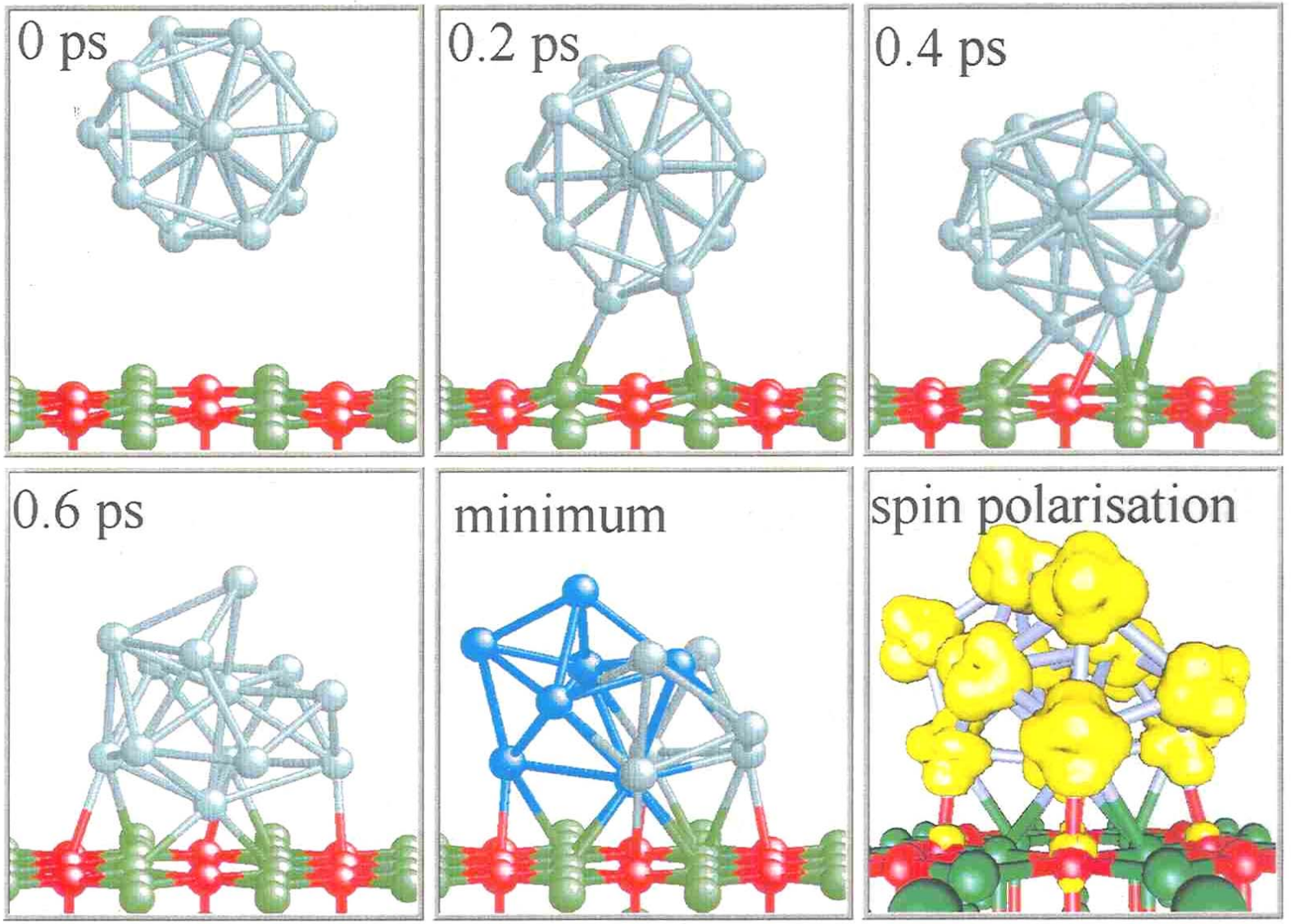
0 ps
0.2 ps
0.4 ps
0.6 ps
minimum
spin polarisation

Surface States of Excess Electrons on Water Clusters

R. N. Barnett, Uzi Landman, and C. L. Cleveland
School of Physics, Georgia Institute of Technology, Atlanta, Georgia 30332

and

Joshua Jortner
School of Chemistry, Tel Aviv University, 69978 Tel Aviv, Israel
(Received 29 April 1987)

Electron attachment of water clusters was explored by the quantum path-integral molecular-dynamics method, demonstrating that the energetically favored localization mode involves a surface state of the excess electron. The cluster size dependence, the energetics, and the charge distribution of these novel electron-cluster surface states are explored.

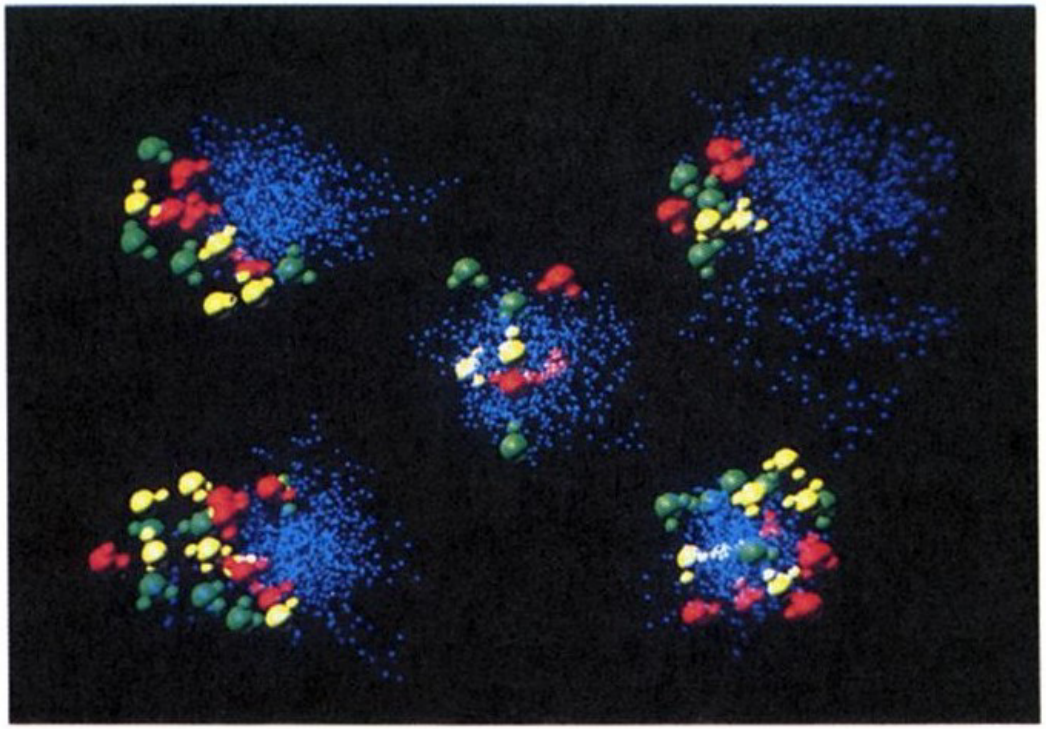

VOL 26 NUMBER 1 SPRING 1991

COMPUTING AND COMMUNICATIONS IN COLLEGES AND UNIVERSITIES

EDUCOM review

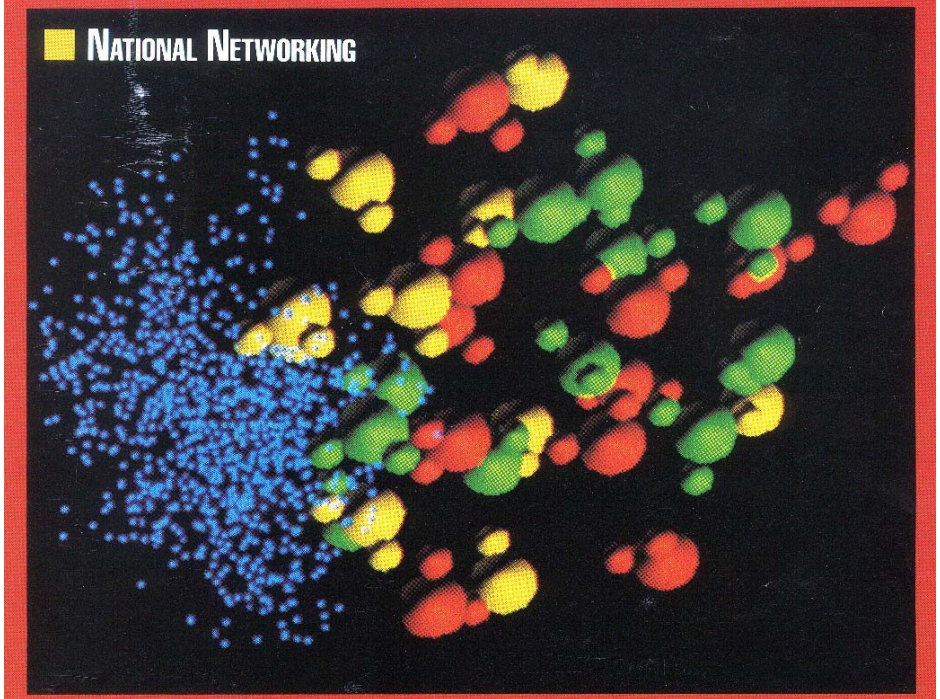

National Networking

NREN Enlightenment

Computing in the Curricula

Information Services

Supercomputing

Nonprofit Org.
U.S. Postage
PAID
Hanover, PA 17331
Permit No. 4

Dynamics of Electron Localization, Solvation, and Migration in Polar Molecular Clusters

R. N. Barnett,[1] Uzi Landman,[1] and A. Nitzan[2]

[1]*School of Physics, Georgia Institute of Technology, Atlanta, Georgia 30332*

[2]*School of Chemistry, Tel Aviv University, 69978, Tel Aviv, Israel*

(Received 19 August 1988)

The time evolution of electron localization, migration, and solvation in water and ammonia clusters is investigated via computer simulations. The attachment of an electron to a cold molecular cluster in a diffuse weakly bound surface state, the dynamics of solvation, the nonhopping mechanism of migration leading to the formation of an internally solvated state, and the spectral manifestation of these processes are demonstrated.

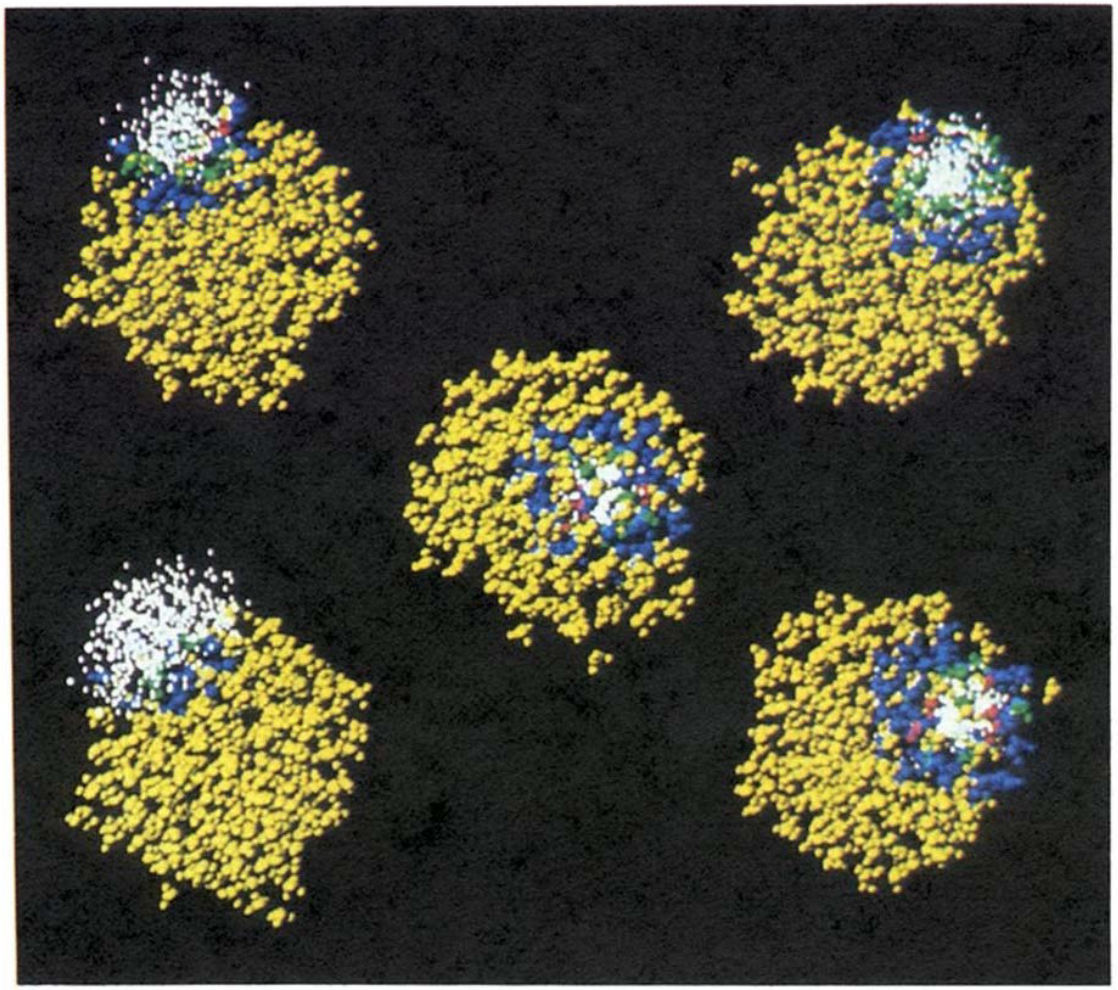

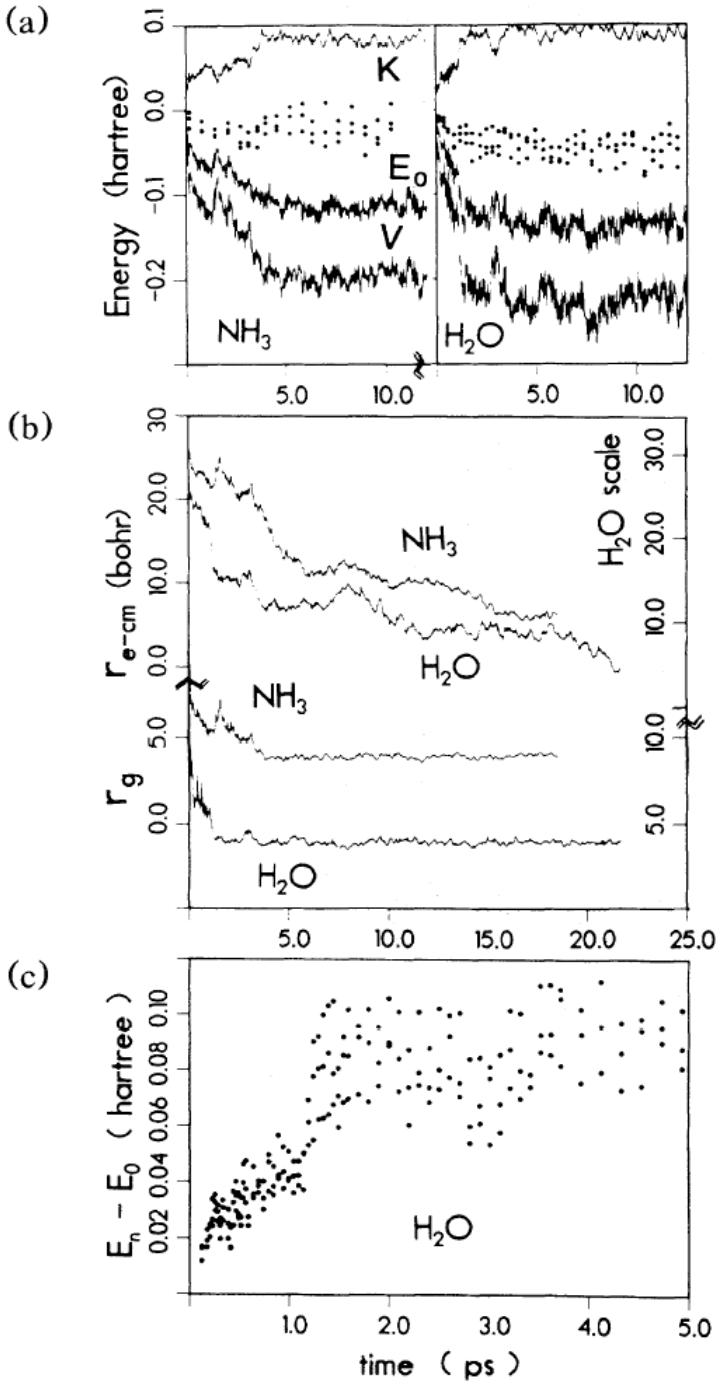
(a)
Energy (hartree)
0.1
0.0
−0.1
−0.2
K
E_o
V
NH_3
H_2O
5.0
10.0
5.0
10.0
(b)
r_{e-cm} (bohr)
r_g
30
20.0
10.0
0.0
5.0
0.0
NH_3
H_2O
NH_3
H_2O
H_2O scale
30.0
20.0
10.0
10.0
5.0
5.0
10.0
15.0
20.0
25.0
(c)
$E_n - E_0$ (hartree)
0.02 0.04 0.06 0.08 0.10
H_2O
1.0
2.0
3.0
4.0
5.0
time (ps)

Observation of Large Water-Cluster Anions with Surface-Bound Excess Electrons

J. R. R. Verlet,[1] A. E. Bragg,[1] A. Kammrath,[1]
O. Cheshnovsky,[2] D. M. Neumark[1,3]*

SCIENCE VOL 307 7 JANUARY 2005

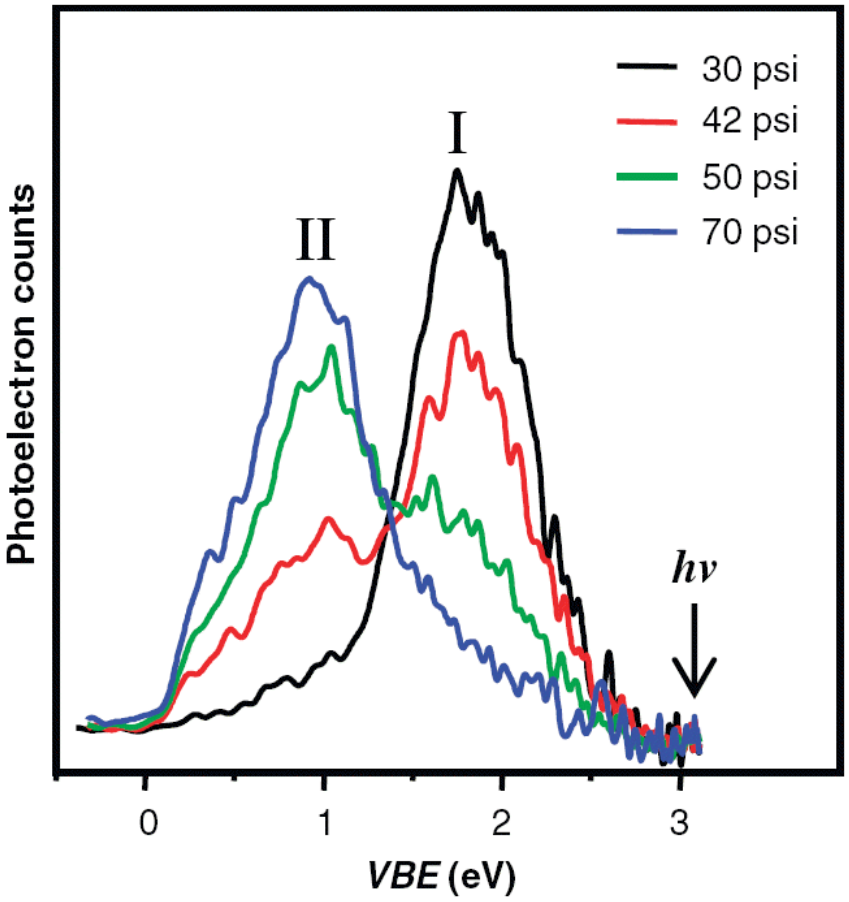

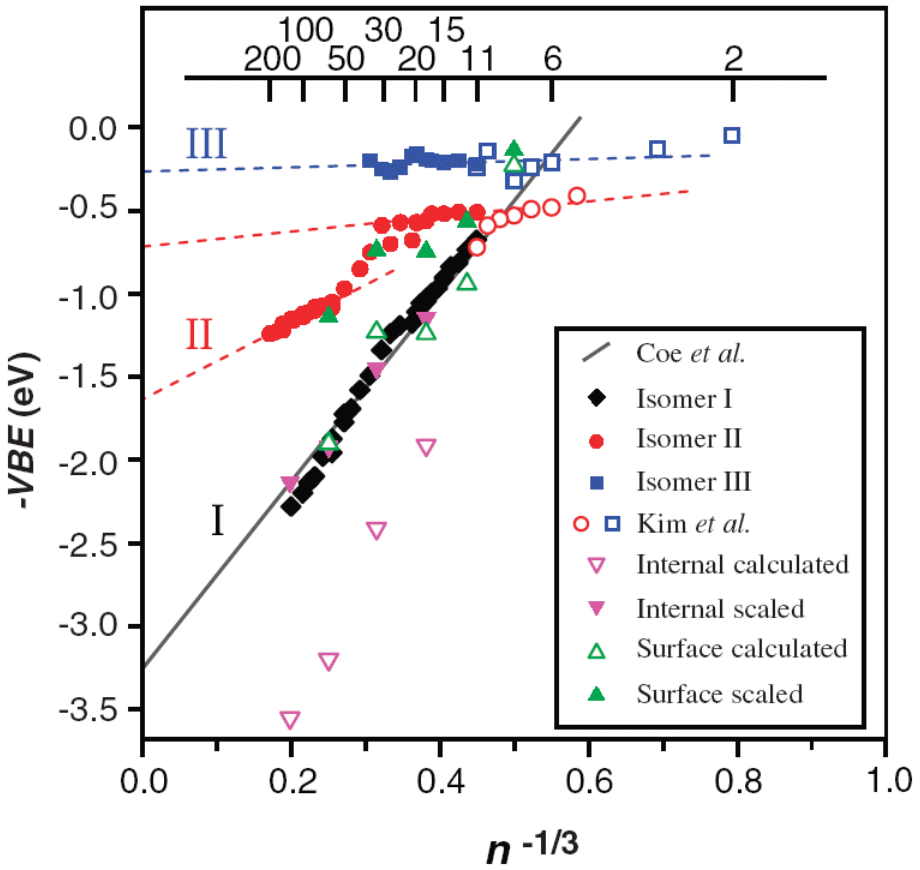

THE INTERSECTION OF TWO MAJOR EMERGENT MOVEMENTS

* *SCIENCE AND TECHNOLOGY AT THE NANOSCALE*

* *COMPUTATIONAL MICROSCOPIES – COMPUTERS AS TOOLS FOR DISCOVERY*

Small is Different

The non-scalable regime